Tesi di Dottorato di TALLARITA ELENA
Matricola 753363

POLITECNICO DI MILANO

EXPRESSION, STRUCTURAL AND FUNCTIONAL CHARACTERIZATION OF THE PROTEIN PROLINE OXIDASE INVOLVED IN DIFFERENT HUMAN DISEASES

**DIPARTIMENTO
DI
CHIMICA,
MATERIALI
E
INGEGNERIA CHIMICA
"Giulio Natta"**

**Dottorato di Ricerca in
Chimica Industriale e
Ingegneria Chimica (CII)**

XXV ciclo
2010 - 2012

Coordinatore: prof. Tiziano Faravelli
Tutore: prof. Stefano Servi
Relatore: prof. Loredano Pollegioni

Si dice spesso che bisogna sperimentare senza idee preconcette. Questo non è possibile; non solamente ciò equivale a rendere sterile ogni esperienza, ma anche se lo si volesse, non si potrebbe. Ciascuno porta con sé la propria concezione del mondo.

Henri Poincaré, 1902.

Acknowledgments

My gratitude to Professor Loredano Pollegioni and Professor Stefano Servi for giving me the opportunity to work on this PhD project. My thanks to Dr. Silvia Sacchi and Dr. Gianluca Molla for their support and their precious help during my work of thesis.

Publications

1. “Expression in Escherichia coli of the catalytic domain of human proline oxidase”.
   Tallarita E., Pollegioni L., Servi S., Molla G.; Protein Expr Purif. 2012 Apr; 82(2): 345-51.

2. “Expression of human proline oxidase in U87 glioblastoma cell line: effect on the concentrations of proline and glutamate”.
   Tallarita E. et al.,

Table of contents

	TABLE OF CONTENTS	**I**
	TABLES OF FIGURES	**III**
	INDEX OF TABLES	**V**
	LIST OF ABBREVIATION	**VII**
	ABSTRACT	**IX**
1.	**INTRODUCTION**	**1**
	1.1 Proline metabolism	**1**
	1.1.1 Proline oxidase: a universal enzyme in life kingdom	**2**
	1.1.2 *PRODH* genes and schizophrenia susceptibility	**7**
	1.1.3 Proline metabolism and cancer	**8**
	1.1.4 Disease related to proline metabolism	**9**
	1.1.5 Proline as a neurotransmitter: physiological significance	**10**
	1.1.5.1 Neurological impairments caused by L-proline	**11**
	1.2 Schizophrenia: a multifactorial psychiatric disorder	**14**
	1.2.1 Schizophrenia: neurochemicals alteration	**15**
	1.2.2 Schizophrenia: role of glial aminoacid transporter	**19**
2.	**AIM OF THE WORK**	**21**
3.	**RESULTS**	**23**
	Expression in Escherichia coli of the catalytic domain of human proline oxidase	**23**
	Effect of PO expression in U87 glioblastoma cell line, on selected amino acid	**30**
4.	**DISCUSSION**	**53**
5.	**REFERENCES**	**59**
4.	**OTHER PUBLICATION**	**67**

Tables of Figures

Figure 1. *Structure of L-proline*

Figure 2. *Reactions catalyzed by L-proline biosynthetic and catabolic enzymes*

Figure 3. *Scheme of the cycle of L-proline*

Figure 4. *Monofunctional PO from T. thermophilus and PO domain of E. coli PutA*

Figure 5. *UV/Visible spectra of EcPutA; reaction of Helicobacter PutA with sulfite*

Figure 6. *Scheme of oxidation of L-proline to L-glutamate catalyzed by the PRODH and the P5C domain of PutA*

Figure 7. *Scheme of PRODH and ΨPRODH genes*

Figure 8. *Model of the NMDA receptor*

Figure 9. *Summary plot of the proposed role of NMDAR in pathophysiology of schizophrenia*

Figure 10. *Schematic reaction involved in glutamatergic neurotransmission*

Index of tables

Table 1. *Apparent kinetic parameters of PRODH from different sources on L-proline as substrate*

List of abbreviation

ATP: Adenosine triphosphate

BD: Bipolar disorder

Bp: Base pairs

CNS: Central nervous system

CSF: Cerebro spinal fluid

C-terminal: Carboxyl terminal

CTRL: Control

DAAO: D-amino acid oxidase

DCPIP: Dichlorophenolindophenol

DGRC: Di George syndrome chromosomal region

EAAT: Excitatory amino acid transporter

E.Coli: *Escherichia coli*

EYFP: Enhanced yellow fluorescent protein

FAD: Flavin adenine dinucleotide

GABA: Gamma-aminobutyric acid

GAT: GABA transporter

GLAST: Glutamate aspartate transporter

Gln: Glutamine

GLT-1: Glutamate transporter 1

Glu: Glutamate

GSA: Glutamate semialdehyde

G-protein: Guanine nucleotide-binding proteins

hDAAO: Human D-amino acid oxidase

HPI: Hyperprolinemia

Kb: Kilo base pairs

Kd: Dissociation costant

KDa: kilodalton

Km: Michaelis constant

Leu: Leucine

Mb: Mega base pairs

mGluR: Metabotropic glutamate receptor

mRNA: Messanger ribonucleotide acid

NAD: Nicotinammide adenine dinucleotide

NADP: Nicotinammide adenine dinucleotide phosphate

NMDAR: N-methyl-D-aspartate receptor

N-terminal: Amino terminal

o-AB: o-aminobenzaldehyde

Orn: Ornithine

PO: Proline oxidase

Pro: Proline

PRODH: Proline dehydrogenase

PROT: Proline transporter

PuTA: Proline utilization A

P5C: Δ^1-pyrroline-5-carboxylate

P5CDH: Δ^1-pyrroline-5-carboxylate dehydrogenase

ROS: Reactive oxygen species

SNARE: SNAP (Soluble NSF Attachment Protein) Receptor

SNP: Single nucleotide polymorphysm

TCA: Tricarboxilic acid

THFA: Tetrahydro-2-furoic acid

UV: Ultraviolet

U87: Human glioblastoma cell line

VAMP: Vesicle associated membrane proteins

V_{max}: Maximum reaction rate

Abstract

Intracellular synthesis and degradation of free L-proline occur through a distinct set of enzymes with unique properties and regulatory mechanism: together they constitute a "proline cycle" which represents an important connection with other metabolic pathways. Proline oxidase (PO) is a mitochondrial inner-membrane flavoenzyme that catalyzes the first step in the L-proline degradation pathway. All organisms oxidize proline to glutamate in two enzymatic steps coupled by a non-enzymatic equilibrium: in the first step, proline oxidase (PO) catalyzes the oxidation of proline to Δ^1-pyrroline-5-carboxilyc acid (P5C) a reaction that involves flavin adenine dinucleotide (FAD) as a cofactor. P5C is then alternatively subjected to three metabolic reactions: oxidation to glutamate, transamination to ornithine or reduction back to proline. Even if the biosynthetic pathways and biological role of proline have been well established, the role of proline oxidation in the cell remain largely unknown. PO is encoded by the *PRODH* gene, which maps in a genomic region (22q11) which is affected by mutation and deletion involved in different (and possibly related) neurological pathologies, and where several studies have localized genes that potentially confer increased susceptibility to schizophrenia.

Delections of the 22q11 locus are found in 0.3-2% of patients with schizophrenia; this made *PRODH* a positional candidate gene for schizophrenia. Moreover, microdeletion of chromosome 22q11 is associated with velo-cardio-facial syndrome (VCFS) (or Di George syndrome) and patients with 22q11 deletion also exhibit cognitive deficits similar to those observed in schizophrenia. Association between plasma proline level and schizophrenia revealed that this parameter in affected individuals is significantly higher than in healthy individuals and that subjects with hyperprolinemia (HPI) have a 6-fold greater chance to develop schizophrenia than controls. HPI is an autosomal recessive disorder characterized by plasma proline concentration above normal, caused by absence or reduced activity of PO. At least 16 *PRODH* missense mutations on the *PRODH* gene have been identified with moderate to severe effect on PO activity; notably the L441P substitution, which results in severe reduction of PO activity, is one of the allele typically found in individuals affected by HPI and schizophrenic patients. Schizophrenia is a common chronic and disabling brain disease of still largely unknown etiology and pathogenesis, that affects about 1% population worldwide. Schizophrenia occurs in all populations and is considered a

complex disease with multiple factors contribution: the most widely accepted neurodevelopmental hypothesis of schizophrenia integrates environmental influences and causative genes. Several experimental evidences suggest that the pathology is related to a deficiency of glutamate-mediated excitatory neurotransmission. Glutamate is the primary excitatory amino acid neurotransmitter in the mammalian CNS, thus dysfunction of the glutamate system is responsible of neuronal toxicity. In schizophrenia an hypofunction of N-methyl-D-aspartate (NMDA) receptors is reported to cause the complex pattern of symptoms and cognitive deficits found in schizophrenia. Recently it has been proposed a putative role of proline as a neuromodulator since a specific proline transporters has been localized within the glutamate pathways, suggesting that proline might serve as a modulator of glutamate transmission. This hypothesis is strongly supported by the observation that proline and glutamate are involved in the same metabolic pathways.

This PhD project was aimed at understanding the role of PO in physiological and/or pathological processes, particularly as a candidate risk factor for schizophrenia.

In the first part of the project, we decided to characterize the recombinant PO by expressing the human protein in an heterologous system and to evaluate its catalytic properties. *E. coli* is usually the most used organism for heterologous expression of recombinant proteins; nevertheless the expression of mammalian proteins, such as PO, turns out to be sometimes difficult in this host since it does not perform most post-translational modifications. Moreover, human PO is in the mitochondrial inner membrane, so it could possess regions that negatively affect its expression in *E. coli* as a soluble protein. Therefore, by using an accurate bioinformatic analysis, several PO deletion variants were produced: all PO variants include a core region corresponding to the catalytic domain but they lack regions which could negatively affect the expression. Among the expressed PO variants, the PO-barrelN-His variant was expressed as a soluble protein and was subjected to a detailed biochemical characterization.

A second aspect of the project focused on the expression of the wild-type and L441P inactive PO variant in a mammalian cell system. The U87 human glioblastoma cell line was used as *in vitro* model of astroglia, which in the brain is the responsible of the release and reuptake of signaling molecules, among which the key neurotransmitter glutamate. U87 clones stably expressing wild-type and L441P inactive variant PO, were successfully produced, as confirmed by Western blot analysis. The subcellular localization was also confirmed by the over-expression of the PO variants as chimeric proteins with EYFP fluorescent protein and immunostaining. Confocal images show that the fluorescent signal corresponding to PO-EYFP displays a peculiar “spaghetti like” pattern

typical of mitochondria. Furthermore, PO-EYFP variants signal distribution largely overlapped with a specific mitochondrial marker. The investigation of the functional differences between U87 cells transfected with the wild-type or the mutant PO was subsequently carried out. The cells growth was monitored over a period of 7 days: the growth curves (cell density/well vs time) display the typical trend of exponential growth. No significant difference was evident between cells stably expressing the mutant or the wild-type PO, while both showed a lower growth rate with respect to untransfected U87 cells. This result could indicate that the over-expression of PO negatively affected U87 cells metabolism and proliferation capacity, this independently from the enzyme activity. The next step was the investigation of proline cellular content by HPLC analysis, since variation in the concentration of the amino acid, in U87 transfected is indicative of the activity of expressed PO variant. Proline is reported to be directly involved in glutamatergic transmission (even though the biochemical mechanism by which this happens is still unknown) two hypotheses have been formulated: proline may accumulate in the synaptic terminals inhibiting glutamate release or act on a cell surface transporter inhibiting the release through a complex signaling cascade. For these reasons we measured the proline/glutamate levels in cellular and extracellular space of U87 cells by HPLC analysis. At the same time we started the investigation of the expression level of the glutamate transporters GLT-1 and GLAST by Western blot analysis to verify if expression of active or inactive PO variants could affect glutamatergic functionality.

In conclusion, the purification of a soluble, active human PO variant (encompassing the whole catalytic domain of the enzyme), as reported in the first part of the project, represents the fundamental step to investigate structure-function relationships in human proline oxidase and to compare the biochemical properties of the mammalian enzyme to those of the prokaryotic homologues. Further studies will be necessary for the identification of the effect of the reported polymorphisms of the enzyme on its structure and activity and to understand how they could affect the proline/P5C redox cycle.

In addition, the expression of the wild-type and L441P inactive variant, as obtained in the second part of the project, allowed a preliminary characterization of proline oxidase function in the framework of glutamate metabolic pathways. Further investigation are required to elucidate the role of proline as a putative neuromodulator in physiological and pathological conditions, through the characterization of proline oxidase regulatory mechanism in the glutamatergic synapses.

1 Introduction

1.1 Proline metabolism

L-Proline is a non-essential amino acid: because it possesses only one hydrogen atom attached to the nitrogen atom inserted in a pyrrolidine ring, it is usually referred to as “imino acid” [Fig. 1].

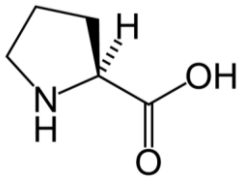

Fig.1- Structure of L-proline.

Proline can be synthesized from glutamate or ornithine through the common intermediate Δ^1-pyrroline-5-carboxylic acid (P5C). P5C is the main precursor of proline but also its immediate degradation product [Fig. 2]. The metabolic connection between P5C and proline constitutes a “proline cycle” allowing the transfer of reducing potentials from cytoplasm into mitochondria. In addition, P5C constitutes a metabolic interlock with other metabolic pathways and it is related to the synthesis and degradation of glutamate [1, 2].

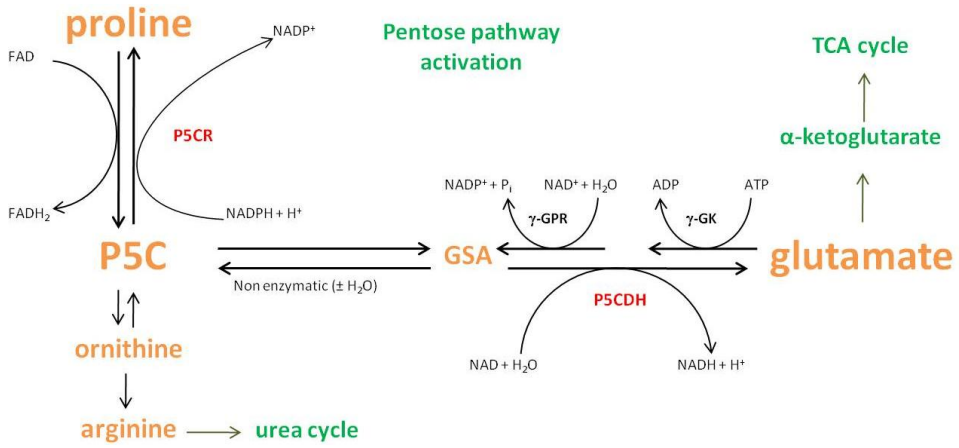

Fig.2 - Reactions catalyzed by proline biosynthetic and catabolic enzymes. PO = proline oxidase; P5C = Δ^1-pyrroline-5-carboxylate; γ-GK = γ-glutamil kinase; γ-GPR = γ-glutamil phosphate reductase; GSA = glutamate semialdehyde; P5CR = Δ^1-pyrroline-5-carboxylate reductase; P5CDH = Δ^1-pyrrolline-5-carboxylate dehydrogenase.

Because proline metabolism is distinct from that of primary amino acids, especially due to the unique structure of pyrrolidine ring, the synthetic reaction and related interconversions of proline can play a regulatory role and can be involved in special physiological or pathophysiological situations [2].

1.1.1 Proline oxidase: a universal enzyme in life kingdom

Proline dehydrogenase (PRODH, EC 1.5.99.8), also known as proline oxidase (PO/POX), catalyzes the first step in the two step oxidation of proline to glutamate in bacteria and eukaryotes. Proline oxidation not only contributes to modulate the amount of proline in the cell, but also generates various molecules such as ATP, reactive oxygen species (ROS) NAD^+/$NADPH+H^+$ and α-ketoglutarate. PO is an ubiquitous protein, but enzymes from different sources are structurally different and possess distinct cellular and physiological roles. The mitochondrial localization of PO in eukaryotes suggests that electrons originating from proline oxidation could be transferred to an acceptor of the membrane electron transport chain [3-6]. Even though the biosynthetic pathways and biological role of proline itself have been well established, the role of proline oxidation in the cell remain largely unknown [2].

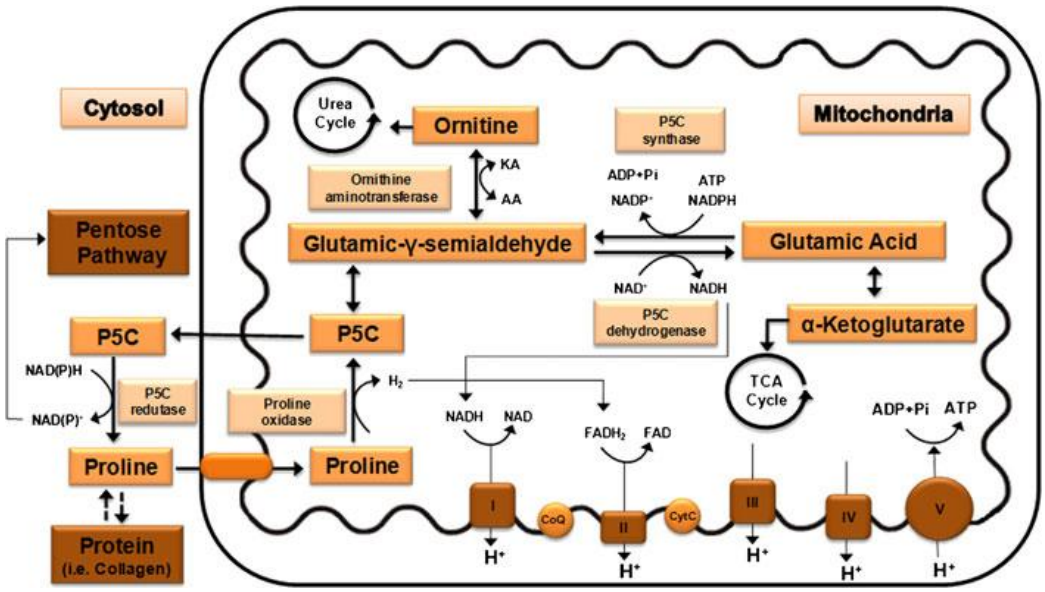

Fig.3- Scheme of the cycle of proline [33].

Some of the specific functions of proline have been elucidated in model organisms. For example proline can be used as a defense against osmotic challenge in prokaryotes and plants [7] or as a redox shuttle in insects [2, 8]. Proline content in higher plants increases under different environmental stresses and accumulation has been reported during condition of drought, high

salinity, high light/UV irradiation, in the presence of heavy metals or under oxidative stress. Thus it has been proposed that proline accumulation in stressed plants could have a protective function [7, 8]. All organisms oxidize proline to glutamate in two enzymatic steps coupled by a nonenzymatic equilibrium. In the first step, the FAD-containing enzyme proline oxidase catalyzes the oxidation of proline to P5C; P5C has three possible metabolic fates: oxidation to glutamate, a reaction catalyzed by P5C dehydrogenase (P5CDH, EC 1.5.1.12); transamination to ornithine in a reaction catalyzed by ornithine aminotransferase (OAT, EC 6.1.13); or the reduction back to proline, catalyzed by P5C reductase (P5CR, EC 1.5.1.2) using NADPH as cofactor [Fig. 2] [8]. Both PO and P5CDH are highly conserved in eukaryotes and bacteria. The general structural organization of PO in several organisms belonging to all kingdoms has been clarified based on the availability of several genomic and structural data [9]. PO activity is found in mono-, bi- and trifunctional enzymes. In eukaryotes and some prokaryotes, PO and P5CDH are separate monofunctional enzymes localized in mitochondria, while in several bacteria they are combined into a single polypeptide chain known as proline utilization A (PutA) [10].

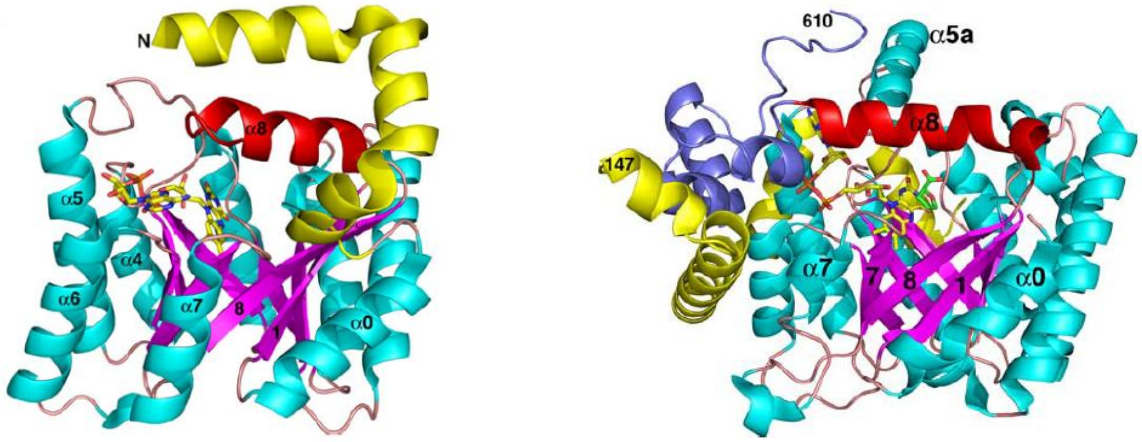

Fig. 4 - Monofunctional PO from *T. thermophilus* (left) and PO domain of E. *coli* PutA (right). *β*-strands and α-helices of the $(\beta\alpha)_8$ barrel are colored magenta and cyan, respectively; helix 8 is colored in red. The FAD cofactor is shown in yellow sticks, the THFA inhibitor is shown in green steacks. From [9].

Bacterial PutAs are further classified as bifunctional or trifunctional enzymes: trifunctional PutAs are distinguished by the presence of an additional DNA binding domain located in the first 50 residues of the polypeptide chain. In fact in addition to function as a PO/P5C enzyme, the DNA binding domain of the trifunctional enzyme represses the transcription of the *put* regulon (which

contains the genes encoding PutA and the proline transporter PutP) when environmental proline level are low. [10, 11].

Protein sequences encoded by *PRODH* genes from 63 different eukaryotic species were aligned to generate an unrooted phylogenic tree [2]. The analysis reveals distinct clusters of sequence similarities. The residues of the active site of proline catabolic enzymes belonging to PutA family are highly conserved, indicating that the three dimensional structure of catalytic domains is conserved in these enzyme. Many of the enzyme domains used for structure determination derive from bacterial sources, this reflects the relative ease of isolation and purification of the bacterial enzymes compared to the eukaryotic ones. Three dimensional crystal structure has been solved for different PO/P5C enzymes from microorganisms such as the PRODH and P5CDH from *Thermus thermophilus* (TtPRODH, TtP5CDH) and *Bradyrhizobium japonicum* (BjPutA), and the PRODH domain of *E. coli* (EcPUTA) [12, 13]. Comparison between the crystal structures of TtPRODH and the PRODH domain from *E. coli,* showed that PO enzymes adopt a distorted $(\alpha\beta)_8$ barrel fold [9, 10, 12]. This barrel fold consist of eight parallel β-strands arranged like the staves of a barrel; each strand is followed by an α-elix, and these helices are arrayed on the outside of the β-barrel next to the strands. The strands and helices are numbered 1 to 8 with helix 8 containing residues that are critical for substrate recognition, including a conserved Arg-Arg motif. In both structures the FAD is bound at the C-terminal ends of the strands of the barrel [Fig. 4] [10].

Despite both the PutA PRODH domain and the monofunctional enzyme exhibit a similar distorted $(\alpha\beta)_8$ barrel fold, there is an important difference between monofunctional PRODH and PutA: the latter possesses an extra helix (α5a) and an additional structure element in helix α8 of the barrel structure; this results into a different FAD conformation in the catalytic site of the enzymes from *E. coli* and *Thermus thermophilus* and in a different arrangement of the substrate-channeling cavity [14, 15]. PutA also have extra domains (alpha helical arm at the N-terminus) not found in the monofunctional PRODH enzymes, that possesses a localization critical for proper orientate the two active sites of the proteins and facilitate substrate channeling [10]. Enzymes or domains have been crystallized in the presence of substrate analogs to provide insights into substrate recognition [9]; e.g., structures of the EcPUTA PO domain complexed with reversible inhibitors such as L-tetrahydro-2-furoic acid (THFA) or L-lactate. Residues in the active site of the PRODH domain that are in direct contact with THFA are highly conserved: seven of the nine residues contacting the inhibitor are present also in the human enzyme. Based on the high sequence conservation of the active site residues throughout the PutA/PRODH family, it is likely that all PO enzymes (including the human one) bind the substrate in the $(\alpha\beta)_8$ barrel active site [9]. By comparing TtPRODH crystal structure to that of PutA/THFA, it was discovered that helix 8 of the

distorted $(\alpha\beta)_8$ barrel, constitutes a flexible element of the structure: it protects the flavin cofactor in the active site from the solvent and moves in response to substrate binding and product release [10]. Further investigations on the flexibility of helix 8 may be relevant to elucidate the oxygen reactivity of some PO enzymes and in particular, it will be useful to explain how superoxide is generated and how molecular oxygen can access to the reduced flavin [9, 12, 13].

All the PO enzyme characterized displayed the typical absorption spectrum of flavooxidase with maxima at ~ 280 nm, 380 nm and 450 nm [Fig 5]. The flavin cofactor can be reduced by potentiometric tritation (e.g., TtPRODH [14]) or proline tritation (e.g., PutA [12, 16] and Put1p [17]), in the absence of O_2. During these experiments, no significant stabilization of semiquinone species are observed. The flavoenzymes that directly reacts with molecular oxygen during catalytic turnover typically form reversible sulfite adducts at the N-5 position of the isoalloxazine ring of FAD, which is observed as a variation of the flavin absorbance at 450 nm [18]. Accordingly, *Helicobacter* PutA (HpPutA) which shows a high reactivity with O_2, rapidly reacts with sodium sulfite (showing a decrease in the absorbance of the FAD cofactor at 450 nm); in contrast EcPUTA, having a poor O_2-reactivity, does not react with sulfite up to 50 mM concentration [16].

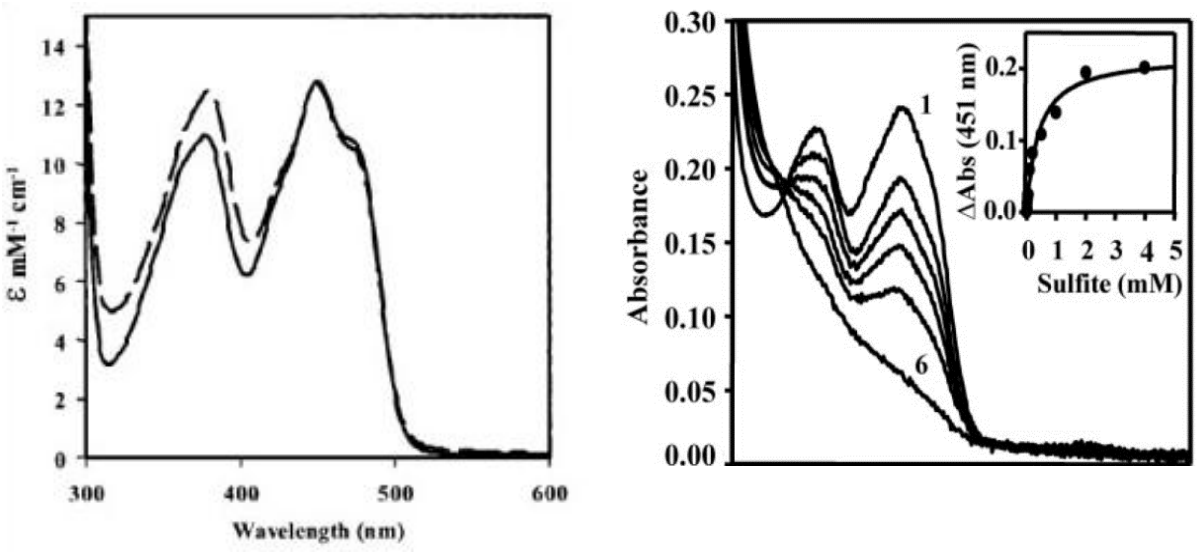

Fig. 5 –UV/Visible spectra of EcPutA (left); reaction of *Helicobacter* PutA with sulfite (right): curves 1 to 6 correspond to 0, 0.05, 0.1, 0.5, 1 and 4 mM sodium sulfite. Inset is a plot of the decrease in absorbance at 451 nm vs sulfite concentration [16, 19].

The catalytic mechanism of PO/PRODH activity can be divided into two reactions: reductive and oxidative half-reaction. In the reductive half-reaction, two electrons are transferred from proline to the flavin cofactor, whereas in the oxidative half-reaction, two electrons are transferred from the reduced flavin to an electron acceptor such as ubiquinone or molecular oxygen [12]. PutA shows a two-site ping-pong mechanism for the proline:ubiquinone reductase activity with a k_{cat} of 5.2 s^{-1} and a K_m of 42 mM and 112 µM for proline and CoQ_1, respectively. Because of sequence conservation in the PRODH active site among bacterial PutAs and eukaryotic PRODHs, it is conceivable that eukaryotic enzymes (such as human PO) will follow kinetic mechanism similar to that of *E. coli* PutA [12].

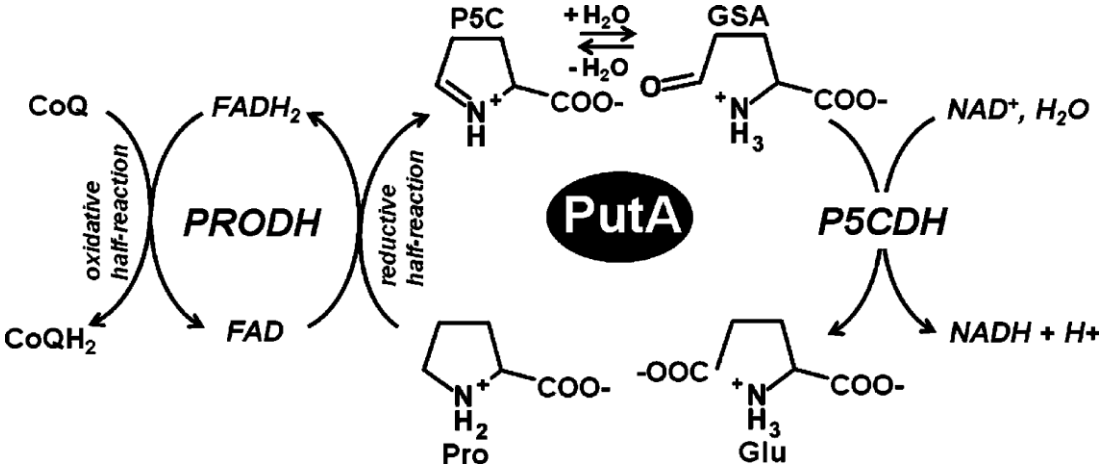

Fig. 6- Scheme of oxidation of proline to glutamate catalyzed by the PRODH and the P5C domain of PutA [20] .

Rapid reaction kinetic studies allowed the calculation of the microscopic reaction rates of the reaction catalyzed by PutA. A rate constant of 27.5 s^{-1} was determined for proline reaction during the reductive half reaction, while a rate constant of 5.4 s^{-1} was obtained for the oxidation of the flavin by CoQ_1. This indicates as this oxidative step is rate limiting in turnover.

The apparent kinetic parameters of different PO enzymes were calculated using the dichlorophenolindophenol (DCPIP) assay (DCPIP was used as final electron acceptor) or the o-aminobenzaldehyde (o-AB) assay, where the O_2 was the final electron acceptor. The ratio of the specific activity determined from the DCPIP assay vs the o-AB assay, indicates the preference of utilizing DCPIP over O_2 as the electron acceptor [Tab. 1] [14].

All prokaryotic and eukaryotic PRODH enzymes exhibited K_m values for proline in the mM range. Indeed, all PRODH (both prokaryotic and eukaryotic) show high K_m values for proline (27 -146 mM range) and similar k_{cat} values (8 -27 s^{-1}) [Tab. 1].

Table 1: [1] [14]; [2] [18].

Apparent kinetic parameters of PRODH from different sources on proline as substrate				
	TtPRODH[1]	***E.coli* PutA[1]**	***H. pylory* PutA[1]**	***S.cerevisiae* Put1p[2]**
e^- acceptor: DCPIP				
DCPIP assay				
K_m (mM)	27	100	146	36 ± 5
units/mg of protein	20.5	10	3.6	18
k_{cat} (s^{-1})	13	12	8	27
K_i for THFA (mM)	1	0.2	0.35	5.3
e^- acceptor: O_2				
o-AB assay				
K_m (mM)	1.3	-	150	50
units/mg of protein	0.335	< 0.002	0.230	-
k_{cat} (s^{-1})	0.2	< 0.005	0.5	0.013
DCPIP/O_2 activity ratio	61	>2500	16	-

The oxygen reactivity of *Helicobacter* PutA is about 100-fold faster than that of EcPUTA; it seems that for the *E. coli* the weak oxygen reactivity is necessary to protect the substrate-derived reducing equivalents until the flavoenzyme reacts with the physiological partner (e.g., ubiquinone). Moreover, the K_m values determined for HpPutA in the two assays are very similar. The different reactivity of reduced FAD with molecular oxygen may depend on the electrostatic environment of the active site, because of the formation of superoxide anion during the reaction [21]. Differences in charge distribution between EcPutA and HpPutA are not obvious by primary structure analysis alone. The only relevant difference is Tyr345 that is replaced by Asn291: this substitution could increase active-site accessibility in HpPutA [16].

The activity of PRODH on compounds similar to proline was also tested. The activity of yeast PRODH on trans-4-hydroxy-L-proline and L-pipecolic acid is very low (0.008 and 0.004 U/mg, respectively). In addition, the enzyme is strictly stereospecific since is does not show any activity on D-Pro. Trans-4-hydroxy-L-proline is neither inhibitor nor substrate for TtPRODH, while THFA is a competitive inhibitor for EcPutA and HpPuTA too [Tab. 1] [14, 16, 17].

1.1.2 *PRODH* genes and schizophrenia susceptibility

Human proline oxidase is encoded by *PRODH,* a gene spanning 23.8 kb with 15 exons and localized to 22q11.2 at 17.3 Mb [6]. The human genome contains two other genes with high sequence similarity to *PRODH.* The first is a nonfunctional pseudogene (*ΨPRODH*) that is the result of *PRODH* duplication. It is located 1.4 Mb telomeric on 22q and has > 95% sequence identity to *PRODH* but with a complex internal deletion [22]. Although *ΨPRODH* does not encode a functional protein, it appears to contribute to sequence variability in *PRODH* by acting as a

source of gene conversion events in which variations accumulated in *ΨPRODH* are transferred to *PRODH*. The second *PRODH*-related sequence is located on 19q and encodes hydroxyproline oxidase (OHPRODH), an enzyme that catalyzes the first step in hydroxyproline degradation and has very little activity towards proline [23].

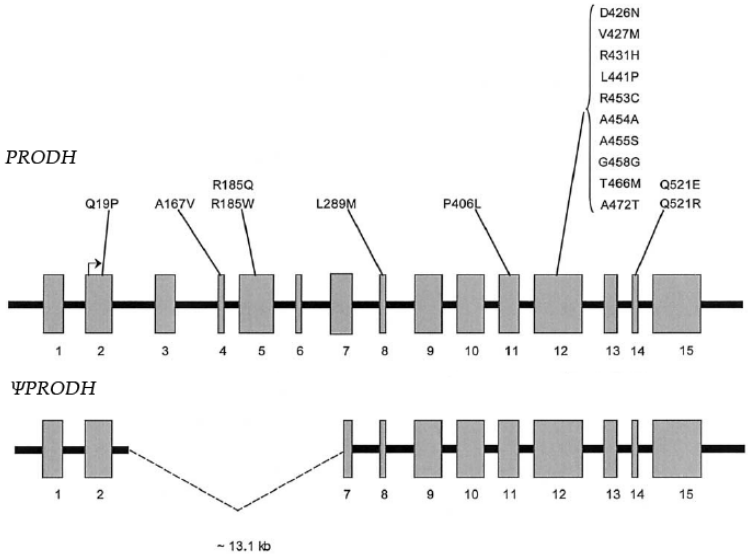

Fig.7 – Scheme of *PRODH* and *ΨPRODH* genes. Grey rectangles represent exons and the black heavy lines the intronic regions (not to scale). The missense mutations are indicated above the rectangles. The dashed lines in the lower panel indicate the deletion in *ΨPRODH* [6].

1.1.3 Proline metabolism and cancer

In 1997, Polyak et al. analyzed the trascriptome in order to identify the genes responding to p53. *PRODH* was one of the 14 genes identified because induced by p53 (more than seven-fold) [24]. Soon after, several laboratories independently demonstrated that over-expression of PO was responsible of proline-mediated apoptosis, suggesting a possible role of the flavoenzyme in apoptosis and proliferative disorders [25, 26].

Despite during the last decade cancer research gained important insights thanks to the advances in genomics which allowed the identification of oncogenes, suppressor genes and signaling networks, many aspects still need to be deeply investigated, especially concerning the fact that many cancer networks “accommodate” the bioenergetic requirements for survival or to supply the necessary building blocks for rapid proliferation. Important considerations concern also the differential metabolic requirements along the timeline of tumorigenesis and the metabolic adaptation of tumor cells to nutrient depletion that seems strongly related to the tumor

microenvironment [27]. After the discovery that *PRODH* is among a selected group of genes strongly induced by p53 a putative role of PO in tumor suppression was investigated.

The mechanism of PO pro-apoptotic effect is dependent on the generation of ROS, linking PO to the induction of mitochondrial apoptosis. Such a process involves the release of cytochrome c by mitochondria, the activation of the caspase cascade and culminates with the condensation of chromatin and formation of apoptotic bodies, thereby leading to cell death [28]. Proline oxidase can also lead to cell death by activating the extrinsic apoptotic pathway: the over-expression of this protein, in fact, leads to an increase of NFAT (Nuclear Factor of Activated T-cells), a transcription factor that allows the activation of the transcription of TRAIL (TNF-Related Apoptosis Inducing Ligand), which, upon binding to its receptor, activates the caspase cascade [29]. Nevertheless, PO was also described to play a role in induction of autophagy, as its overexpression is sufficient to induce cell protective autophagy in a colon cancer cell line [30].

Autophagy is a process known as 'self-eating', which plays a housekeeping role and degrades damaged or unwanted organelles. Autophagy also serves to control energy during stress conditions: beyond a threshold, this process may eventually lead to cell death [31]. Therefore, PO seems to act as a balance between survival and apoptosis, likely depending on the type and extent of stress that is inducing it.

In tumors cells, proliferation requires a nutrient supply for cell mass and the two main sources are glucose and glutamine. Although glutamine is known as the source of carbon skeletons and amino group from one tissue to another, it has been speculated that is the conversion of glutamate to P5C and subsequently to proline which provides the necessary regulation to optimize glucose utilization for cell proliferation. Accordingly glutamine and proline, together with arginine, constitute a metabolic system [5].

1.1.4 Diseases related to proline metabolism

Proline is one of the most abundant amino acids in higher organism, together with hydroxy-L-proline it constitutes over 25% of the amino acids in collagen [32]. As previously described, the cycling of proline and P5C between mitochondria and cytosol participates and activates the metabolism of glucose through the pentose phosphate pathways. In addition, proline can be a direct substrate for ATP production providing the transfer of reducing potentials to the mitochondrial respiratory chain; moreover its degradation can generate glutamate and α-ketoglutarate, which can play an anaplerotic role in the Krebs cycle [8, 33].

Inherited disorders of proline metabolism may entail severe effects on human health. They include hyperprolinemia type I, hyperprolinemia type II, ornithine aminotransferase (OAT)

deficiency, hydroxylprolinemia and P5C syntase deficiency [34]. Each of those conditions is caused by mutations or deletions in one of the genes encoding for enzymes involved in proline metabolic pathways [35].

In particular, impairments in proline degradative pathways cause hyperprolinemia [8]. Various studies have been performed in order to understand the biological function, the physiopathology, as well as the behavioral and neurochemical effects of hyperprolinemia, even in relation to diseases such as cancer and psychiatric disorders.

Hyperprolinemia type I (HPI) is an autosomal recessive condition characterized by the deficiency or the reduced activity of PO. Tissue accumulation of proline occurs in affected patients: the observed levels are 5- to 10-fold higher compared to physiological values. On the other hand, hyperprolinemia type II (HPI II) is a disorder related to deficiency in Δ^1 – pyrroline – 5 –carboxylic acid dehydrogenase activity. Also in this case the disease is biochemically characterized by the accumulation of proline and P5C in plasma, urine and cerebro spinal fluid (CSF) [33].

Typically HPI is a "diagnosis of exclusion": all cases of familial hyperprolinemia not due to a deficiency of P5C dehydrogenase are assumed to be HPI [8]. For this reason, causal relationships between proline oxidase deficiency in HPI and clinical outcome are difficult to prove.

HPI is a relatively benign condition in most individuals [8], but some observations raised the possibility that proline oxidase deficiency and proline accumulation could play a causative role in certain complex pathological phenotypes [8, 33, 34].

1.1.5 Proline as a neurotransmitter: physiological significance

The *PRODH* gene is widely expressed in brain and other tissues [35]: indeed P5C (derived from the oxidation of proline) can be converted in glutamate and GABA, two main neurotransmitters implicated in the physiology of schizophrenia and other mental illnesses [36, 37]. In addition, proline fulfills several of the classic criteria used to define well characterized amino acid neurotransmitters in the mammalian CNS such as: biosynthesis and uptake into synaptosomes, release after K^+ induced depolarization and regional distribution in the brain [8, 38, 39]. The role of proline as a putative synaptic regulatory molecule in excitatory synaptic transmission, is also supported by the presence of a brain high affinity L-proline transporter (Na^+/Cl^- - dependent proline transporter – PROT) which belongs to a large superfamily of plasma membrane neurotransmitter transporter proteins (the Na^+/Cl^- dependent GAT1 family of plasma membrane transporters including norepinephrine, dopamine, serotonin, GABA and glycine transporters), with which it exhibits 42-50% of amino acid sequence identity [40]. *In situ* hybridization revealed that PROT in the rat brain is mainly expressed by a subpopulation of

glutamatergic neurons belonging to the hippocampus and corticostriatal pathways [38, 41], and that its specific target localize into presynaptic terminals [40-42]. For all those reasons, proline could be considered as a component of the excitatory synaptic transmission system, functioning as a modulator of specific excitatory regulatory pathways within the CNS. In fact high affinity L-proline uptake may regulate the ability of extracellular proline to potentiate excitatory transmission at those synapses where its specific transporter is expressed [38]. Proline likely regulates the basal function of some glutamatatergic synapses by maintaining them in a partial potentiate state [38]; proline-induced potentiation requires the activation of NMDA receptors but is still not clear how exactly the mechanism is turned on/off [38].

1.1.5.1 Neurological impairments caused by L-proline

Experimental evidences show that altered proline level can be the principal cause of some neurological impairments: mice and flies (*D. melanogaster*) bearing a mutation in the gene encoding proline oxidase, exhibit high plasma proline levels and depressed locomotor activity [43, 44]. Intracerebral proline administration in chickens can cause retrograde amnesia and impairment in memory processes [45]; in an experimental model of developing rats affected by chronic hyperprolinemia, impairments of spatial memory in adults animals and degenerative changes in brain is observed [46].

In the brain glutamate is the major excitatory neurotransmitter. In physiological conditions it is essential for plastic processes which underlie memory and learning as well as developmental and environmental adaptation. In contrast, an excessive glutamate mediated excitation due to an abnormal high release of the neurotransmitter in the synaptic cleft, gives rise to prolonged stimulation of its receptors which leads to an enzymatic cascade in post-synaptic neurons ultimately resulting in cell death (excitotoxicity) [47]. Glial cells are responsible of the maintenance of glutamate concentration below neurotoxic level in the synaptic cleft, and this is achieved through the high affinity Na^+-dependent glutamate transporter named GLAST and GLT-1, expressed mainly in astrocytes [48].

On the other hand, the localization of proline transporter PROT in glutamate terminals suggested that proline might itself modulate excitatory transmission at certain excitatory synapses, although the mechanism of its action is actually poorly understood. Proline possesses excitotoxic properties: it has been demonstrated that millimolar concentrations of proline directly evoke NMDA receptor-mediated current or can reduce synaptic glutamate reuptake [40, 49]. Thus, high-affinity proline uptake may regulate the ability of extracellular proline to potentiate excitatory transmission at those neuronal pathways that express PROT [50]. Alternatively, high-affinity

proline uptake may achieve a novel metabolic function for proline as precursor of glutamate: it could be necessary to buffer the cytoplasmic glutamate level in certain specific excitatory nerve terminals [49]. Abnormal elevated proline concentration in CSF (such as those observed in hyperprolinemic patients) are likely responsible of the impaired cognitive function associated with the disease in which an hyperstimulation of glutamate transmission by proline may occur [8, 38]. Elevated proline concentration could also induce lipoperoxidation and reduce enzymatic and non-enzymatic antioxidant defenses in rat brain [51], suggesting that during proline oxidation the electrons from proline can reduce oxygen to yield superoxide [33, 52]. In this situation, high proline concentration might produce neurochemical effects arising from the imbalance between free radical production and antioxidant defense: it is possible that oxidative stress may in part contribute to the effects of proline on energy metabolism and excitotoxicity, both acting synergistically with the brain dysfunction observed in hyperprolinemia [50].

In hyperprolinemia, an increased in plasma proline concentration is accompanied by an equivalent increase in the (CSF) proline content [53]. Experimental evidences report that in a hyperprolinemic mouse model, elevated proline level in the CNS, are associated with neurocognitive dysfunction such as learning and memory deficits [44]; moreover, in a mouse model with heterozygous *PRODH* mutation associated with loss of PO activity, plasma proline level results abnormally high (two to tenfold with respect to the normal one), as observed in hyperprolinemia type I [44].

Existing data suggest that severe hyperprolinemia occurs in individuals with large deletions and/or *PRODH* missense mutations with the most severe effect on its catalytic activity, while modest hyperprolinemia is associated with *PRODH* alleles with a moderate reduction in activity [6, 53]. Hyperprolinemia has also been associated with schizophrenia, autism, epilepsy as well as neuronal disorders which include mental retardation and delays in psychomotor development.

Two main evidences support the hypothesis of functional involvement of hyperprolinemia in schizophrenia are: first, *PRODH* knockdown mice, miming the loss of PO activity, have elevated plasma and brain proline level, locally decreased glutamate and GABA levels in some brain regions and present deficits in sensimotor gating neurons (all features common to schizophrenia) [44]. Secondly, it was reported that 25-30% of patients with the 22q11 microdeletion met diagnostic criteria for schizophrenia or schizoaffective disorders [54]. In addition, it has been demonstrated that two heterozygous *PRODH* missense mutation (L441P and L289M), were associated with increased plasma proline level and were detected only in a group of schizophrenic patients but not in controls [34]. At least 16 *PRODH* missense mutations have been identified with moderate to severe effect on PO activity [54] and several lines of evidences indicate *PRODH* gene as a

candidate causative gene for schizophrenia [35, 44, 55]. To assess the genetic underpinnings of a disease, clinical genetic studies should provide information about the extent of genetic contributions to its development, linkage studies should identify and localize potential relevant risk genes in the genome and association studies should provide information about which particular gene variation modifies the risk for the disease. In particular, linkage analysis involves the search for polymorphic sequences within families that tend to be shared by affected family members but not by unaffected individuals. The selection of candidate genes arises from their known function (functional candidate) or from their chromosomal localization (positional candidates). Genetic epidemiological data collected from large scale family studies, together with twins and adoption studies, have consistently implicated genetic factors in the development of schizophrenia [56, 57]. In the last decade, it has been established that most promising susceptibility loci for schizophrenia were localized on chromosome 6q, 13q, 18 and 22q, where also the *PRODH* gene maps, and these regions were also implicated in maniac depressive illness or bipolar disorder [6, 33, 35, 55, 58].

Susceptibility gene for schizophrenia (as previously described) is likely to be located on 22q11 since there is an increased prevalence of cognitive deficits, similar to those observed in schizophrenia, among patients with 22q11 interstitial deletion [54]. Even though the heterozygous deletion of the *PRODH* gene in 22q11 in not sufficient *per se* to lead the development of hyperprolinemia, it may account for the hyperprolinemia observed in some Di George patients [35, 54, 55]. Notably the deletion within the Di George syndrome chromosomal region (DGRC) involves the entire *PRODH* locus, and it is also associated with hyperprolinemia in schizophrenic patients [4, 34].

Association between plasma proline level and schizophrenia revealed that schizophrenic patients had significantly higher plasma proline levels than controls ($p<0.0001$) and subjects with hyperprolinemia have six times greater odds of schizophrenia. Notably the association studies were developed excluding schizophrenic patients that were receiving mood stabilizers (due to the known influences that this kind of drugs have on plasma proline) to confirm the association between hyperprolinemia and schizophrenia [53]. The fact that proline oxidase encoding gene maps to a region of the genome where several genes supposed to confer increased susceptibility to schizophrenia localize, together with the evidence that proline may function as a neuromodulator, suggests that proline oxidase should be considered as a consistent candidate risk factor for schizophrenia.

1.2 Schizophrenia: a multifactorial psychiatric disorder

Schizophrenia is a widely diffused chronic and disabling brain disease of still unknown etiology and pathogenesis [59-61]. Because schizophrenia has neither unique causative factors nor biological markers, the diagnostic criteria are determined by the concomitant appearance of specific symptoms with a duration of at least 6 months [61]. Symptoms of schizophrenia are conventionally divided into “positive”, “negative” and “cognitive”; positive symptoms include delusions (fixed false beliefs that are impervious to rational refutation), hallucinations (realistic sensory perceptions that are not generated by stimuli outside of the subject experiencing them), “thought disorder” and bizarre behavior. Negative symptoms include emotional flattening, social withdraw, apathy, impaired judgment, difficulty in planning, impaired problem solving, abstract reasoning and decreased care for personal hygiene. Finally, cognitive symptoms consist of conceptual disorganization, disorientation and poor attention [60, 61].

Schizophrenia has about 1% population prevalence and occurs in all cultures. In general it is considered to be a complex disease with multiple factors that contribute to the pathogenesis: the most widely considered neurodevelopmental hypothesis of schizophrenia integrates environmental influences and causative genes and despite its clinical onset usually takes place in young adulthood, the neuronal abnormalities are hypothesized to evolve early during the first phases of brain development [60]. The disease can’t be simply defined by several major genes but is characterized by multiple genetic susceptibility elements that determine the genetic vulnerability of an individual [61]. Genetic factors and gene-environment interactions together contribute over 80% of the liability for developing schizophrenia: they need to be considered together since both neither appear to operate in isolation [58]. The phenotypic heterogeneity of the disease underlines the difficulties in a precise delineation of its genetic basis; it has been suggested that the “schizophrenia genes” are not accountable for schizophrenia *per se*, but also for the broader clinical outcome such as psychosis or neurocognitive deficits that occur also in other disorders [58]. A variety of specific environmental risk factors have been related to the etiology of schizophrenia: these include biological or psychosocial events from the antenatal periods (maternal infection and nutrition deficiency) to childhood, adolescence and early adulthood (trauma, head injury, parental separation or death, cannabis use) [62].

Nevertheless, which specific exposure and how they can influence the onset of neurochemical alteration, is still unknown [61].

1.2.1 Schizophrenia: neurochemicals alterations

A widely considered neurodevolpmental hypothesis of schizophrenia is the “dopamine hypothesis”, based on the evidences that positive or negative symptoms of schizophrenia may result from excessive dopaminergic neurotransmission in specific brain areas [61]. It was supported by two major clinical observations: first of all, schizophrenia-like symptoms always occur in amphetamine abusers especially due to the excessive dopamine release; secondly, it has been demonstrated how D_2 antagonists can be effective drugs in schizophrenia treatment [63]. In fact, among the most used antipsychotic drugs for schizophrenia treatments are antagonists or partial agonists of the dopamine D_2 receptor. Nonetheless, the schizophrenia neurochemical model based upon dopamine, accounts poorly for negative and neurocognitive dysfunction and the mechanisms underlying the differential cortical and subcortical dopaminergic abnormalities, remain to be defined [59].

An alternative to the “dopamine hypothesis” was first proposed based upon the observation that phencyclidine, ketamine and other psychotomimetic compounds achieve their effects by blocking neurotransmission at N-methyl-D-aspartate (NMDA) glutamate receptors [59, 62]. Subsequently, another indication of an impaired glutamatergic system in schizophrenia was provided by the observation of reduced glutamate level in cerebro spinal fluid of patients affected by the disease [63, 64]. Thus, recognizing that there has to be more to the onset of schizophrenia than simply dopamine hyperactivity, it was proposed a “glutamatergic hypothesis”, in which the pathology is suggested to be related to a deficient glutamate-mediated excitatory neurotransmission [65, 66].

Glutamate is responsible of the excitation of neurons and glia through the activation of various glutamate receptors. NMDA Receptors are among the most important synaptic receptors in the CNS: broadly distributed throughout the brain, they play a major role in glutamatergic synaptic transmission and participate in synaptic events associated with outstanding physiological processes. NMDA Receptors have been found at both synaptic and extrasynaptic sites, but are present at much higher density at the synapsis [67]. They are organized as heteromeric complexes of different subunits (NR1, NR2a, NR2b, NR3), composed of spliced variants of NR1 subunit combined with at least one of four NR2 subunits. A third subunit, NR3, which is less common, can co-assemble with NR1/NR2 complex. The NMDA receptors are unique in their requirement for more than one agonist to operate: the receptor channel is blocked by Mg^{2+}, depolarization removes this block and enables ion flux when the receptor binds both glutamate (on NR2 subunit) and a co-agonist (on NR1 subunit) [Fig. 8] [68-70]. This regulation of NMDAR activity by a second agonist may be regarded as a safety mechanism to protect against the deleterious effects of overstimulation of the NMDAR (excitotoxicity) [71]. Co-agonist binding increases the receptor's

affinity for glutamate, decreases its desensitization and promotes NMDAR turnover by internalization. The influx of Ca^{2+} through ionotropic glutamate receptors stimulates intraneuronal signal transduction cascades that determine cellular plasticity and cell death. Depending on which signals transduction pathways are activated, the proteins synthesized are involved in the construction of new synapses and reinforcement of existing synapses, or the controlled disassembly of the neurons in a cell death program. This findings indicate that glutamate has a critical role in neuroplasticity, neurotoxicity and neurodevelopment, it is thus suggested that disregulation of those neuronal processes are implicated in the pathology of schizophrenia [65].

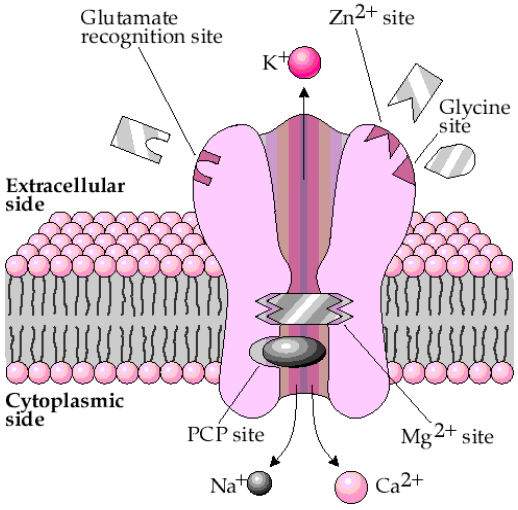

Fig.8 - Model of the NMDA receptor. It is organized as heteromeric complexes of different subunits; the channel pore is formed by three transmembrane domains and a hairpin bend within the membrane. The integral ion channel is blocked by magnesium in a voltage-dependent manner; depolarization of the neuron (for example, by the action of glutamate on other classes of ion channels) removes this block. Binding of both glutamate and the co-agonist (e.g., glycine or D-serine) results in the opening of the channel, allowing calcium to enter.

Neuroplasticity refers to the ability of neurons to adapt to changes in the environment and is crucial for neurons survival and important brain functions concerning learning and memory. Indeed, schizophrenia is thought to be a neurodevolpmental disorder, with defective connectivity, decreased synaptic density and reduction in the density of spines. Notably glutamate transmission is critically involved in neuronal development thanks to the ability of neurons to synthesize and release adequate amount of glutamate to determine the formation of a sufficient number of synapses. Presynaptic neurons that cannot provide enough glutamate may prevent the formation of a postsynaptic site, which decrease the likelihood of synapse formation [72]. The initial fate of a

synapses is thus determined by presynaptic glutamate release: reduced levels of glutamate or reduced activity of NMDA receptors impact the number of synapses established.

Moreover, throughout life glutamate controls synapses morphology and influences its strength, to proper carry out cognitive function; the cognitive deficit observed in schizophrenic patients may be caused, in some extent to impairment in the glutamate system [68].

Finally, excessive stimulation of glutamate receptors can compromise neuronal viability by limiting structural and functional integrity: this process is known as "excitotoxicity". Under extreme conditions, excessive activation of NMDAR can cause unexpected Na^+ and Cl^- influx which can cause cell brake for osmotic pressure. Moreover irreversible intracellular Ca^{2+} elevation cause mitochondrial damage, build up of reactive oxygen species (ROS) and apoptotic cell death [73]. Interestingly, also a decrease in the activity of NMDA receptors (as suspected in schizophrenia) can cause excitotoxicity: the attenuated inhibitory tone of GABA neurons on glutamate neurons, leads to an increase activity of postsynaptic glutamate neurons, excessive glutamate release and finally neurotoxicity [65, Fig. 9].

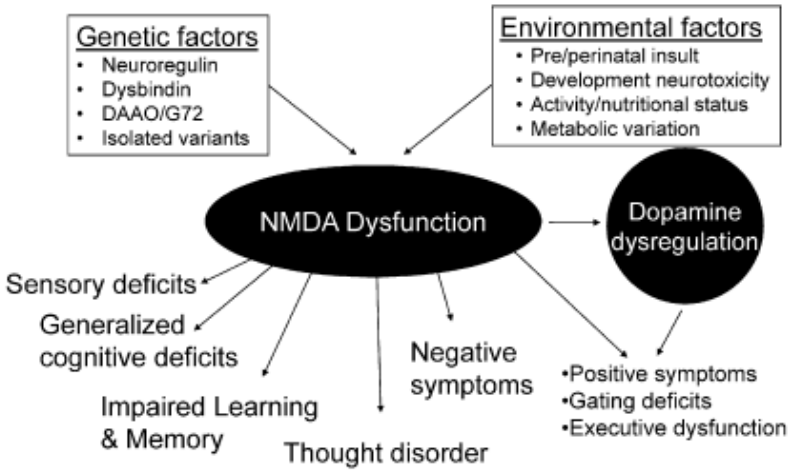

Fig. 9 - Summary plot of the proposed role of NMDAR in pathophysiology of schizophrenia. In this model, NMDAR dysfunction or dysregulation reflects final common pathways leading to the complex pattern of symptoms and cognitive deficits seen in schizophrenia, with multiple potential causes of NDMAR dysfunction, including both genetic and environmental contributions [74].

To summarize, the dopamine hypothesis is like the tip of the iceberg, and could not fully describe what is beneath. The glutamatergic hypothesis and the NMDA hypo-function looks deeper and suggest that probably disregulated NMDA receptors, often upstream dopaminergic neuronal circuits, are the actual cause of the dopamine hypothesis. Hence, NMDA receptor may be the key in their own hypothesis, but more globally, if any genetic mutation impact on a protein functionality along glutamatergic pathways [Fig. 10], it consequently results in alteration along various neuronal circuits and in the production of the same effects as inheriting hypofunctioning NMDA alone [74].

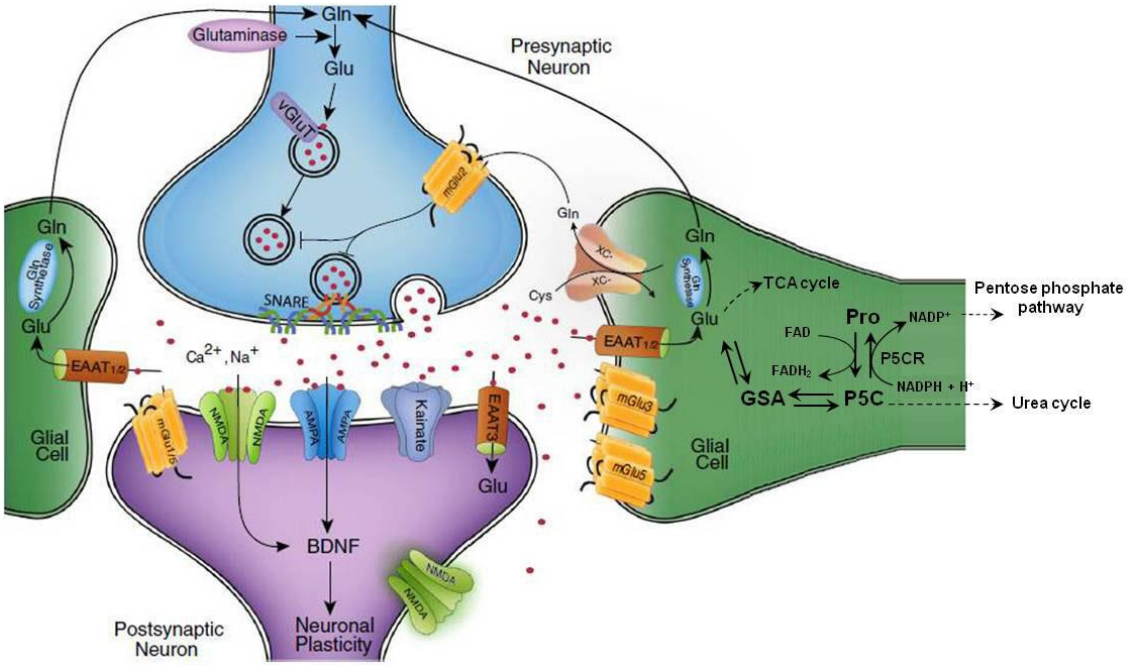

Fig. 10 - Schematic reaction involved in glutamatergic neurotransmission. Glutamine (Gln) is converted to glutamate (Glu) by glutaminase though glutamate may also be derived from the TCA cycle and from precursor linked with the "proline cycle". Glu is packaged into presynaptic vesicles by vesicular Glu transporter (VGLUT) proteins and synaptically released in a voltage-dependent manner through vesicular interactions with SNARE proteins. Synaptically-released Glu is recycled from the extracellular space by excitatory amino acid transporters (EAATs) expressed predominantly on astroglia. In astrocytes, Glu is converted to Gln by Gln synthetase and exported extracellularly to be taken up again by neurons. Additionally, system x-C is a cystine/glutamate antiporter expressed on glia that also contributes to Glu recycling [adapted from 75].

1.2.2 Schizophrenia: role of glial amino acid transporter

The glutamate hypothesis of schizophrenia postulates an hypofunction of NMDA receptors at critical sites in local brain circuits [59]. In the last years, also the glial glutamate and aspartate transporter (GLAST) have been associated with schizophrenia [76-78]. Five plasma membrane glutamate transporter subtypes, called excitatory amino acid transporter (EAAT), have been identified so far: 1) GLAST (EAAT1) is an astroglial transporter and the principal transporter present during CNS development [79]; 2) GLT-1 (EAAT2) is an astroglial transporter expressed postnatally and is responsible for up to 90% of all glutamate transport in adult tissue [80]; 3) EAAC1 (EAAT3), is a neuronal glutamate transporter with high density on postsynaptic membranes [81, 82]; 4) EAAT4 is a glutamate transporter largely limited to the Purkinje cells of the cerebellum [83] and 5) EAAT5 is found primarily in the retina on photoreceptors and bipolar cells [84].

Glutamate transport dysfunction may be caused by different events: abnormalities in glutamate transporter expression (as result of altered transcription or splicing) increased turnover of the transporter, altered trafficking of glutamate transporters, abnormal phosphorylation or cleavage of the protein and reduced transport capacity. The EAATs are usually compartementalized to selected regions of neuronal and astroglial membranes and are activated by interacting proteins (glutamate transporter associated protein, GTRAP) which can regulate their cellular and membrane trafficking by anchoring glutamate transporter to cytoskeletal protein. One potential mechanism by which glutamate transporter may be damaged is the redox modulation of reactive amino acids: oxidation of certain intracellular amino acidic residues of GLT-1 by oxygen free radicals could alter functional transport of glutamate and elicit an increasing concentration of glutamate in the synaptic cleft, further hyperactivation of glutamate receptors and a typical signalling cascade of glutamate neurotoxicity [85]. Finally, another possible mechanism for glutamate transporter protein dysfunction involves ATP depletion: in fact, a depletion of ATP reserves may result in reversal of Na^+-dependent transporter and diffusion of glutamate into the extracellular space, exacerbating accumulation of extracellular glutamate [85].

2 Aim of the work

The intracellular synthesis and degradation of L-proline occurs through a distinct set of enzymes with unique properties and regulatory mechanisms. Interestingly, proline metabolic enzymes constitute a "proline cycle" which represents an important crossroad with other metabolic pathways, involving interconversion of proline with glutamate and ornithine. Proline oxidase (PO) is a mitochondrial flavoenzyme that catalyzes the first step of proline degradation; the mitochondrial localization of PO suggests that oxidation of proline may play an important role in redox transfer between cellular compartments. Although the biosynthetic pathways of proline have been investigated in details, the role of proline oxidation in the cell remains largely unknown.

This PhD project is aimed at characterizing the human PO from a biochemical and cellular point of view. In fact, despite the intriguing role of this protein in different human diseases, a correlation between genotype and phenotype of PO is still lacking mainly because the structural and functional characterization of the human protein has not yet been carried out. For this reason, the first part of the project, focused on the expression and biochemical characterization of the recombinant human PO in *E. coli.* The cDNA coding the full length human PO (600 amino acid) was designed by *in silico* back translation and was optimized for the expression in *E. coli.* Despite different growth conditions were attempted, a very low amount of recombinant full length PO was produced (< 0.1 mg/L of fermentation broth). *In silico* analyses allowed to design 7 different PO deletion variants: all variants encompassed the catalytic domain (identified by alignment of the human sequence with that of monofunctional bacterial PO) and differed for upstream or downstream sequences. Moreover, regions with high propensity to structural disorder (that may prevent the expression of a soluble protein in *E. coli*) were also identified using RONN bioinformatic server.

Interestingly, in the *PRODH* gene, encoding for PO, has accumulated several recognized mutations that occur at polymorphic frequency (> 0.01) with mild to severe effect on PO activity; in particular, we focused on the L441P substitution, as it is reported to yield to an inactive form of the enzyme.

The *PRODH* gene, is considered a positional candidate gene for schizophrenia and several lines of evidences supports the hypothesis that proline may act as a neuromodulator, especially at glutamatergic synapses. For this reason, the second part of the project, we focused on the effect

of the over-expression of PO on the cellular and extracellular levels of selected molecules, in the human cellular model of U87 glioblastoma cell line. The cells were stably transfected in order to obtain the expression of the wild-type and the L441P inactive variant of the enzyme; the two PO variants were also expressed as chimeric proteins with the enhanced yellow fluorescent protein (EYFP), in order to verify the subcellular localization of the over-expressed PO. Since it has been reported that reduced activity of PO is responsible of hyperprolinemia type I and that hyperprolinemic patients have significantly higher chance (6-fold) to be associated with schizophrenia than healthy individuals, functional differences between cells stably transfected with the wild-type or the L441P variant were investigated. In particular we investigated the proline and glutamate levels in U87 cells by HPLC analysis. Noteworthy proline is not only a metabolic precursor of glutamate, but itself fulfills several criteria to define a neuromodulator, such as the presence of a Na^+/Cl^--dependent proline transporter (PROT) mainly expressed into presynaptic terminals. Differences in the expression of two main glutamate transporter GLT-1 and GLAST, were thus investigated.

The final aim is to formulate the potential mechanism exerted by PO, in physiological glutamate metabolism as well as in pathological conditions. Understanding the complex biochemical network linking proline to glutamate and its potential role in the onset of schizophrenia, will pave the way to the design of new drugs that modulating PO activity should be used as new therapeutic target for schizophrenia treatment.

3 Results

Protein Expression and Purification 82 (2012) 345–351

Contents lists available at SciVerse ScienceDirect

Protein Expression and Purification

journal homepage: www.elsevier.com/locate/yprep

Expression in *Escherichia coli* of the catalytic domain of human proline oxidase

Elena Tallarita [a,b,c], Loredano Pollegioni [a,b], Stefano Servi [b,c], Gianluca Molla [a,b,*]

[a] Dipartimento di Biotecnologie e Scienze della Vita, Università degli Studi dell'Insubria, Varese, Italy
[b] The Protein Factory, Centro Interuniversitario di Biotecnologie Proteiche, Politecnico di Milano, ICRM-CNR and Università degli Studi dell'Insubria, Varese, Italy
[c] Dipartimento di Chimica dei Materiali e Ingegneria Chimica G. Natta, Politecnico di Milano, Milano, Italy

ARTICLE INFO

Article history:
Received 30 December 2011
and in revised form 25 January 2012
Available online 8 February 2012

Keywords:
L-Proline
Schizophrenia
Amino acid oxidase
Amino acid metabolism
Neurotransmitter

ABSTRACT

The human *PRODH* gene has been shown to have unique roles in regulating cell survival and apoptotic pathways and it has been related to velocardiofacial syndrome/DiGeorge syndrome and increased susceptibility to schizophrenia. It encodes for the flavoprotein proline oxidase (PO), which catalyzes the conversion of L-proline to Δ^1-pyrroline-5-carboxylate. Despite the important physiological and medical interest in human PO, up to now only microbial homologues of PO have been expressed as recombinant protein and fully characterized. By using a bioinformatics analysis aimed at identifying the catalytic domain and the regions with a high intrinsic propensity to structural disorder, we designed deletion variants of human PO that were successfully expressed in *Escherichia coli* as soluble proteins in fairly high amounts (up to 10 mg/L of fermentation broth). The His-tagged PO-barrelN protein was isolated as an active (the specific activity is 0.032 U/mg protein), dimeric holoenzyme showing the typical spectral properties of FAD-containing flavoprotein oxidases. These results pave the way for elucidating structure–function relationships of this human flavoenzyme and clarifying the effect of the reported polymorphisms associated with disease states.

Introduction

Schizophrenia is a severe psychiatric disorder, affecting about 1% of the population worldwide. Several factors are correlated to an increased susceptibility to schizophrenia (e.g., infections, birth complications, and drug abuse), but an individual's genetic profile constitutes the major risk factor, as demonstrated by a heritability of schizophrenia of up to 50% in monozygotic twins. In past years, several genes, mainly related to glutamatergic neurotransmission, have been associated with an increased susceptibility to this condition [1–3]. Among them we focused our attention on the product of *PRODH*, a gene located in 22q11 near the centromeric end of the region typically deleted in the velocardiofacial syndrome/DiGeorge syndrome (VCFS/DGS)[1]. Interestingly, VCFS/DGS patients show an increased susceptibility to schizophrenia (SZ) [4]. *PRODH* encodes for proline oxidase (PO, EC 1.5.99.8), an enzyme expressed in kidney, liver, and brain and that is localized on the inner mitochondrial membrane [5,6]. PO catalyzes the oxidation of L-proline (L-Pro) to Δ^1-pyrroline-5-carboxylate (P5C), a key metabolite that has several destinations: (1) nonenzymatic hydrolysis to glutamic semialdehyde, that can be further oxidized to glutamate by P5C dehydrogenase (P5CDH, EC 1.5.1.12); (2) conversion to ornithine that enters the urea cycle; (3) transport to the cytosol, where it is reduced to L-Pro in a cycle that transfers reducing equivalents from mitochondria to cytosol and that represents an interlock with the pentose phosphate pathway [7,8]. A peculiar aspect of enzymes involved in proline catabolism is that PO and P5CDH comprise separate proteins in eukaryotes and archaea while the two enzymes are fused in prokaryotes (e.g., the proline utilization A, PutA protein, in *Escherichia coli*) [6,9]. Moreover, the membrane localization of PO (both in eukaryotes and bacteria) suggests that electrons originating from L-Pro oxidation could be transferred to an acceptor of the membrane electron transport chain.

In the brain, L-Pro is a precursor of the neurotransmitter glutamate and is itself an inhibitory neurotransmitter, at least in subpopulations of glutamatergic neurons [2,8,10]. Indeed, *PRODH* is a "hot-spot" for mutations [8]. At least 16 *PRODH* missense mutations have been identified in individuals suffering from hyperprolinemia type I [11] or schizophrenia [11–13]; five of the identified polymorphisms result in a severe (>70%) reduction in PO activity when expressing the PO variants in CHO-K1-C9 cells [14]. Furthermore, human PO expression is upregulated by the tumor suppressor p53 protein, inducing cell death pathways and helping to prevent cancer progression [15]. The validation of the proposed correlation between *PRODH*, glutamatergic neurotransmission, and schizophrenia

* Corresponding author at: Dipartimento di Biotecnologie e Scienze della Vita, Università degli Studi dell'Insubria, Varese, Italy. Fax: +39 0332 421500.
E-mail address: gianluca.molla@uninsubria.it (G. Molla).

[1] *Abbreviations used:* DCPIP, dichlorophenolindophenol; IPTG, isopropyl β-D-1-thiogalactopyranoside; PO, proline oxidase (EC 1.5.99.8); L-Pro, L-proline; P5C, Δ^1-pyrroline-5-carboxylate; P5CDH, P5C dehydrogenase (EC 1.5.1.12); PutA, proline utilization A; SZ, schizophrenia; THFA, L-tetra-hydro-2-furoic acid; VCFS/DGS, velocardiofacial syndrome/DiGeorge syndrome.

1046-5928/$ - see front matter © 2012 Elsevier Inc. All rights reserved.
doi:10.1016/j.pep.2012.01.021

(which is still being debated, see [2,13]) requires that the effect of the reported mutations in the *PRODH* gene on the enzyme activity and the *in vivo* levels of L-Pro be investigated at the molecular level. For such studies, it is mandatory to overexpress the human enzyme in a heterologous system. Up to now, except for one preliminary report on the expression of human PO in *E. coli* [16] – that does not give details on the production level and protein quality – the only eukaryotic PO expressed as recombinant protein and fully characterized was the one from *Saccharomyces cerevisiae* [17]. On the other hand, bacterial homologues have been successfully expressed in *E. coli*: bacterial POs are FAD-dependent enzymes with a $(\alpha\beta)_8$ barrel catalytic core [9].

Here we report on the design, expression, purification, and basic characterization of a human PO deletion variant possessing proline oxidation activity.

Materials and methods

Design, synthesis, and cloning of cDNA coding for human PO

The synthetic cDNA coding for the full-length PO was designed by *in silico* back translation of the amino acid sequence reported in the data bank (GenBank accession code NM_016355) [14]. Codon optimization for expression in *E. coli* was performed according to the Codon Usage Database (http://www.kazusa.or.jp/codon/) by eliminating rare codons (i.e., codons used with a <10% frequency for coding a given amino acid). Synthetic cDNA was produced by GENEART (Germany). See Fig. 1A. Deletion mutants of synthetic PO cDNA were produced by mutagenic PCR using the primers reported in Suppl. Table 1.

The cDNA molecules coding for full-length PO and for the deletion variants were cloned into pET24b (Novagen, USA) or pT7.7 [18] expression vectors, thus yielding C-terminal or N-terminal His-tagged proteins, respectively.

Growth conditions, enzyme expression, and purification

For protein expression, plasmids containing the PO cDNA were transferred into *E. coli* BL21(DE3)pLysS host cells (Novagen, USA) [19,20]. Starter cultures were prepared from a single colony of *E. coli* cells carrying the recombinant plasmid in LB medium (Luria–Bertani broth: 10 g/L bacto-tryptone, 5 g/L yeast extract, and 5 g/L NaCl), to which the appropriate antibiotic was added (kanamicin, 30 μg/mL final concentration for pET24b, or ampicillin, 100 μg/mL final concentration for pT7.7, and chloramphenicol, 34 μg/mL final concentration), and then grown under vigorous shaking at 37 °C. For protein purification trials 2 L baffled flasks containing 500 mL of LB medium were inoculated with the starter culture (initial $OD_{600\ nm}$ = 0.2) and cells were grown at 37 °C under shaking (180 rpm) until $OD_{600\ nm}$ = 0.8 was reached. Protein expression was induced by adding 1 mM isopropyl β-D-1-thiogalactopyranoside (IPTG). To promote the expression of the holoprotein form of recombinant PO, 1 μM FAD was also added. Cells were harvested by centrifugation (at 8000*g* for 10 min, at 4 °C) 3 h after adding IPTG. Cells were stored at −20 °C.

Cells were lysed by sonication (5 cycles of 30 s each, with 30-s intervals) on ice in 50 mM TrisHCl pH 8.0, 40 μM FAD, 0.5 mM phenylmethylsulfonyl fluoride, 1 mM 2-mercaptoethanol, and 10 μg/mL deoxyribonuclease I. Cell lysates were centrifuged at 39,000*g* for 1 h at 4 °C; the insoluble fraction contained the inclusion bodies [19,20]. The crude extract was loaded on a HiTrap Chelating column (GE Healthcare, USA) preloaded with Ni^{2+} and equilibrated in 50 mM sodium pyrophosphate, pH 7.2, 1 M NaCl, 10 μM FAD, and 5% glycerol. The bound protein was then eluted from the column using 20 mM sodium pyrophosphate, pH 7.2, 0.5 M imidazole, 10 μM FAD, and 5% glycerol [19,20]. The pure protein was then transferred into the storage buffer (20 mM Tris–HCl, pH 8.0, and 10% glycerol) by chromatography on a PD10 desalting column (GE Healthcare, USA).

SDS–PAGE electrophoresis and Western blot analysis

Protein samples from expression trials were analyzed by SDS–PAGE; gels were stained for proteins with Coomassie Blue R-250. For Western blot analysis, proteins were transferred onto an Immobilon-P transfer membrane (Millipore, USA) and recombinant PO was identified using anti-His-tag mouse monoclonal antibodies (His-probe) and goat anti-mouse IgG HRP-conjugated antibodies or anti-PRODH goat polyclonal antibody (all from Santa Cruz Biotechnology, USA) and donkey anti-goat IgG HRP-conjugated antibodies (Jackson ImmunoResearch, USA). The immunorecognition was detected using the ECL Plus Western Blotting Detection System (GE Healthcare, USA).

Enzyme assay and spectral measurements

Absorbance spectra in the UV/Vis regions were recorded using a JASCO V-560 spectrophotometer; fluorescence measurements were performed using a Jasco FP-750 spectrophotometer. See [19,21,22] for details.

The PO activity assay was conducted at 25 °C as previously described [17,23]. Briefly, L-Pro:dichlorophenolindophenol (DCPIP) oxidoreductase activity assay was performed in 1 mL reaction volume: changes in absorbance were recorded at 595 nm (ε = 16,100 M^{-1} cm^{-1}). The reaction mixture contained 2 μM PO, 0.25 mM phenazine methosulfate, 50.4 μM DCPIP, 10 mM $MgCl_2$, 10% glycerol and 50–500 mM of L-Pro in 10 mM MOPS, pH 7.5 [17]. One unit of PO is defined as that amount of enzyme which transfers electrons from 1 μmol of L-Pro to DCPIP in 1 min at 25 °C. The inhibition studies were carried out using the same assay and by adding increasing concentrations of L-tetra-hydro-2-furoic acid (THFA), or L-lactate or L-pipecolate to the L-Pro:DCPIP assay mixture.

Results

Design of PO variants for E. coli expression

The nucleotide sequence of the cDNA coding for full-length human PO (600 amino acids) was designed by *in silico* back translation of the amino acid sequence (GenBank accession code NM_016335) [14]. The optimized full-length human PO cDNA (Fig. 1A) was subcloned into the pET24b expression vector (between the *Nde*I-*Xho*I restriction sites), thus adding a sequence coding for a 6xHis-tag at the C-terminal end of PO. Using the pET24 vector, BL21(DE3)pLysS *E. coli* host cells, and the conditions reported in [16], a very low amount of recombinant PO was produced (<0.1 mg/L of fermentation broth). The deletion of the N-terminal mitochondrial targeting sequence (residues 1–48) [24] did not increase the amount of expressed protein either (not shown).

Since human PO is localized on the inner mitochondrial membrane, it could possess regions that negatively affect the expression of a soluble recombinant PO form in *E. coli*. The putative catalytic domain of human PO was identified by aligning its sequence and the *E. coli* PutA and *Thermus thermophilus* monofunctional PO proteins (Fig. 1B) [9,25]: all fundamental, active site residues of *E. coli* PutA are conserved in the human protein (Fig. 1B, arrows). Then, a model of the three-dimensional structure of the catalytic domain of human PO was built using an I-Tasser server [26] and based on the structure of domain III of *E. coli* PutA as template (PDB code: 1k87) [9]. Compared to the *E. coli* enzyme, all of the secondary

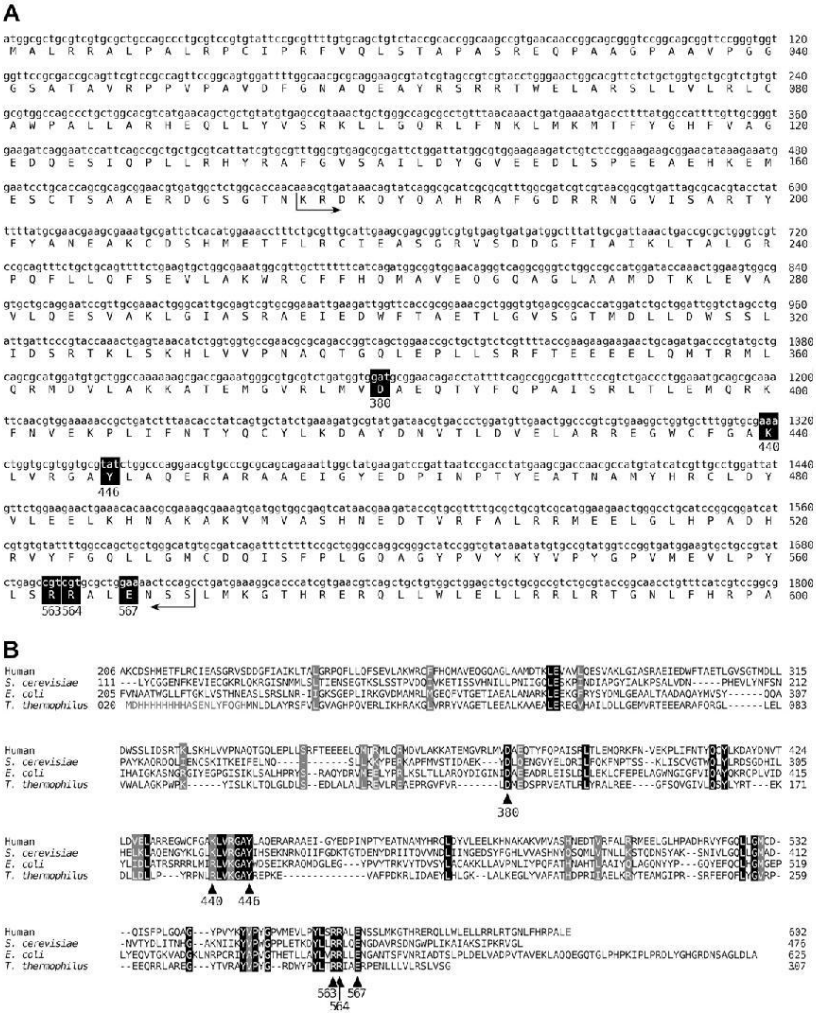

Fig. 1. (A) Nucleic acid and corresponding amino acid sequence of the optimized human PO gene expressed in this study. The protein sequence of full-length PO corresponds to the wild-type sequence of PO as in [14], with the only Q521R substitution. Arrows show the region of the gene corresponding to the PO-barrelN-His variant; boxes indicate proposed active site residues. (B) Multiple alignment of the amino acid sequences of significant POs from different sources; only regions corresponding to domain 2 and 3 (see Fig. 2) are shown. Multiple alignment was carried out by Clustal X [37]. Black boxes: conserved residues; grey boxes: similar residues. Arrows: proposed active site residues.

structure elements of the $(\alpha\beta)_8$-barrel were correctly placed in the human PO model (Fig. 2A and B), including the additional α-helix 5a and the α-helix 8 (according to the PutA numbering) [9]. This latter helix hosts three important active site residues (Arg563, Arg564, and Glu567, Fig. 2B).

Protein regions with a high intrinsic propensity to structural disorder may affect the solubility of the recombinant protein: accordingly, these regions were identified in PO using the RONN server [27] (see pink regions in Fig. 2A). Based on these analyses, 7 different PO deletion variants were designed and produced (Fig. 2A and Table 1). All deletion variants encompass a core region corresponding to the entire predicted αβ-barrel (containing the catalytic site) and differ for the presence of additional upstream and/or downstream sequences.

Expression and characterization of PO deletion variants

All PO deletion variants were produced by mutagenic PCR and subcloned into the pET24b (thus introducing a C-terminal His-tag) or the pT7.7 (thus introducing an N-terminal His-tag) expression vectors, using a subcloning strategy similar to the one employed for full-length PO. His-PO-dom2-barrel (residues

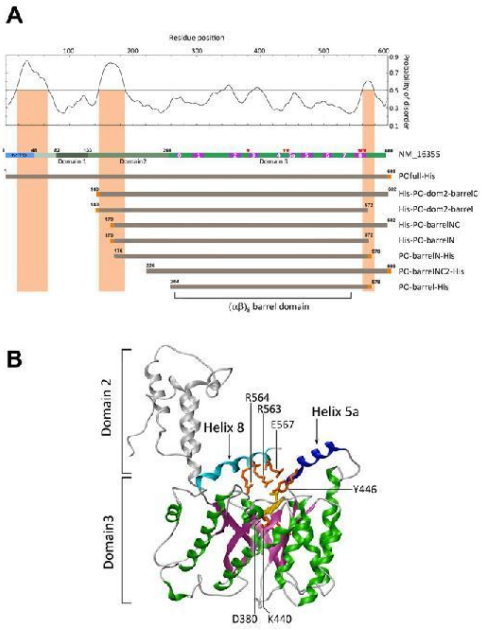

Fig. 2. (A) Scheme of the deletion variants of human PO designed in this work. (Top) Plot of the RONN analysis of human PO. (Bottom) Scheme of full-length and deletion variants of human PO. Regions with high propensity to structural disorder are shown in pink. α-Helices of the $(\alpha\beta)_8$-barrel domain, helix 5a and helix 8 are shown in purple. Orange boxes: His-tag. Red symbols indicate conserved catalytic residues (as shown in panel B). (B) Model of the three-dimensional structure of PO-barrelN-His variant. The $(\alpha\beta)_8$-barrel region of the protein (catalytic domain, domain 3) is represented in green and mauve; α-helix 5a is in blue and α-helix 8 in cyan. Helices are named according to the *E. coli* PutA numbering. Conserved residues proposed to be important for catalysis are indicated (orange). FAD cofactor (yellow) was modeled into the active site based on the structure of *E. coli* PutA [9].

140–572) was the only PO variant whose expression was never detected by Western blot using antibodies against His-tag or human PO. On the other side, the highest expression yield was obtained for the PO-barrelNC2-His variant (residues 226–608) growing BL21(DE3)pLysS *E. coli* recombinant cells in LB broth at 37 °C after adding 1 mM IPTG (up to 100 mg of recombinant PO/liter). Anyway, the His-PO-barrelNC and PO-barrelNC2-His were expressed almost exclusively in the insoluble fraction of the cell lysate (i.e., as inclusion bodies, Table 1). A decrease in IPTG concentration (up to 0.1 mM final) or in the growth temperature (up to 18 °C) did not increase the solubility of the recombinant protein (not shown). Solubilization of inclusion bodies and refolding of PO-barrelNC2-His variant using different refolding strategies [28], did not isolate soluble and active PO.

All the further PO variants reported in Fig. 2A were partially expressed as soluble proteins (Fig. 3A) and purified by chelating chromatography. Only for His-PO-barrelN (residues 170–572) and PO-barrelN-His (residues 176–578) was the final enzyme preparation yellow and active (even in the absence of exogenous FAD in the assay mixture). About 1.2 mg of His-PO-barrelN/L of fermentation broth and 5–10 mg of PO-barrelN-His/L of fermentation broth (corresponding to 1.2 mg/g cell paste) were purified, with a purity >90% (estimated by SDS–PAGE, Fig. 3B and C, lane 6). These PO variants differ each other only for the location of the His-tag and distinguish from the other designed PO variants because encompass the entire αβ catalytic domain and only partially extend into the putative disordered regions (see Fig. 2A).

Characterization of the PO-barrelN-His variant

Size exclusion chromatography of the purified PO-barrelN-His variant (at 3 mg/mL protein concentration) resulted in a yellow, single peak with a retention volume corresponding to a molecular mass of 94.9 ± 7.6 kDa. Since the theoretical mass of the monomer is 46,276 Da, PO-barrelN-His is a holodimer in solution under native conditions.

The purified PO-barrelN-His variant (as well as the His-PO-barrelN, not shown) possesses the classical absorbance spectrum of FAD-containing flavoproteins with two absorbance maxima in the visible region at 455 and 380 nm (Fig. 4). A molar extinction coefficient at 455 nm of 11.0 $mM^{-1}\,cm^{-1}$ and a ratio of 10.3 between the absorbance values at 280 and 455 nm were calculated. The FAD cofactor is noncovalently bound to the apoprotein moiety since it is released by heat treatment of the holoenzyme. In the holoenzyme form, the fluorescence of flavin cofactor is largely quenched by the protein moiety (∼78% as compared to the value for free FAD, not shown). The far-UV circular dichroism spectrum of the PO-barrelN-His variant was analyzed by means of K2D2 web server [29]: the protein's secondary structure content was estimated as 40.9% α-helices and 9.9% β-strands (Suppl. Fig. 2), which is in good agreement with that deduced from the 3D model (44.1% α-helices and 9.7% of β-strands).

The FAD bound to PO-barrelN-His was anaerobically photoreduced in the presence of EDTA and 5-deazariboflavin as catalyst [19,22]. The maximum amount of flavin semiquinone (∼55% of the initial enzyme) was reached after ∼30 min of irradiation and the fully reduced form of the enzyme was observed after 90 min of irradiation (Fig. 4A). The semiquinone form of PO variant is kinetically stabilized; in fact, it fully dismutates after overnight

Table 1
PO deletion variants expressed in this study.

Variant	Length[a]	Molecular mass (kDa)	Yield (mg PO/L culture)	Solubility	Protein form
His-PO-dom2-barrelC	146–600	53.6	5 (Whole cells)	50% Soluble	Apoprotein
His-PO-dom2-barrel	146–572	49.9	No expression	–	–
His-PO-barrelNC	176–600	49.9	0.12 (Purified)	<10% Soluble	Apoprotein
His-PO-barrelN	176–572	46.2	1.2 (Purified)	50% Soluble	Holo
PO-barrelN-His	176–572	46.2	10 (Purified)	50% Soluble	Holo
PO-barrelNC2-His	226–600	44.1	100 (Whole cells)	IB[b]	–
PO-barrel-His	264–600	36.1	1 (Whole cells)	<30% Soluble	Apoprotein

[a] Numbering refers to wild-type PO sequence. Two amino acids and six histidines were added to PO variants possessing the His-tag at the C-terminus. Six histidines were added to the PO variants possessing the His-tag at the N-terminus.
[b] IB = inclusion bodies.

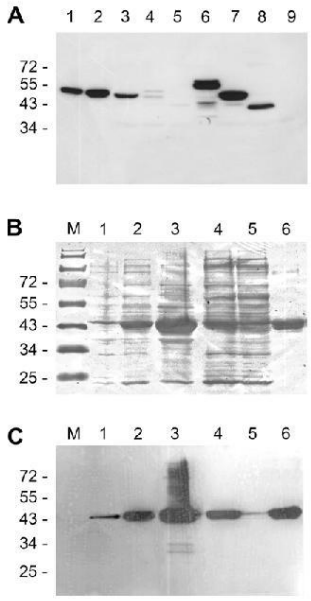

Fig. 3. Electrophoretic analysis of the expression of different human PO variants and of PO-barrelN-His purification. (A) Western blot analysis of the crude extracts of the recombinant PO variants tested in this study as obtained using anti-His-tag antibodies. In each lane an amount of sample corresponding to 0.1 mL of *E. coli* cultivation broth was loaded. Lanes: (1 and 2) 0.1 and 0.5 μg of pure PO-barrelN-His; (3) His-PO-barrelN; (4) His-PO-barrelNC; (5): His-PO-dom2-barrel; (6): His-PO-dom2-barrelC; (7) PO-barrelN-His; (8) PO-barrel-His; (9) PO-barrelNC2-His. (B) SDS–PAGE electrophoresis of samples from purification of PO-barrelN-His variant stained with Ponceau S. (M): Standard proteins; (1): whole cells before adding IPTG; (2): whole cells collected 3 h after adding 1 mM IPTG; (3): insoluble fraction of cell lysate; (4): crude extract; (5): HiTrap chromatography flow-through; (6): pure PO-barrelN-His variant after HiTrap chelating chromatography. All lanes were loaded with an amount of protein corresponding to 100 μL of the cultivation broth. (C) Western blot analysis of the samples in panel B using anti-His-tag mouse monoclonal antibodies.

incubation. The fully reduced flavin of PO-barrelN-His was quickly reoxidized by readmitting dioxygen in the cuvette.

Reactivity of flavoproteins with sulfite (a small-sized reducing agent) falls into two general classes: only the members of the oxidase class form an N(5)-adduct, with spectral properties resembling those of reduced flavin [30,31]. PO-barrelN-His reacts readily with sulfite, giving the typical spectral modifications (Fig. 4B): for the adduct a K_d of 10.4 ± 1.1 mM at 15 °C and pH 8.0 was calculated (inset of Fig. 4B). Sulfite binding is significantly (~100-fold) weaker than for other known amino acid oxidases: for example, K_d for sulfite is 0.1 mM for D-amino acid oxidase from *Rhodotorula gracilis* [31] and 0.4 mM for the homologue PutA from *Helicobacter* [23]. Indeed, the PO homologue from *S. cerevisiae* was reported to not react with sulfite [17]. The FAD N(5)-sulfite adduct in PO-barrelN-His is reversible: complete recovery of the original, oxidized spectrum of FAD was observed when the excess of sulfite was removed from the solution by PD10 desalting.

Enzymatic activity of the PO-barrelN-His variant

The enzymatic activity of PO-barrelN-His on its physiological substrate L-Pro was tested using the L-Pro:DCPIP assay [17]: a decrease in the absorbance at 595 nm related to DCPIP reduction demonstrating activity (Fig. 5A). The specificity of the reaction was confirmed by the lack of absorbance changes in the absence of L-Pro as well as in the presence of L-Pro and of the inhibitor THFA (PO-barrelN-His is fully inhibited at 1 mM THFA, see Fig. 5A). From the Michaelis–Menten plot, a V_{max} of 0.032 ± 0.007 U/mg protein (~0.8 s^{-1}) with a K_m of 0.47 ± 0.20 M was estimated; this analysis reveals that saturation was not achieved up to 1 M L-Pro (Fig. 5B). The K_m for L-Pro of human PO is 5–10 fold higher than that determined for microbial PutA from *Helicobacter* (K_m > 100 mM) [23] or for *E. coli* PutA and *Saccharomyces* Put1P (30–50 mM) [32,17]. Noteworthy, the kinetic properties of human, as well as microbial proline oxidases strongly depend on the electron acceptor used [12,23].

Concerning enzyme inhibition, the homologues Put1p from *S. cerevisiae* and PutA from *Helicobacter* are also fully inhibited by THFA, with a K_i of 5.3 and 0.35 mM, respectively [17,23]. Spectral titration of PO-barrelN-His with increasing concentrations of THFA yielded small changes in the visible spectrum of the oxidized enzyme. The most significant change was the hyperchromic change at 305 nm (not shown): from this a K_d = 1.5 ± 0.5 mM was estimated. L-Lactate is also a good inhibitor of PO-barrelN-His – under conditions as those reported in Fig. 5A the activity was fully inhibited at 5 mM lactate – while no inhibition was observed up to 50 mM L-pipecolate.

Discussion

Since the very first schizophrenia susceptibility locus was identified and published in *Nature* more than two decades ago [33], several studies have reported that "rare alleles of susceptibility genes" are involved in the onset of this disease. The unsuccessful search for causal mutations in these genes and the difficulty in

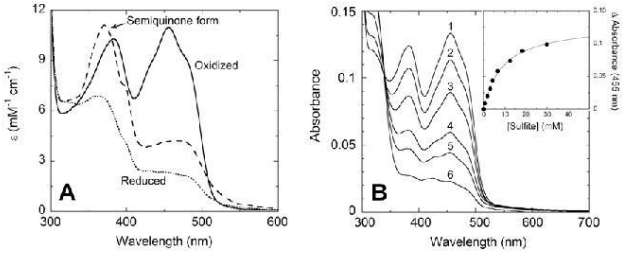

Fig. 4. Spectral properties of PO-barrelN-His. Conditions: 20 mM Tris–HCl buffer, pH 8.0, and 10% glycerol at 15 °C. (A) Absorbance spectra of recombinant PO-barrelN-His in the oxidized (—), half (- - -), and fully reduced (. . .) states. The spectrum of the latter two PO forms was generated by anaerobic photoirradiation in the presence of 5 mM EDTA and 0.5 μM 5-deazaflavin. (B) Sulfite binding to PO-barrelN-His: (1) 12 μM recombinant PO variant; (2–6) after the addition of 0.9, 4.3, 6.7, 18.4 and 30.0 mM sodium sulfite ($HSO_3^- + SO_3^{2-}$), respectively. Inset: replot of change in $Abs_{455\ nm}$ as a function of sulfite concentration. The K_d value was calculated by hyperbolic fit.

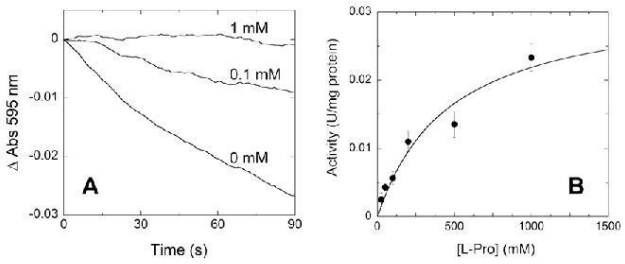

Fig. 5. L-Pro:DCPIP oxidoreductase assay of PO-barrelN-His activity. The reaction mixture contains 2 μM PO, 0.25 mM phenazine methosulfate, 50.4 μM DCPIP in 10 mM MOPS, pH 7.5 and 25 °C. (A) Activity assay in the presence of 100 mM L-Pro and increasing (0, 0.1 and 1 mM) concentrations of L-THFA. (B) Michaelis–Menten plot of PO-barrelN-His activity on L-Pro. Error bars indicate ±SE for at least three measurements.

replicating genetic studies [1,5,34] thus require that the products of the proposed susceptibility genes be biochemically characterized in detail in order to validate the genetic findings at the molecular level, e.g., [35]. We have focused our attention on the human enzyme PO, the product of the schizophrenia susceptibility candidate gene *PRODH*. Human PO was related to the control of plasma L-Pro level, an amino acid proposed to serve as a modulator of synaptic transmission in mammalian brain [36]. Furthermore, L-Pro is readily available from the breakdown of extracellular matrix, pointing to an important role of PO during nutrient stress, mainly in the metabolic adaptation of tumor cells to nutrient limitation [7].

Expression of a recombinant eukaryotic protein in a prokaryotic host such as *E. coli* is often hampered by the presence of specific eukaryotic post-translational modifications, peculiar protein features (i.e., transmembrane domains), and/or targeting sequences to specific subcellular compartments. This is the case for human PO, an enzyme localized on the mitochondrial inner membrane [5]. Although bioinformatics analysis failed to identify potential transmembrane regions, an examination of the primary sequence of PO using RONN software revealed the presence of two large regions with a high propensity to structural disorder in the N-terminal end of the protein (residues 15–65 and 150–190). Accordingly, the full-length and the variants encompassing at least one of the putatively disordered regions of PO were not expressed in *E. coli* as soluble protein. His-PO-barrelN and PO-barrelN-His were the only human PO variants that were successfully produced as soluble, active holoenzymes in *E. coli*; these PO variants are constituted by the C-terminal half of domain 2 (excluding the disordered region), the whole catalytic αβ-barrel, which contains most of the conserved fundamental residues, and the C-terminal helix 8, which hosts 2 additional important catalytic residues. Adding the last 28 C-terminal residues of PO also negatively affected the expression and solubility of these latter variants. Compared to the 3D structure of *E. coli* PutA, all the secondary structure elements of the αβ-barrel catalytic domain and the most important active site residues are correctly placed in the human PO model (Fig. 2).

Fairly high amounts of the His-tagged PO-barrelN protein were isolated as soluble and active, dimeric holoenzyme showing the typical spectral properties of flavoproteins oxidases. PO-barrelN-His variant shows a specific activity of ~3-fold lower than the value previously estimated for the full-length PO (~0.032 and 0.1 U/mg protein, respectively) [16] and a high K_m value for L-Pro. The reason for the observed discrepancy in activity is not straightforward because information on the previously reported recombinant full-length PO is limited [16]. Although the structural determinants not included in the sequence of the PO-barrelN-His variant could affect the overall conformation of PO and could prevent the enzyme from reaching full activity, differences in the primary sequence of the genes used for recombinant expression (frequently not defined in previous works on PO) or differences in activity assay/protein preparation (e.g., previous recombinant PO was equilibrated in phosphate buffer containing 100 mM KCl, 10% glycerol and 10% sucrose [16]) might account for such a discrepancy. Our conclusion that the fold of the PO-barrelN-His variant strictly resembles that of full-length PO is supported by the tight interaction with the flavin cofactor and the inhibitor THFA, the flavin reactivity, and the spectral properties (CD and UV-visible spectra). Hence, our results confirm the low turnover of human PO in the L-Pro:DCPIP assay as compared to microbial counterparts [16].

Conclusions

In conclusion, the purification of a soluble, active human PO variant (encompassing the whole catalytic domain) represents a crucial step in elucidating the structure–function relationships of this enzyme. This result paves the way for studying the effect of the reported polymorphisms associated with disease states at the molecular level so as to answer the many questions regarding proline/P5C redox cycle [2] and to design new and structure-based drugs that will modulate the cellular concentration of L-Pro and glutamate by affecting PO activity. As stated by [2]: "... we are entering a new era when patients newly diagnosed with a neuropsychiatric disorder should be evaluated with metabolic and molecular testing" and "... all new diagnosed SZ patients should be evaluated with a fasting plasma amino acid determination... as well genotyping for *COMT*, *PRODH*, and other risk genes for SZ".

Acknowledgments

This work was supported by grants from Fondo di Ateneo per la Ricerca (University of Insubria) to G. Molla and L. Pollegioni. We are grateful to Luciano Piubelli e Mattia Valentino for help in protein production.

Appendix A. Supplementary data

Supplementary data associated with this article can be found, in the online version, at doi:10.1016/j.pep.2012.01.021.

References

[1] J.A. Gogos, D.J. Gerber, Schizophrenia susceptibility genes: emergence of positional candidates and future directions, Trends Pharmacol. Sci. 27 (2006) 226–233.
[2] A. Willis, H.U. Bender, G. Steel, D. Valle, PRODH variants and risk for schizophrenia, Amino Acids 35 (2008) 673–679.

[3] H.J. Tuominen, J. Tiihonen, K. Wahlbeck, Glutamatergic drugs for schizophrenia: a systematic review and meta-analysis, Schizophr. Res. 72 (2005) 225–234.
[4] K.C. Murphy, Schizophrenia and velo-cardio-facial syndrome, Lancet 359 (2002) 426–430.
[5] T.M. Maynard, D.W. Meechan, M.L. Dudevoir, D. Gopalakrishna, A.Z. Peters, C.C. Heindel, T.J. Sugimoto, Y. Wu, J.A. Lieberman, A.S. LaMantia, Mitochondrial localization and function of a subset of 22q11 deletion syndrome candidate genes, Mol. Cell. Neurosci. 39 (2008) 439–451.
[6] J.J. Tanner, Structural biology of proline catabolism, Amino Acids 35 (2008) 719–730.
[7] J. Pandhare, S.P. Donald, S.K. Cooper, J.M. Phang, Regulation and function of proline oxidase under nutrient stress, J. Cell. Biochem. 107 (2009) 759–768.
[8] C.A. Hu, D.B. Williams, S. Zhaorigetu, S. Khalil, G.H. Wan, D. Valle, Functional genomics and SNP analysis of human genes encoding proline metabolic enzymes, Amino Acids 35 (2008) 655–664.
[9] Y.H. Lee, S. Nadaraia, D. Gu, D.F. Becker, J.J. Tanner, Structure of the proline dehydrogenase domain of the multifunctional PutA flavoprotein, Nat. Struct. Mol. Biol. 10 (2003) 109–114.
[10] J. Phang, C.A. Hu, D. Valle, Disorders of proline and hydroxyproline metabolism, in: C.R. Scriver, W.S. Sly, D. Valle (Eds.), The Metabolic and Molecular Bases of Inherited Disease, McGraw Hill, B.A., New York, 2001, pp. 1821–1838.
[11] H. Jacquet, G. Raux, F. Thibaut, B. Hecketsweiler, E. Houy, C. Demilly, S. Haouzir, G. Allio, G. Fouldrin, V. Drouin, J. Bou, M. Petit, D. Campion, T. Frebourg, PRODH mutations and hyperprolinemia in a subset of schizophrenic patients, Hum. Mol. Genet. 11 (2002) 2243–2249.
[12] H. Liu, S.C. Heath, C. Sobin, J.L. Roos, B.L. Galke, M.L. Blundell, M. Lenane, B. Robertson, E.M. Wijsman, J.L. Rapoport, J.A. Gogos, M. Karayiorgou, Genetic variation at the 22q11 PRODH2/DGCR6 locus presents an unusual pattern and increases susceptibility to schizophrenia, Proc. Natl. Acad. Sci. USA 99 (2002) 3717–3722.
[13] H.J. Williams, N. Williams, G. Spurlock, N. Norton, S. Zammit, G. Kirov, M.J. Owen, M.C. O'Donovan, Detailed analysis of PRODH and PsPRODH reveals no association with schizophrenia, Am. J. Med. Gen. B – Neuropsychiatr. Genet. 120B (2003) 42–46.
[14] H.U. Bender, S. Almashanu, G. Steel, C.A. Hu, W.W. Lin, A. Willis, A. Pulver, D. Valle, Functional consequences of PRODH missense mutations, Am. J. Hum. Genet. 76 (2005) 409–420.
[15] Y. Liu, G.L. Borchert, S.P. Donald, B.A. Diwan, M. Anver, J.M. Phang, Proline oxidase functions as a mitochondrial tumor suppressor in human cancers, Cancer Res. 69 (2009) 6414–6422.
[16] N. Krishnan, M.B. Dickman, D.F. Becker, Proline modulates the intracellular redox environment and protects mammalian cells against oxidative stress, Free Radic. Biol. Med. 44 (2008) 671–681.
[17] S. Wanduragala, N. Sanyal, X.W. Liang, D.F. Becker, Purification and characterization of Put1p from *Saccharomyces cerevisiae*, Arch. Biochem. Biophys. 498 (2010) 136–142.
[18] G. Molla, C. Vegezzi, M.S. Pilone, L. Pollegioni, Overexpression in *Escherichia coli* of a recombinant chimeric *Rhodotorula gracilis* D-amino acid oxidase, Protein Expr. Purif. 14 (1998) 289–294.
[19] G. Molla, S. Sacchi, M. Bernasconi, M.S. Pilone, K. Fukui, L. Pollegioni, Characterization of human D-amino acid oxidase, FEBS Lett. 580 (2006) 2358–2364.
[20] F. Volontè, L. Pollegioni, G. Molla, L. Frattini, F. Marinelli, L. Piubelli, Production of recombinant cholesterol oxidase containing covalently bound FAD in *Escherichia coli*, BMC Biotechnol. 10 (2010) 33.
[21] V. Job, G. Molla, M.S. Pilone, L. Pollegioni, Overexpression of a recombinant wild-type and His-tagged *Bacillus subtilis* glycine oxidase in *Escherichia coli*, Eur. J. Biochem. 269 (2002) 1456–1463.
[22] V. Job, G.L. Marcone, M.S. Pilone, L. Pollegioni, Glycine oxidase from *Bacillus subtilis*. Characterization of a new flavoprotein, J. Biol. Chem. 277 (2002) 6985–6993.
[23] N. Krishnan, D.F. Becker, Oxygen reactivity of PutA from *Helicobacter* species and proline-linked oxidative stress, J. Bacteriol. 188 (2006) 1227–1235.
[24] M.G. Claros, P. Vincens, Computational method to predict mitochondrially imported proteins and their targeting sequences, Eur. J. Biochem. 241 (1996) 779–786.
[25] T.A. White, N. Krishnan, D.F. Becker, J.J. Tanner, Structure and kinetics of monofunctional proline dehydrogenase from *Thermus thermophilus*, J. Biol. Chem. 282 (2007) 14316–14327.
[26] A. Roy, A. Kucukural, Y. Zhang, I-TASSER: a unified platform for automated protein structure and function prediction, Nat. Protoc. 5 (2010) 725–738.
[27] Z.R. Yang, R. Thomson, P. McNeil, R.M. Esnouf, RONN: the bio-basis function neural network technique applied to the detection of natively disordered regions in proteins, Bioinformatics 21 (2005) 3369–3376.
[28] G. Molla, M. Bernasconi, S. Sacchi, M.S. Pilone, L. Pollegioni, Expression in *Escherichia coli* and *in vitro* refolding of the human protein pLG72, Protein Expr. Purif. 46 (2006) 150–155.
[29] C. Perez-Iratxeta, M.A. Andrade-Navarro, K2D2: estimation of protein secondary structure from circular dichroism spectra, BMC Struct. Biol. 8 (2008) 25.
[30] V. Massey, F. Muller, R. Feldberg, M. Schuman, P.A. Sullivan, L.G. Howell, S.G. Mayhew, R.G. Matthews, G.P. Foust, Reactivity of flavoproteins with sulfite - possible relevance to problems of oxygen reactivity, J. Biol. Chem. 244 (1969) 3999–4006.
[31] L. Pollegioni, S. Sacchi, L. Caldinelli, A. Boselli, M.S. Pilone, L. Piubelli, G. Molla, Engineering the properties of D-amino acid oxidases by a rational and a directed evolution approach, Curr. Protein Pept. Sci. 8 (2007) 600–618.
[32] M.A. Moxley, J.J. Tanner, D.F. Becker, Steady-state kinetic mechanism of the proline:ubiquinone oxidoreductase activity of proline utilization A (PutA) from *Escherichia coli*, Arch. Biochem. Biophys. 516 (2011) 113–120.
[33] R. Sherrington, J. Brynjolfsson, H. Petursson, M. Potter, K. Dudleston, B. Barraclough, J. Wasmuth, M. Dobbs, H. Gurling, Localization of a susceptibility locus for schizophrenia on chromosome-5, Nature 336 (1988) 164–167.
[34] T.R. Insel, Rethinking schizophrenia, Nature 468 (2010) 187–193.
[35] S. Sacchi, M. Bernasconi, M. Martineau, J.P. Mothet, M. Ruzzene, M.S. Pilone, L. Pollegioni, G. Molla, pLG72 modulates intracellular D-serine levels through its interaction with D-amino acid oxidase: effect on schizophrenia susceptibility, J. Biol. Chem. 283 (2008) 22244–22256.
[36] J.A. Gogos, M. Santha, Z. Takacs, K.D. Beck, V. Luine, L.R. Lucas, J.V. Nadler, M. Karayiorgou, The gene encoding proline dehydrogenase modulates sensorimotor gating in mice, Nat. Genet. 21 (1999) 434–439.
[37] J.D. Thompson, T.J. Gibson, F. Plewniak, F. Jeanmougin, D.G. Higgins, The CLUSTAL_X windows interface: flexible strategies for multiple sequence alignment aided by quality analysis tools, Nucleic Acids Res. 25 (1997) 4876–4882.

Expression of human proline oxidase in U87 glioblastoma cell line: effect on the concentrations of proline and glutamate

E.Tallarita et al.,

Abbreviations

EAATs, excitatory amino acid transporters; EYFP, enhanced yellow fluorescent protein; FAD, flavin adenine dinucleotide; NMDAr, N-methyl-D-aspartate receptor; PO, proline oxidase; P5C, Δ^1-pyrroline-5-carboxylic acid

Keywords

L-proline; proline oxidase; glutamate; neurotransmitter; schizophrenia.

Abstract

L-Proline is a multifunctional imino acid with an essential role in primary metabolism and physiologic functions. Proline is oxidized to glutamate in the mitochondria, and the rate limiting step is catalyzed by the FAD-containing enzyme proline oxidase. Among human inherited disorder of proline metabolism, hyperprolinemia type I (HPI) results from proline oxidase deficiency and leads to tissue accumulation of the amino acid. Notably, the *PRODH* gene, encoding for proline oxidase has been related to velo-cardio-facial syndrome/Di George syndrome and increased susceptibility to schizophrenia. Despite the recognized physiological and medical interest of proline oxidase, the molecular mechanism by which its function is exerted is still largely unclear. Here we report the expression of proline oxidase and its L441P inactive variant in an eukaryotic cell system, represented by the U87 glioblastoma cell line. We investigated the expression level and the subcellular localization of the flavoenzyme in cells stably expressing the two enzyme variants and the effect on proline and glutamate intracellular and extracellular concentrations. These results allow to propose a regulatory role for proline oxidase in the framework of glutamatergic neurotransmission, thus highlighting the significance of this flavoenzyme as a putative new therapeutic target for neurological diseases, such as schizophrenia.

Introduction

Proline is a non-essential imino acid, with a distinctive cyclic structure [Phang et al., 2001]. Proline has a central role in metabolism and is increasingly being recognized as a critical amino acid in bioenergetics, cellular redox control, apoptosis and cancer [Phang et al., 2001, Maxwell and Rivera, 2003; Pandhare et al., 2009]. Because of its unique structure, proline metabolism is distinct from that of primary amino acids: intracellular synthesis and degradation occur through a distinct set of enzymes with unique properties and regulatory mechanisms [Phang et al., 2001; Servet et al., 2012]. Proline can be endogenously synthesized either from glutamate or ornithine, but it is also readily available from the breakdown of the extracellular matrix. The first step of degradation is performed by the flavoenzyme proline oxidase (PO, EC 1.5.99.8), also known as proline dehydrogenase (PRODH). It catalyzes the oxidation of L-proline to Δ^1-pyrroline-5-carboxylate (P5C), a key metabolite with several metabolic destinations: non enzymatic hydrolysis to glutamate semialdehyde that can be further oxidized to glutamate by P5C dehydrogenase

(P5CDH, EC 1.5.1.12); conversion to ornithine; reduction back to proline by P5C reductase (P5CR, EC 1.5.1.2) [Krishnan et al., 2008; Pandhare et al., 2009; Tanner 2008; Phang et al., 2012]. In the last few years a possible role of proline in neurotransmission has been proposed. It has been suggested to act as a neuromodulator: different studies demonstrated that high proline concentration could activate NMDA receptors "potentiating" glutamatergic neurotransmission [Nadler et al., 1987; Cohen et al., 1997]; moreover, high proline levels likely have a neurotoxic effect inducing changes in different neurotransmitter systems [Wyse and Netto 2011]. In addition, a high affinity transporter for proline has been identified supporting the role of proline in brain function [Yu et al., 2009]. Within the brain the proline transporter is exclusively expressed by a subset of glutamatergic pathways, including those localized in the area CA1 of hippocampus and corticostriatal pathways [Nadler et al., 1987; Cohen and Nadler, 1997; Fremau et al., 1992; Renick et al., 1999].

Furthermore, *PRODH* is a "hotspot" for mutations. At least 16 *PRODH* missense mutations have been identified in individuals suffering from hyperprolinemia type I (MIM 239500) [Jacquet et al., 2002] or schizophrenia [Jacquet et al., 2002; Liu et al., 2002; Williams et al., 2003]. Indeed, five of the identified polymorphisms, among which the Lys441Pro (L441P), result in almost complete (70%) inactivation of the flavoenzyme when the PO variants were expressed in CHO-K1_C9 cells [Bender et al., 2005].

HPI is an inherited disorder of proline metabolism caused by a deficiency of proline oxidase activity [Phang et al., 2001; Mitsubuchi et al., 2008]. Affected individuals show a ten-fold increase in proline concentration in plasma and cerebral spinal fluid [Clelland et al., 2011]. In most cases, hyperprolinemia is a benign condition (hyperprolinemic patients often result asymptomatic), nevertheless several studies demonstrated that proline accumulation could play an important role in certain complex phenotypes [Phang et al., 2001; Wyse and Netto 2011]. In fact, hyperprolinemic patients might present neurological manifestations such as cognitive dysfunction. Moreover, it has been shown that increased proline level can be specifically related to psychotic disorders [Phang et al., 2001; Oresic et al., 2011]. The link between hyperprolinemia and cognitive or psychiatric disorders, was strengthened by the studies on patients affected by velo-cardio-facial syndrome (VCFS), which arises from a 1.5–3 Mb deletion on chromosome 22q11, where the PO encoding gene (*PRODH*) is located [Jacquet et al., 2002]. Worthy of note, increased prevalence of schizophrenia has been reported among patients carring 22q11 interstitial deletion syndrome [Mitsubuchi et al., 2008].

Despite the recognized potential relevant role of proline in the central nervous system, the molecular mechanism by which this small signaling molecule plays its effect is still largely unclear. In order to investigate the possible correlation between proline, PO, glutamatergic neurotransmission and schizophrenia, and to confirm the effects of the reported L441P mutation on the enzyme activity [Bender et al., 2005], we recently successfully produced in *E. coli* and characterized a recombinant human PO deletion variant, PO-barrelN-His, encompassing the whole catalytic domain of human proline oxidase [Tallarita et al., 2012]. The PO variant was obtained in fairly high amounts as soluble and active, dimeric holoenzyme. The comparison of the human PO model to the tridimensional structure of *E. coli* PutA, suggests that the fold of the PO-barrelN-His strictly resembles that of the full length enzyme. This observation is supported by its biochemical properties such as interaction with the FAD cofactor and the inhibitor L-tetrahydro-2-

furoic acid (THFA), the flavin reactivity and the spectral properties [Tallarita et al., 2012]. On the other hand, we did not succeed in expressing in *E. coli* the full length PO as soluble protein.
In the present study, we report on the expression and preliminary characterization of the full length wild-type proline oxidase and the L441P inactive variant in an eukaryotic and "more physiological" cell system, the U87 glioblastoma cell line. We investigated the expression level and subcellular localization of the two PO variants in U87 clones stably expressing the flavoproteins fused to the enhanced yellow fluorescent protein (EYFP). Furthermore, we analyzed the intracellular and extracellular concentration of proline and glutamate, investigated the effect of the overexpression of the PO variants on proline cellular level and the role in the modulation of glutamate intracellular concentration and release.
Although our results are still preliminary, they allow us to propose for PO a regulatory role in the complex processes related to glutamatergic neurotransmission, thus suggesting that the flavoenzyme should represent a new target for therapeutic treatment of neurological diseases, such as schizophrenia.

Experimental Methods

Expression vector

The cDNA coding for the full length human PO was designed based on the sequence information reported [Bender et al,. 2005]. The data bank of "Source Bioscience" – I.M.A.G.E. (Integrated Molecular Analysis of Genomes and their Expression) reported different cDNAs corresponding to different *PRODH* genes. By the sequence alignment of I.M.A.G.E. *PRODH* clones we identified two clones with partially overlapping sequences (pBlue – IRAKp961I0147Q and pCR-BluntII-TOPO-IRCMp5012A1133D), containing the 5'-terminus and the 3'-terminus of the expected full length *PRODH* sequence (the one encoding for human PO, 600 amino acids). The two I.M.A.G.E. clones were purchased and digested with EcoRI and BbvCI restriction enzymes (Thermo Scientific) to obtain the fragments of interest, which were subsequently ligated (T4 DNA ligase, Roche) to produce the pCR-BluntII-TOPO-PRODH cDNA which sequence was confirmed by automated sequencing.
The resulting cDNA encoding human PO was amplified by PCR (using the following primers: 5' – cataaagcttatggctctgaggcgcgccctg-3'; 5'-gttggtaccaaggcagggcgatggaagaggttg-3') and subcloned into Hind III and KpnI restriction sites of the expression vector pEYFP-N1 (Clontech) which allowed the expression of PO fused upstream to EYFP. In order to produce the untagged flavoprotein, the PO cDNA was subcloned into pcDNA3 vector (employing the EcoRI restriction sites). The L441P mutation was introduced into the pEYFP-N1-prodh and pcDNA3-prodh constructs DNA by using the QuikChange Site-Directed Mutagenesis Kit (Stratagene). Enzymatic DNA modifications were carried out following the manufacturer protocols and successful mutagenesis was confirmed by DNA sequencing.

Cell culture and transfection

The U87 human glioblastoma cells (ATCC) were maintained in DMEM supplemented with 10% fetal bovine serum (FBS), 2 mM L-glutamine, 1% penicillin/streptomycin and 1% amphotericin B

(Euroclone) at 37 °C in a 5% CO_2 incubator. U87 cells were transfected using the FuGene®HD transfection reagent (Promega, 8 µL) and 2 µg of the following constructs: pEYFP-N1-prodh, pEYFP-N1-prodh-L441P, pcDNA3-prodh, pcDNA3-prodh L441P. Cell clones stably expressing the different protein variants (PO-EYFP, PO-EYFP L441P, PO, PO L441P) were selected by adding 0.4 mg/mL G418 (Euroclone) to the growth medium. Protein expression level were monitored either by a fluorescence microscope (Olimpus IX51) to detect the EYFP associated signal or by Western blot analysis using anti-PO and anti-GFP specific antibodies.

Cell growth curves

The cell growth was monitored over a 7 days period: the different cell clones were seeded in 24 wells plate (10.5 x 10^3 cells/well starting density) and incubated at 37 °C in a 5% CO_2 incubator. The cells were collected and counted every 24 h. The growth curves were expressed as cell density/well vs time.

Western blot analysis

Stably transfected cells were detached by trypsin treatment, counted, harvested and resuspended in SDS-PAGE sample buffer. 5 x 10^4 cells or 1 x 10^5 of each clone were separated by a 10% SDS-PAGE electrophoresis and transferred on a polyvinylidene difluoride membrane (PVDF – Immobilon-P, Millipore). Western blot analyses were carried out incubating the PVDF membranes over-night at 4 °C in phosphate buffer saline added with 0.1% Tween-20 (TPBS: 10 mM sodium phosphate dibasic, 1.75 mM potassium phosphate monobasic, 137 mM NaCl and 2.7 mM KCl pH 7.4) or in Tris-buffered saline added with 0.1% Tween-20 (TTBS: 10 mM Tris-HCl, pH 8.0, 0.5 M NaCl), containing 4% dried milk or 5% bovine albumin serum (BSA). Subsequently, the membranes were incubated for 1.5 h at room temperature or 37 °C with primary antibodies, washed extensively with TPBS or TTBS and incubated for 1 h at room temperature with specific peroxidase–conjugated immunoglobulins. After washings, the immunoreactivity signals were detected by enhanced chemiluminescence (ECL plus, GE Healthcare). The immunoreactivity signals were detected using the following primary antibodies: rabbit polyclonal anti-PO (1:1000, Davids Biotecnologie); mouse monoclonal anti-GFP (1:500, SantaCruz); rabbit polyclonal anti-actin (1:1000, Sigma); rabbit polyclonal anti-GLT1 (1:1200, Abnova); rabbit polyclonal anti-EAAT1 (1:1000, Thermo Scientific). The different immunorecognition signals were quantified by using the Quantity One software (BioRad). In the following Western blot analyses, the intensity values (immunodetected by anti-PO, anti-GLT1 or anti-EAAT1 antibodies) were normalized to the values obtained with the anti-actin antibody.

Determination of selected amino acid cellular and extracellular concentration by HPLC analysis

8 x 10^4 U87, U87 PO-EYFP or PO-EYFP L441P cells were seeded in 12 wells plate. At different times upon seeding (0, 6, 12, 24, 48, 72 hours), both the culture medium and the cells were collected and used for HPLC analysis. The culture medium was centrifuged at 13000 rpm for 5 min at 4 °C while the cells were detached by trypsin treatment, harvested, washed with PBS; both samples were stored at -80 °C until analyses. The cells extracts were prepared as reported previously

[Sacchi et al., 2008]: the cells were thawed and resuspended (2.5 x 10^5 cells/mL) in ice cold 5% trichloroacetic acid, then sonicated and centrifuged for 30 min at 13000 rpm. The soluble fraction was extracted with water-saturated ether and lyophilized before derivatization. Samples derivatization was carried out using the solution included in the Waters AccQ Tag™ Amino Acid Analysis kit and following the manufacturer instructions. Culture medium samples were diluted 1:20 in 20 mM HCl before derivatization. Derivatized samples were resolved by HPLC chromatography on a 4 µm C18 (3.9 x 150 mm) reverse phase column (Waters) and eluted by a gradient (from 100% aqueous Waters AccQ Tag™ buffer to 60% acetonitrile and 40% Milli-Q water in 36 minutes). Each amino acid was identified and quantified based on the retention time and the corresponding peak area. The calibration curves were determined by injection of increasing concentrations of each amino acid.

Immunofluorescence

2.5 x 10^5 U87 cells stably expressing PO-EYFP or PO-EYFP L441P, were seeded on round glass coverslips and incubated for 24 hours at 37 °C and 5% CO_2. The cells were then extensively washed with PBS solution (10 mM sodium phosphate dibasic, 2 mM potassium phosphate monobasic, 137 mM NaCl and 2.7 mM KCl pH 7.4) and fixed with 4% p-formaldehyde and 4% sucrose in 0.1% sodium phosphate buffer pH 7.4, for 15 min at room temperature. Fixed cells were permeabilized and the unspecific binding sites were blocked by a 30 min incubation in PBS supplemented with 4% horse serum and 0.2% Triton X-100. The coverslips were incubated 24 h or 48 h at 4 °C with primary antibodies against a specific mitochondrial marker (1:50 anti-mitochondria antibody, surface intact mitochondria, clone 113-1, Millipore), or the glutamate transporter GLAST (anti-EAAT1 1:200, Thermo Scientific) and GLT-1 (anti EAAT2 1:20, Abnova). Immunoreactivity was detected with donkey anti-mouse Alexa 546-conjugated antibody (1:1000, Invitrogen) donkey anti-rabbit Alexa 647-conjugated antibody (1:1000, Invitrogen). Immunostained coverslips were imaged using an inverted laser scanning confocal microscope (TCS SP5, Leica Microsystems equipped with a 63.0 x 1.25 NA plan apochromate oil immersion objective). Confocal image stacks were collected with Leica SP5 software avoiding interference between each channel and without saturating any pixel.

PO activity assay

Activity of PO variants expressed in U87 cell clones was measured by the o-aminobenzaldehyde (o-AB) spectrophotometric assay as previously reported [Pandhare et al., 2009]. Briefly, P5C (Δ^1-pyrroline-5-carboxylic acid) formed by proline enzymatic oxidation was reacted with o-AB and the resultant o-AB-P5C complex was quantified measuring the absorbance of the reaction mixture at 440 nm. U87 cells and U87 cells expressing untagged PO or L441P inactive mutant, were grown in 9 cm plates up to 80% of confluence. Subsequently cells were rinsed and scraped in cold PBS buffer (Euroclone), collected, resuspended in cold sucrose buffer (250 mM sucrose, 3.5 mM Tris, 1 mM EDTA pH 7.4). Cells were then sonicated for 20 s and the cells extracts were clarified by centrifugation at 13000 rpm 20' at 4 °C . The total protein content was determined using the Bradford protein assay (Sigma). A 200 µL reaction mixture containing, 0.12 mg/ml o-AB, 0.012 mg/mL cytochrome c, 0.5 mM proline in 0.1 M KPO_4 pH 7.2 and a volume of cell extract

corresponding to 50 µg of total protein, was blocked for 30 min at 37 °C. The reaction was terminated by adding of 20 µL of o-AB (10 mg/mL in 6 N HCl).
All the analyses were replicated three times for each condition and statistical analyses were performed using Kaleidagraph software (Synergy Software). Variation between groups was evaluated by one way ANOVA.

Results

Selection of U87 cell clones stably expressing PO variants

The U87 human glioblastoma cell line was chosen as an eukaryotic expression system, since it represents a useful *in vitro* model of astroglia: it has been previously used to express the human flavoenzyme D-amino acid oxidase and to investigate the processes involved in the metabolism of the neuromodulator D-serine [Shoji et al., 2006; Sacchi et al., 2008; Sacchi et al., 2011].
U87 cells were transfected with pEYFP-N1-prodh, pEYFP-N1-prodh L441P, pcDNA3-prodh, or pcDNA3-prodh L441P constructs, encoding for wild-type or L441P inactive PO variants. Upon selection, several clones stably expressing the protein variants were obtained (U87 PO-EYFP, U87 PO-EYFP L441P, U87 PO and U87 PO L441P) as confirmed by Western blot analysis: single bands corresponding to the chimeric fluorescent protein (95 kDa) were detected in U87 PO-EYFP, PO-EYFP L441P using either anti-PO or anti-EYFP specific antibodies [Fig. 1, A-B]. Indeed, an anti-PO specific signal at the predicted molecular mass (68 kDa) was observed in U87 PO and U87 PO L441P clones expressing the untagged proteins. In U87 PO-EYFP L441P cell extract, the anti-PO antibody detected a further band of lower molecular mass, probably corresponding to a proteolytic product and possibly indicating a partial degradation of the PO-EYFP L441P variant. Interestingly, in the same sample, anti-GFP antibody detected only the band corresponding to the full length chimeric fluorescent protein, indicating that probably the proteolytic cleavage occurs at the C-terminal end of PO thus yielding to loss of part of EYFP. The observation that the level of expression of PO-EYFP L441P are comparable to PO-EYFP when detected with anti-PO antibodies while appear sensibly lower when revealed with the anti-GFP antibody, further confirms this hypothesis.
PO has been previously reported to be a mitochondrial protein [Maynard et al., 2008]. Since it is possible that the EYFP tag modifies the cellular targeting of the overexpressed chimeric proteins, the subcellular localization of the two PO variants was verified by immunostaining experiments. Confocal analyses show that the fluorescent signal corresponding to the chimeric proteins displays a peculiar “spaghetti like” pattern (Fig. 1, C, D; yellow channel), typical of mitochondria. Moreover, their distribution largely overlapped with the specific mitochondrial stain (Fig. 1, C, D; merge panel). No significant differences in subcellular localization of the wild-type and the L441P variant chimeric proteins were observed, indicating that the PO targeting is not affected by the introduced point mutation as well as by the EYFP tag.

Growth of U87 cells stably expressing wild-type and L441P PO

Since we demonstrated the expression of PO in U87 cells, the functional differences in U87 clones expressing wild-type or mutant PO were investigated. At first, the possibility that the

overexpression of the two PO variants differently affect cells proliferation capability was investigated: the U87 PO-EYFP, PO-EYFP L441P, PO and PO L441P clones were seeded at 10.5 x 10^3 cells/well starting density in 12 wells plates and the cell growth rate was monitored over a period of 7 days, collecting and counting the cells at different time points. The growth curves (cell density/well vs time) display an exponential trend because during the incubation time (although the medium has not been replaced) the nutrient sources were not entirely depleted. No significant difference in the growth rate of U87 clones expressing the chimeric fluorescent proteins or the untagged PO variants was apparent. Anyway, for all the transfected clones a lower growth rate is observed as compared to untransfected mock U87 cells (Fig. 2). This result suggest that the over-expression of PO negatively affected the growth of transfected U87 cells: the average doubling time of the transfected U87 cells is 1.5-fold higher with respect to U87 control cells. On the other hand, the expression of the wild-type or the inactive L441P PO variants does not affect further growth capability.

To verify that the introduced L441P substitution negatively affects PO functionality, the enzymatic activity was assayed on cellular extracts of U87 PO and U87 PO L441P clones by using the o-aminobenzaldehyde assay and the previously described conditions [Pandhare at al., 2009]. Unfortunately, unless different amount of samples were assayed (cell extract corresponding to 50 µg of total protein) we failed in obtaining a consistent determination of PO activity: the measurements were poorly reproducible and no significant differences were observed between crude extracts from U87 cells expressing the wild-type or the inactive PO variant (data not shown). For this reason, we decided to analyze the proline intracellular content since variations in the concentration of the amino acid might be indicative of the activity of the different over-expressed PO variants.

Determination of L-proline and L-glutamate levels

Proline has been reported to be involved in glutamatergic transmission (see Introduction section). It has been demonstrated that while physiological concentration of proline in cerebrospinal fluid little affects glutamate release, the accumulation of the amino acid at concentration above 30 µM at the synaptic terminals yields to inhibition of glutamate release [Coehen and Nadler, 1997]. To investigate whether variations in proline cellular levels due to PO overexpression might affect glutamate level, cellular and extracellular content of the two signaling molecules in cultures of U87 PO-EYFP, PO-EYFP L441P clones and U87 control cells was determined. 8 x 10^4 cells were seeded in 12 wells plate and at different times upon seeding, both the culture medium and the cells were collected and subjected to HPLC analysis.

The time course of proline intracellular concentration is quite different in the analyzed cell types: while in control U87 cells the proline cellular levels appear relatively constant over time, U87 PO-EYFP L441P shows a gradual accumulation of the amino acid over time (Fig. 3A). On the other hand in U87 PO-EYFP cells proline cellular content decreases (Fig. 3B). Notably, the most evident difference is observed at 72 h: U87 PO-EYFP proline cellular content is 2.3-fold lower compared to U87 controls cells, while in U87 PO-EYFP L441P it is 1.6-fold with respect to U87 control cells. These results indicate that the chimeric wild-type is active and it is responsible of proline intracellular consumption; on the contrary, the L441P substitution effectively inactivates the enzyme, preventing proline degradation.

Unexpectedly, the over-expression of the mutant L441P PO in U87 cells yield to an increase in proline cellular level with respect to U87 control cells (Fig. 3A). It is possible to suppose that the inactive L441P variant binds and inactivates the endogenously produced active PO thus inducing a disequilibrium in proline metabolic pathway, resulting in the accumulation of the amino acid (further studies are needed to explain this observation). An additional hypothesis is that the L441P PO mutant binds the substrate sequestering it and inducing the metabolic "proline cycle" to shift towards the production of proline.

This latter hypothesis is partially supported by the analysis of the time course of glutamate cellular content: the concentration of glutamate (a proline precursor) is always significantly higher in U87 PO-EYFP L441P cells compared to U87 PO-EYFP and U87 control cells (Fig. 3B). Interestingly, the increase in proline level observed at ≥ 48 is paralleled by a concomitant decrease in glutamate cellular content for all the cell types. This suggests that glutamate is consumed by the cells in an attempt to restore proline cellular levels (depleted by the enzymatic activity or by the binding to the inactive mutant PO). This observation rises an additional interesting question: why glutamate cellular level in U87 PO-EYFP are so low compared to U87 PO-EYFP L441P and resembles that detected in U87 control cells? As previously observed, in the cells expressing the PO-EYFP, proline is actively degraded to P5C, which is supposed to act as a glutamate precursor. P5C (produced in large amount by the over-expressed PO-EYFP), should be exported outside mitochondria, where the P5C reductase converts it back to proline which could be transferred to the mitochondrial matrix to compensate the disequilibrium in the cycle induced by the increase in PO level and activity. Accordingly, the excess of produced glutamate should be released by the cell. To support this hypothesis, analysis of the concentrations of this signaling molecule (as well as of proline) in the culture medium were performed. Under the experimental conditions used the extracellular proline concentration was below the resolution limit of the HPLC method. On the other hand, significant levels of glutamate concentration were detected in the extracellular medium of the different cell types. Interestingly, despite the fact that U87, U87 PO-EYFP and U87 PO-EYFP L441P show similar glutamate extracellular level up to 6 h after seeding, at later times the concentration of the amino acid in the extracellular medium of U87 PO-EYFP cells is significantly and statistically higher (≈ 80 µM at 12 h; ≈ 60 µM at 24 h) with respect to that measured in the U87 PO-EYFP L441P (≈ 70 µM at 12 h; ≈ 55 µM at 24 h). These results support the hypothesis that cells expressing the wild-type flavoenzyme show an increase in glutamate release. An increase in the extracellular glutamate concentration compared to U87 control cells is also evident for U87 PO-EYFP L441P cells (≈ 70 µM at 12h; ≈ 55 µM at 24 h), but in this case the effect is probably related to its high intracellular concentration.

Notably, the detected glutamate extracellular concentration, reflects the values reported in literature for glioma cells [Ye and Sontheimer, 1999].

Expression of glutamate transporter

Several studies have reported impaired glutamate transporter expression in glioma cell line [Maragakis and Rothstein, 2004]. GLAST and GLT-1 are the major Na^+-dependent glutamate transporters in the CNS. Thus, in an effort to further justify the observed differences in glutamate extracellular levels, we compared the expression levels of GLAST and GLT-1 in U87 cells stably

expressing PO-EYFP or PO- EYFP L441P variant as well as U87 control cells by Western blot and confocal analysis.

GLAST and GLT-1 are both expressed in all the analyzed cell clones, as demonstrated by the specific immunorecognition signals detected by Western blot at the predicted molecular mass (56 kDa and 65 kDa for GLAST and GLT-1, respectively) (Fig. 4A, 4C). Densitometric analyses (Fig. 4B) indicate that the over-expression of both the PO-EYFP variants in U87 cells affects GLAST cellular levels: the signal corresponding to the 56 kDa immunodetected band is 2.5-fold higher in U87 cells expressing PO-EYFP and U87 PO-EYFP L441P (showing comparable levels) than in control cells. Worthy of note, in U87 cell extracts a band at higher mass (≈ 70 kDa), which is absent in cells expressing the PO-EYFP variants, was observed. It might correspond to a modified form of the transporter. In fact it has been reported that abnormal posttranslational modifications, such as glycosylation, could affect the transporter, reducing its stability or decreasing its surface expression; in particular, impaired glycosylation might prevent the correct targeting to the plasma membrane decreasing the glutamate reuptake capability of the cells [Ye at al., 1999; Escartin et al., 2006; Bauer et al., 2010].

GLAST expression levels in U87 PO-EYFP and U87 PO-EYFP L441P cells are very similar, although the amount of the expressed PO variants are significantly different (1.6-fold higher in U87 cells expressing PO-EYFP L441P) (Fig. 4D). Confocal analysis supported the Western blot observations: the intensity of anti-GLAST signal (showed in red, Fig. 5A, a)) is sensibly higher in the cell expressing the chimeric PO variants with respect to that observed in U87 control cells. Moreover, in the previous cells the transporter's staining is localized at the cell membrane (as observed in U87 cells) but also diffused in the cytosol. Notably, no significant colocalization between signals for GLAST and chimeric PO variants was observed (Fig 5, c)).

On the other hand, GLT-1 (which is always detected as a single band at the expected molecular mass in Western blot analisis) exhibits comparable levels of expression in U87 cells expressing PO-EYFP and in controls cells, while the amount of the transporter is at least 2-fold higher in the cells expressing the inactive PO mutant (Fig. 4D). The transporter is correctly located at the cell membrane, as it is evident from confocal analyses (Fig. 5B): the corresponding immunofluorescence signal is distributed along the cell surface where it localizes in punctuate cluster (Fig. 5B, a)) as previously reported [Lee et al., 2012].

These results indicate that the levels of expression of specific glutamate transporters, is affected by the intracellular proline content. Notably, the cells expressing the inactive PO-EYFP variant, that leads to proline intracellular accumulation, exhibit a prominent expression of GLT-1 transporters. Altogether these results suggest that the over-expression of PO in U87 cells modulates the expression of glutamate transporters. Although further studies are required to confirm that the observed effect is specifically due to the expression of proline oxidase, the increase in glutamate transporters explains the observed increase in the glutamate extracellular level (Fig. 3C).

Discussion

Proline is a unusual non essential amino acid that might be derived from dietary proteins as well as from extracellular matrix, connective tissue, and bone breakdown. Proline is released from these "reservoirs" by the sequential action of specific dipeptidase and prolidase enzymes which can hydrolyze the peptide bond linked to the pyrrolidine ring [Phang et al., 2008]. Since its α-

nitrogen is contained within a pyrrolidine ring, proline is not a substrate for the classical amino acid-metabolizing enzymes (decarboxylases, aminotransferases and racemases). Worthy of note, a family of proline metabolic enzymes evolved with specific cellular localization and regulation mechanisms [Phang et al., 2001]. Because proline metabolism is distinct from that of the other amino acids, it can be reserved for special physiological functions [Phang et al., 2008]. Interestingly, proline metabolic enzymes constitute a "proline cycle" which represents an important and complex crossroad with other metabolic pathways, involving interconversion of proline with glutamate and ornithine through P5C (which is in tautomeric equilibrium with glutamic-γ-semialdehyde). Ornithine and glutamate can be precursors of proline with P5C as the common intermediate; on the other hand, proline itself can be considered a precursor of glutamate [Phang et al., 2001; Phang et al., 2008; Wyse and Netto, 2011]. With the exception of the conversion of P5C to proline, which takes place in the cytosol of the cell, all the other metabolic steps catalyzed by P5C reductase take place into mitochondria. Outside this organelles, proline and P5C participates to the pentose phosphate pathway, the TCA cycle and the urea cycle, so this makes proline a crucial amino acid in bioenergetic and cellular control [Phang et al., 2001]. All these metabolically relevant relationships shall be taken into account in the attempt to define the biological functions of this atypical molecule.

Several inborn errors of proline metabolism, caused by impairements in the functionality of the enzymes involved in the "proline cycle", have been reported. They usually lead to the accumulation of metabolic intermediates [Mitsubuchi et al., 2008]. In the present study, we focused our attention on proline oxidase (PO), a mitochondrial flavoenzyme that catalyzes the first step of L-proline degradation. PO deficiency has been related to hyperprolinemia type I, a disorder characterized by elevated plasma proline levels. Interestingly, in a significant fraction of hyperprolinemic patients, the disease is frequently associated with mental seizures [Cohen and Nadler, 1997]; moreover several experimental evidences demonstrated that hyperprolinemia could affect patients with 22q11 deletion syndrome (Di George syndrome, velo-cardio-facial syndrome). Over the past years it has been shown that the deletion predisposes to a variety of psychotic conditions: this prompted to propose that the deleted region may contain a predisposition locus for psychotic illness. Notably, increased frequency of microdeletions in the 22q11 locus has been found in patients with schizophrenia [Paterlini et al., 2005] and a recent study on metabolic profiles associated with psychotic disorders demonstrated that increased levels of serum proline was specific to schizophrenia [Oresic et al., 2011]. The *PRODH* gene, encoding for proline oxidase, is located on chromosome 22q11. Functional studies on the *PRODH* gene suggested that severe reduction of PO activity caused by inactivating *PRODH* mutations, has the potential for causing substantial neurological abnormalities [Willis et al., 2008]. In particular among the reported 16 missense mutations that could affect PO functionality [Bender et al., 2005], the L441P substitution results in severe reduction of PO activity and, worthy of note, is one of the allele typically found in schizophrenic patients [Willis et al., 2008]. L441P is considered one of the most deleterious mutations since it affects the active site of the enzyme, by disrupting the correct interaction between the substrate (proline) and the FAD cofactor [Bender et al., 2005].

In light of the intriguing putative role of proline oxidase in several human pathological conditions, we focused our attention on the functional and biochemical characterization of the human PO enzyme. As a step forward with respect to our previous investigation in which we reported the production of a soluble and active PO deletion variant in *E. coli* (PO-barrelN-His), the human

recombinant full length PO was expressed in U87 glioblastoma cells. The wild-type and the L441P inactive mutant PO enzyme, were also expressed as a chimeric protein fused with EYFP at the C-terminus (to leave the N-terminal targeting sequences unmasked). Confocal analysis of PO-EYFP and PO-EYFP L441P showed that both enzyme variants are correctly targeted to the mitochondria. This observation suggests that the introduced substitution does not affect the correct folding of the mutant protein which is targeted to the correct subcellular compartment with no evidence of protein aggregates. Since the fused EYFP tag could affect the catalytic activity of the expressed PO variants, we also expressed the untagged wild-type and L441P PO variant, as confirmed by Western blot analysis using a specific anti-PO antibody.

To investigate PO biological function in the U87 cell system, we evaluated the PO activity in the cell extracts of clones stably expressing PO and PO L441P. Unfortunately we were unable to obtain consistent proline oxidase activity values previously reported procedure [Pandhare et al., 2009], we thus decided to evaluate the proline oxidase activity indirectly by measuring variations in the intracellular proline content in the cells expressing the chimeric wild-type enzyme or the inactive PO mutant. The proline content is 2.3-fold lower in U87 PO-EYFP with respect to U87 control cells (Fig. 3A). Interestingly, in U87 cells expressing the inactive PO-EYFP L441P variant, a progressive accumulation of proline is observed: proline cellular levels are 1.6-fold higher compared to control cells. These results demonstrate at the cellular level that PO-EYFP is active, while PO-EYFP L441P is largely inactive.

In order to expande the overview on this particular and complex metabolic network and to take into account a more complicated and dynamic mechanism we tempted to correlate proline oxidase activity with glutamate cellular concentration. U87 cells stably expressing PO-EYFP L441P show higher intracellular glutamate level as compared to U87 cells expressing PO-EYFP and the control untransfected cells: in this scenario, if we consider glutamate as a precursor of proline it is conceivable that when the proline degradation is largely prevented (by the over-expression of an inactive PO form) the “proline cycle” is unbalanced thus resulting in glutamate accumulation within the cells.

The extracellular glutamate content significantly differed among cultures of cells expressing the different PO variants; in particular, higher glutamate level were observed in U87 PO-EYFP cell culture medium. Considering that in these cells the rate of proline degradation is boosted by the over-expression of the flavoenzyme, proline itself can cause the unbalance of the “proline cycle” (being proline the most abundant metabolic glutamate precursors): the excess of glutamate produced could be subsequently released by these cells.

To better understand the observed results related to the extracellular glutamate levels, we investigated the expression of two glial glutamate transporters. Under physiological conditions GLAST and GLT-1 are the two major Na^+-dependent glutamate transporters in CNS. Termination of glutamatergic activity occurs through the glial uptake of the neurotransmitters: the maintenance of the extracellular glutamate concentration below neurotoxic levels is a critical function of glial glutamate transporters [Lopez-Bayghen and Ortega, 2011]. Interestingly, glioma cells demonstrate impaired glutamate transporter expression [Maragakis and Rothstein, 2004] and in particular the transporter results most likely mislocalized, drastically reducing the cells capability of glutamate uptake. Moreover these tumor cells display a strong Na^+-indipendent cystine/glutamate exchange which induces glutamate efflux outside the cells and outweighs the inward glutamate transport leading to the accumulation of glutamate in the extracellular space

[Ye et al., 1999]. Notably, in the U87 model cell system, we observed that the over-expression of the PO-EYFP L441P variant, which increases proline cellular level, might directly influence the levels of selected glutamate transporter. In fact, in U87 PO-EYFP L441P cells, a prominent expression of GLT-1 at the cellular membrane is apparent. On the other hand, GLAST expression level in U87 PO-EYFP and U87 PO-EYFP L441P cells appear very similar, even though the amount of expressed PO between the two cells clones is substantially different. Confocal analysis shows that the transporters are mainly located in the cell membrane, but also partially diffused in the cytosol: this result agrees with previously reported observations that the transporters are often mislocalized and their expression and traslocation at the plasma membrane is reduced in glioma cell indicated [Ye et al., 1999].

Our results represent preliminary but interesting evidence of the physiological relevance of proline oxidase activity in the intriguing scenario that links the “proline cycle” with other essential metabolic pathways. Further investigations are required to elucidate the mechanism by which proline might exert its function as a putative neuromodulator in physiological and pathological conditions. Understanding the complex biochemical network linking proline to glutamate in the CNS and its potential role in regulating the onset of schizophrenia, will pave the way to the design of new drugs that modulating proline oxidase activity could be potentially used as new therapeutic target for schizophrenia treatment.

References

[1] J.M. Phang, C. A. Hu, D. Valle, Disorders of proline and hydroxyproline metabolism. The Metabolic and Molecular Bases of Inherited Disease, 8th ed. Scriver C.R., Beaudet A.R., Sly W., Valle D (eds.), McGraw-Hill, New York, 1821-1838, 2001.

[2] S.A. Maxwell, A. Rivera, Proline oxidase induces apoptosis in tumor cells, and its expression is frequently absent or reduced in renal carcinomas; The Journal of Biological Chemistry 278: 9784-9789, 2003.

[3] J. Pandhare, S.P. Donalds, S.K. Cooper, J.M. Phang, Regulation and function of proline oxidase under nutrient stress; Journal of cellular Biochemistry 107: 759-768, 2009.

[4] C. Servet, T. Ghelis, L. Richard, A. Zilberstein, A. Savoure, Proline dehydrogenase: a key enzyme controlling cellular homeostasis; Frontiers in Bioscience 17 (1): 607-620, 2012.

[5] N. Krishnan, M.B. Dickman, D.F. Becker, Proline modulates the intracellular redox environment and protects mammalian cells against oxidative stress; Free Radical Biology and Medicine 44: 671-681, 2008.

[6] J.J.Tanner, Structural biology of proline catabolism; Amino Acids 35:719-730, 2008.

[7] J.M Phang, W.Liu, Proline metabolism and cancer; Frontiers in Bioscience 17, 1835-1845, 2012

[8] J.V. Nadler, Sodium-dependent proline uptake in the rat hyppocampal formation: Association with ipsilateral commissural projection of CA3 pyramidal cells; Journal of Neurochemistry 49: 1155-1987, 1987;

[9] S.M.Cohen, J.V. Nadler, Proline induced inhibition of glutamate release in hippocampal area CA1; Brain Research 769: 333-339, 1997.

[10] A.T.S. Wyse, C.A. Netto, Behavioral and neurochemical effects of proline; Metabolic Brain Disease 26: 159-172, 2011.

[11] X.C. Yu, W. Zhang, A. Oldham, E. Buxton, S. Patel, N. Nghi, D. Tran, T.H. Lanthorn, C. Bomont, Z.C. Shi, Q. Liu, Discovery and characterization of potent small molecule inhibitors of the high-affinity proline transporter; Neuroscience Letter 451: 212-216, 2009.

[12] R. T. Fremau-Jr, M.G. Caron, R.D. Blakely, Molecular cloning and expression of high affinity proline transporter expressed in putative glutamatergic pathway of rat brain; Neurons 8: 915-926, 1992.

[13] S.E. Renick, D.T. Kleven, J. Chan, K. Stenius, T. A. Milner, V. M. Pickel and R.T. Fremau Jr, The mammalian brain high-affinity L-proline transporter is enriched preferentially in synaptic vescicles in a subpopulation of excitatory nerve terminals rat forebrain; The Journal of Neuroscience 19 (1): 21-33, 1999.

[14] H. Jacquet, G. Raux, F.Thibaut, B. Hecketsweiler, E. Houy, C. Demilly, S. Haouzir, G.Allio, G. Fouldrin, V. Drouin, J. Bou, M.Petit, D. Campion, T. Frebourg, PRODH mutation and hyperprolinemia in a subset of schizophrenic patients; Human Molecular Genetics 11: 2243-2249, 2002.

[15] H. Liu, S.C. Heath, C. Sobin, J.L. Roos, B.L. Galke, M.L. Blundell, M. Lenane, B. Robertson, E.M. Wijsman, J.L. Rapoport, J.A. Gogos, M. Karayiorgou, Genetic variation at the 22q11 PRODH2/DGCR6 locus presents an unusual pattern and increases susceptibility to schizophrenia; Proceedings of the National Academy of Sciences of the United States of America 99, 3717-3722, 2002.

[16] H.J. Williams, N. Williams, G. Spurlock, N. Norton, S. Zammit, G. Kirov, M.J. Owen, M.C. O'Donovan, Detailed analysis of PRODH and PsPRODH reveals no association with schizophrenia. American Journal of Medical Genetics Part B-Neuropsychiatric Genetics 120B, 42-46, 2003.

[17] H.U. Bender, S. Almashanu, G. Steel, C.A Hu, W.W. Lin, A. Willis, A. Pulver, D. Valle, Functional consequences of PRODH missense mutations; American Journal of Human Genetics 76, 409-420, 2005.

[18] H. Mitsubuchi, K. Nakamura, S. Matzumoto, F. Endo, Inborn errors of proline metabolism; The Journal of Nutrition 138: 2016-2020, 2008.

[19] C.L. Clelland, L.L. Read, A.N. Baraldi, C.P. Bart, C.A. Pappas, L.J. Panek, R. H. Nadrich, J.D. Clelland, Evidence for association of hyperprolinemia with schizophrenia and a measure of clinical outcome; Schizophrenia Research 131:139-145, 2011.

[20] M. Orešič, J. Tang, T. Seppänen-Laasko, I. Mattila, S.E. Saarni, S.I. Saarni, J. Lonnqvist, M.Sysi-Aho, T. Hyotylainen, J. Perälä and J. Suvisaari, Metabolome in schizophrenia and other psychotic disorders: a general population–based study; Genome Medicine 3: 19-33, 2011.

[21] E. Tallarita, L. Pollegioni, S. Servi, G. Molla, Expression in *Escherichia coli* of the catalytic domain of human proline oxidase; Protein Expression and Purification 82: 345-351, 2012.

[22] S. Sacchi, M. Bernasconi, M. Martineau, J.P. Mothet, M. Ruzzene, M.S. Pilone, L. Pollegioni, and G. Molla, pLG72 Modulates Intracellular D-serine levels through its interaction with D-amino acid oxidase – effects on schizophrenia susceptibility; The Journal of Biological Chemistry 283 (32): 22244-22256, 2008.

[23] K. Shoji, S. Mariotto, A.R. Ciampa, H. Suzuki, Regulation of serine racemase activity by D-serine and nitric oxide in human glioblastoma cells; Neuroscience letter: 392 (1-2): 75-78, 2006.

[24] S. Sacchi, P. Cappelletti, S. Giovannardi, L. Pollegioni, Evidence of the interaction of D-amino acid oxidase with pLG72 in glial cell line; Molecular and Cellular Neuroscience 48: 20-28, 2011.

[25] T.M. Maynard, D.W. Meechan, M.L. Dudevoir, D. Gopalakrishna, A.Z. Peters, C.C. Heindel, T.J. Sugimoto, Y. Wu, J.A. Lieberman,1, A.-S. LaMantia, Mitochondrial localization and function of a subset of 22q11 deletion syndrome candidate genes; Molecular and Cellular Neuroscience 39: 439-451, 2008.

[26] Z.C. Ye and H. Sontheimer, Glioma cells release excitotoxic concentrations of glutamate; Cancer Research 59: 4383-4391, 1999.

[27] N.J. Maragakis and J.D. Rothstein, Glutamate transporters: animal models to neurologic disease; Neurobiology of Disease 15: 461-473, 2004.

[28] Z.C. Ye, J.D. Rothstein, H. Sontheimer, Compromised glutamate transport in human glioma cells: reduction-mislocalization of sodium-dependent glutamate transporters and enhanced activity of cystine-glutamate exchange; The Journal of Neuroscience 19 (24): 10767-10777, 1999.

[29] C. Escartin, E. Brouillet, P. Gubellini, Y. Trioulier, C. Jacquard, C. Smadja, G.W. Knott, L. Kerkerian-Le Goff, N. Déglon, P. Hantraye, G. Bonvento, Ciliary neurotrophic factor activates astrocytes, redistributes their glutamate transporters GLAST and GLT-1 to raft microdomains, and improves glutamate handling *in vivo*; The Journal of Neuroscience 26 (22): 5978-5989, 2006.

[30] D. Bauer, V. Haroutunian, J.H. Meador-Woodruff, R.E. McCullumsmith, Abnormal glycosylation of EAAT1 and EAAT2 in prefrontal cortex of elderly patients with schizophrenia; Schizophrenia Research 117 (1): 1-14, 2010.

[31] A. Lee, A.R. Anderson, S.J. Beasley, N.L. Barnett, P. Poronnik, D.V. Powa, A new splice variant of the glutamate–aspartate transporter: cloning and immunolocalization of GLAST1c in rat, pig and human brains; Journal of Chemical Neuroanatomy 43: 52-63, 2012.

[32] J.M. Phang, S.P. Donald, J. Pandhare, Y. Liu, The metabolism of proline, a stress substrate, modulates carcinogenic pathways; Amino Acids 35: 681-690, 2008.

[33] M. Paterlini, S.S. Zakharenko, W.S. Lai, J. Qin, H. Zhang, J. Mukai, K. Westphal, B. Olivier, D. Sulzer, P. Pavlidis, S.S. Siegelbaum, M. Karayiorgou, J.A. Gogos, Transcriptional and behavioral

interaction between 22q11.2 orthologs modulates schizophrenia–related phenotypes in mice; Nature Neuroscience 11 (8): 1586-1594, 2005.

[34] A. Willis, H.U. Bender, G. Steel, D. Valle, Prodh variants and risk for schizophrenia; Amino Acids 35: 673-679, 2008.

[35] E. Lopez-Bayghen, A. Ortega, Glial glutamate transporters: new actors in brain signaling; Life 63 (10): 816-823, 2011.

Fig. 1. Expression of PO in stably transfected U87 clones. Western blot analysis performed using mouse anti-GFP or rabbit anti-PO antibodies confirm the expression of both the fluorescent PO-EYFP wild-type and PO-EYFP L441P fusion proteins (A) or the untagged proteins (B) in transfected U87 cells. The same amount of sample, corresponding to 5 x 10^4 cells or 50 μg of crude extract (EG) was loaded in each lane, as further confirmed by using an anti-actin antibody as internal control. The level of endogenous PO in U87 control cells is below the detection limit (1 ng). The PO EYFP L441P variant detected with anti-PO show a further band of lower molecular mass corresponding to a partial proteolyzed form of the protein. (C, D) Confocal analysis of proline oxidase subcellular distribution in cultured U87 glioblastoma cells stably expressing PO-EYFP wild-type and PO-EYFP L441P. Both the chimeric proteins display a perinuclear "spaghetti like" distribution (yellow channel) which largely overlap (merge panel) with mitochondria specific immunostain (red channel). Scale bar 5 μm.

Fig. 2. U87 cells growth monitored over a period of 7 days. U87 control cells and U87 cells stably expressing PO-EYFP wild-type, PO-EYFP L441P, PO wild-type and PO L441P were seeded in 24 wells plate (10.5 x 10^3 cells/well starting density) and incubated at 37 °C in a 5% CO_2 incubator. The cells were collected and counted every 24 h. The growth curves were expressed as cell density/well vs time.

Fig. 3. HPLC analysis of proline and glutammate cellular level. 8 x 10^4 U87 cells stably expressing PO-EYFP or PO-EYFP L441P were seeded and growth for 72 h. At different incubation times both the culture medium and the cells were collected and analyzed to assay the proline and glutamate content. Panel A shows intracellular proline content: proline concentration remains almost constant over time in control cells (•, continuous black line), while for cells expressing PO EYFP L441P variant (♦, dashed gray line) shows a progressive accumulation; conversely PO-EYFP wild-type variant (■, dotted gray line) proline content shows a decrease. Panel B shows intracellular glutamate content: PO-EYFP L441P (♦, dashed gray line) shows significant higher glutamate content with respect to control U87 not transfected (•, continuous black line) and U87 PO-EYFP expressing cells (■, dotted gray line). Panel C shows extracellular glutamate content; similar glutamate concentrations are evident until 6 h for all U87 cells, while at later incubation time the glutamate concentrations decrease with a different time course. *$p<0.03$; **$p<0.003$; ***$p<0.0003$.

Fig. 4. Western blot analysis of GLAST and GLT-1 glutamate transporters in U87 clones. The same amount of sample corresponding to 1 x 10^5 (lane 1-3-5) or 5 x 10^4 (lane 2-4-6) cells was loaded in each lane, as further confirmed by using an anti-actin antibody as internal control. Panel A and B) the level of PO expression was evaluated using an anti-PO specific antiboby. Quantification analysis (panel B) shows that the GLAST level in U87 cells stably expressing PO-EYFP or PO-EYFP L441P is at least 2-fold higher with respect to U87, while the PO expression level is 1.6-fold higher for PO-EYFP L441P cells then for PO-EYFP wild-type expressing cells. Panel C and D) Western blot analysis of GLT-1 glutamate transporter: quantification analysis shows that U87 and PO-EYFP expressing cells exhibit a comparable level of expression while GLT-1 expression is 2-fold higher in U87 cells stably expressing PO-EYFP L441P.

Fig. 5. Immunohistochemical localization of GLAST and GLT-1 glutamate transporters in control U87 cells and U87 cells stably expressing wild-type and PO-EYFP L441P. Panel A: a) anti-GLAST staining displays predominant signal in correspondence of the plasma membrane with less intense and less diffused labeling in U87 not transfected cells. b) Signals corresponding to the expressed chimeric fluorescent PO-EYFP protein (both the wild-type and the L441P variants) displays a mitochondrial distribution (yellow channel). c) Overlap of the two signals corresponding to the mitochondrial stain (yellow channel) of the overexpressed PO variants and GLAST stain (red channel) confirm the different subcellular distribution of the glutamate transporter vs the PO protein. Panel B): a) anti-GLT-1 staining displays predominant signal in correspondence of the plasma membrane with less intense labeling in control U87 not transfected cells and in U87 stably expressing PO-EYFP. b) Signals corresponding to the expressed chimeric fluorescent PO protein (yellow channel) display a mitochondrial distribution. c) Overlap of the two signals corresponding to the mitochondrial stain (yellow channel) of the overexpressed PO variants and the GLT-1 stain (red channel) confirm the different subcellular distribution of the glutamate transporter (mainly in the plasma membrane) vs the PO proteins (mitochondria).

Fig. 1

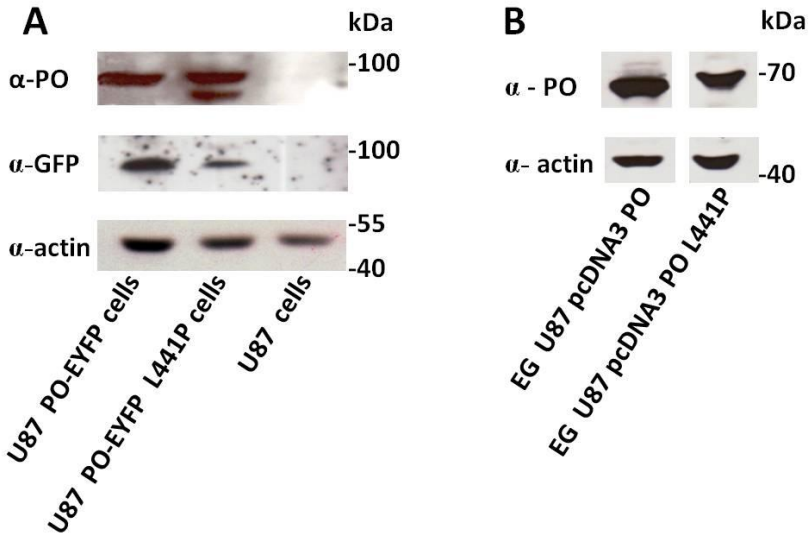
A
kDa
α-PO
-100
α-GFP
-100
α-actin
-55
-40
U87 PO-EYFP cells
U87 PO-EYFP L441P cells
U87 cells
B
kDa
α - PO
-70
α- actin
-40
EG U87 pcDNA3 PO
EG U87 pcDNA3 PO L441P

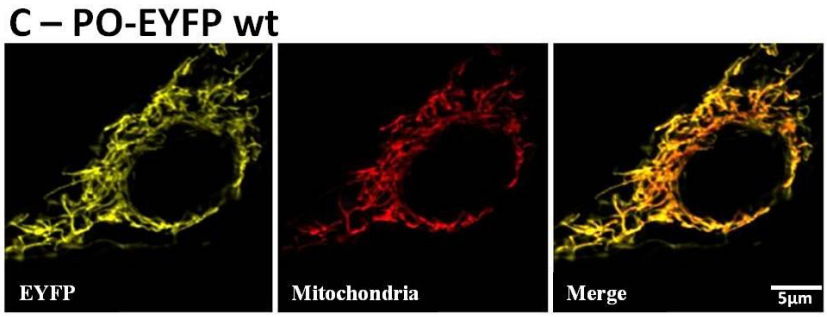
C – PO-EYFP wt
EYFP
Mitochondria
Merge
5µm

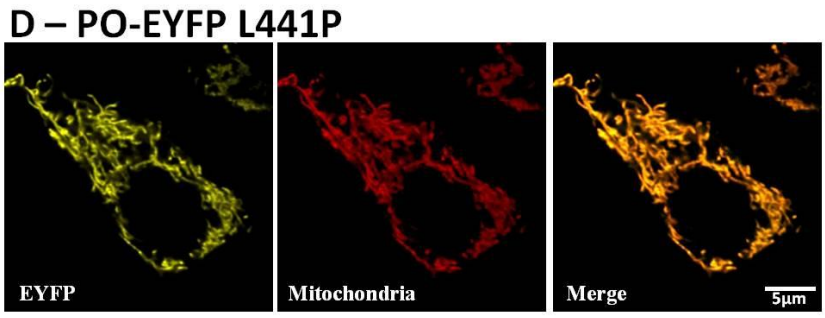
D – PO-EYFP L441P
EYFP
Mitochondria
Merge
5µm

Fig. 2

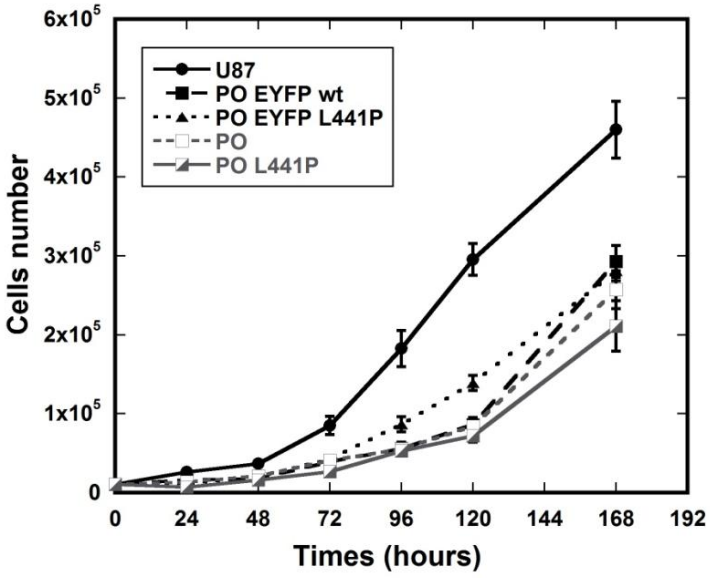
6x10^5
5x10^5
4x10^5
3x10^5
2x10^5
1x10^5
0
Cells number
0
24
48
72
96
120
144
168
192
Times (hours)
U87
PO EYFP wt
PO EYFP L441P
PO
PO L441P

Fig. 3

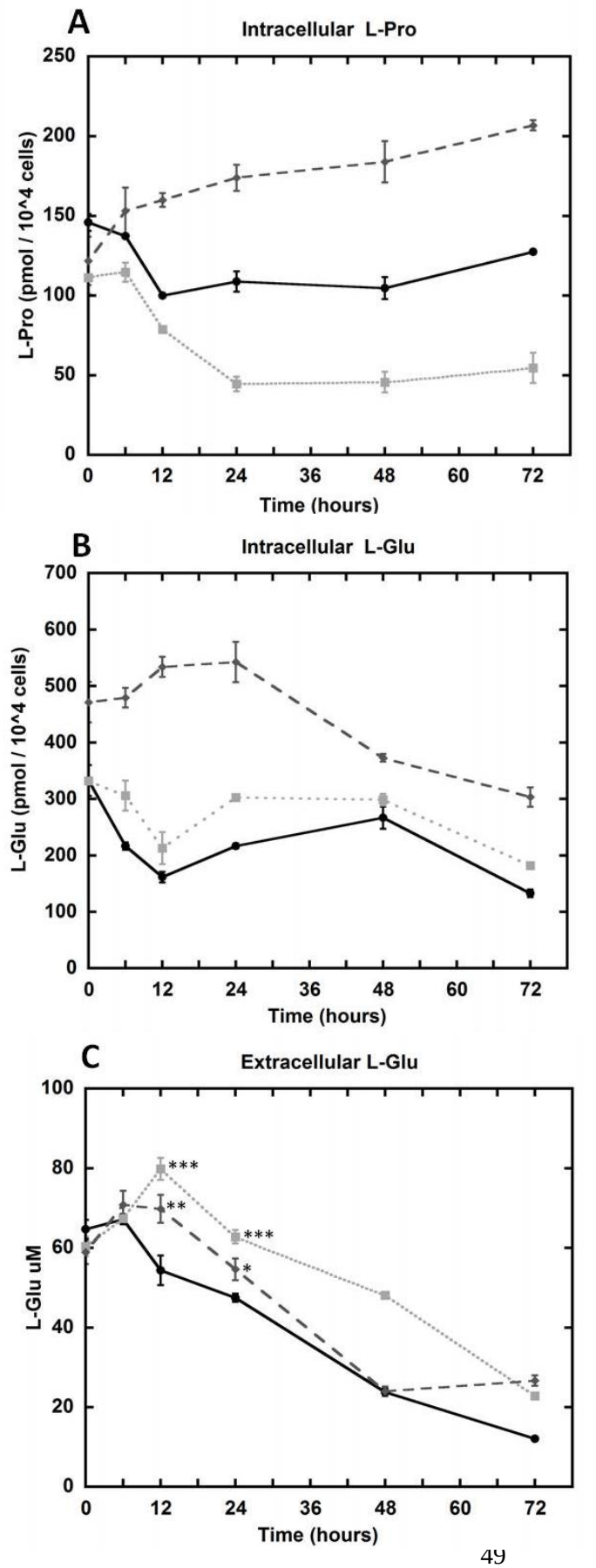
A
Intracellular L-Pro
L-Pro (pmol / 10^4 cells)
250
200
150
100
50
0
0
12
24
36
48
60
72
Time (hours)
B
Intracellular L-Glu
L-Glu (pmol / 10^4 cells)
700
600
500
400
300
200
100
0
0
12
24
36
48
60
72
Time (hours)
C
Extracellular L-Glu
L-Glu uM
100
80
60
40
20
0
***
**
***
*
0
12
24
36
48
60
72
Time (hours)

Fig. 4

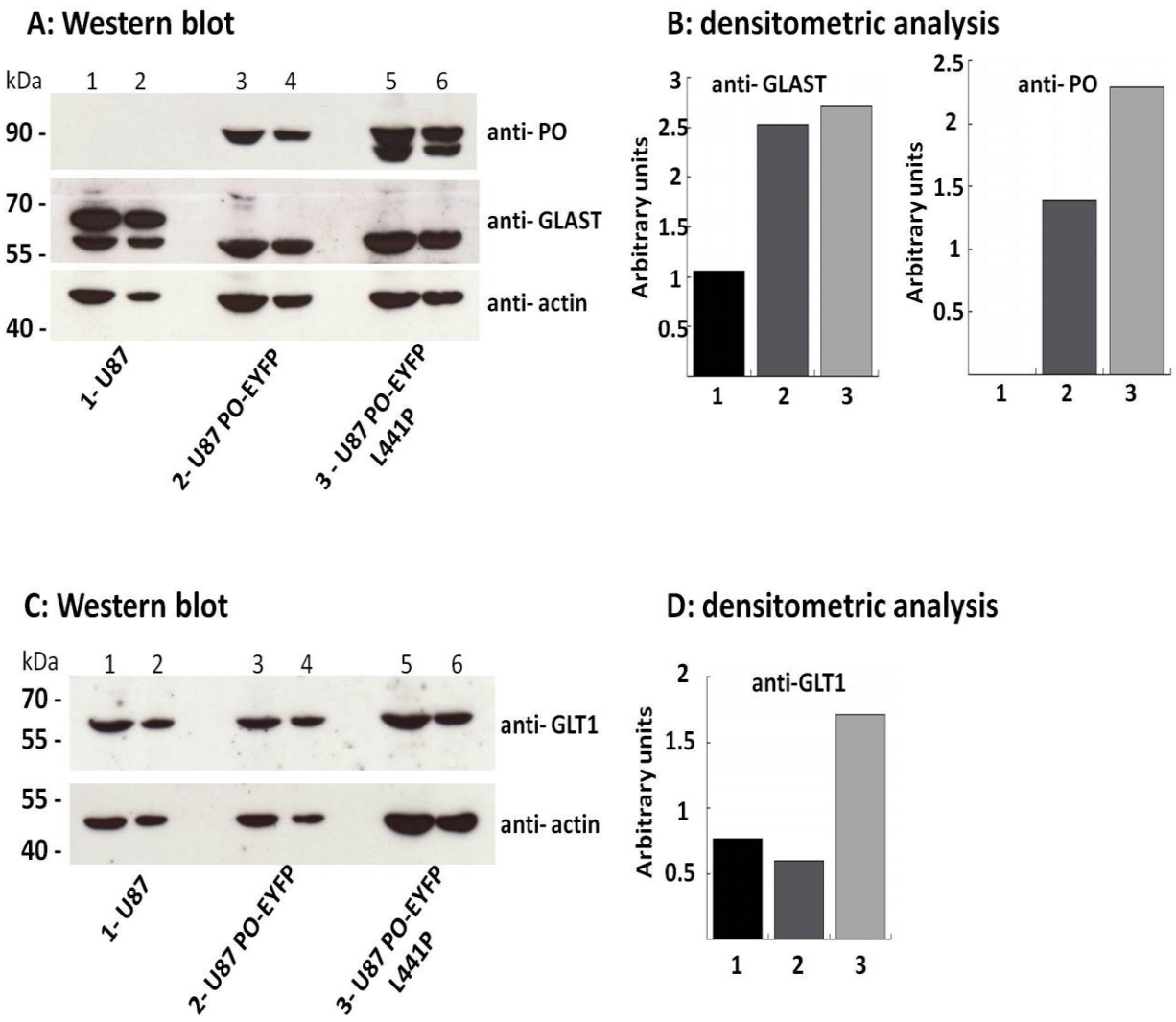
A: Western blot
kDa
1 2 3 4 5 6
90 -
70 -
55 -
40 -
anti- PO
anti- GLAST
anti- actin
1- U87
2- U87 PO-EYFP
3 - U87 PO-EYFP L441P
B: densitometric analysis
anti- GLAST
Arbitrary units
anti- PO
Arbitrary units
C: Western blot
kDa
1 2 3 4 5 6
70 -
55 -
55 -
40 -
anti- GLT1
anti- actin
1- U87
2- U87 PO-EYFP
3- U87 PO-EYFP L441P
D: densitometric analysis
anti-GLT1
Arbitrary units

Fig. 5

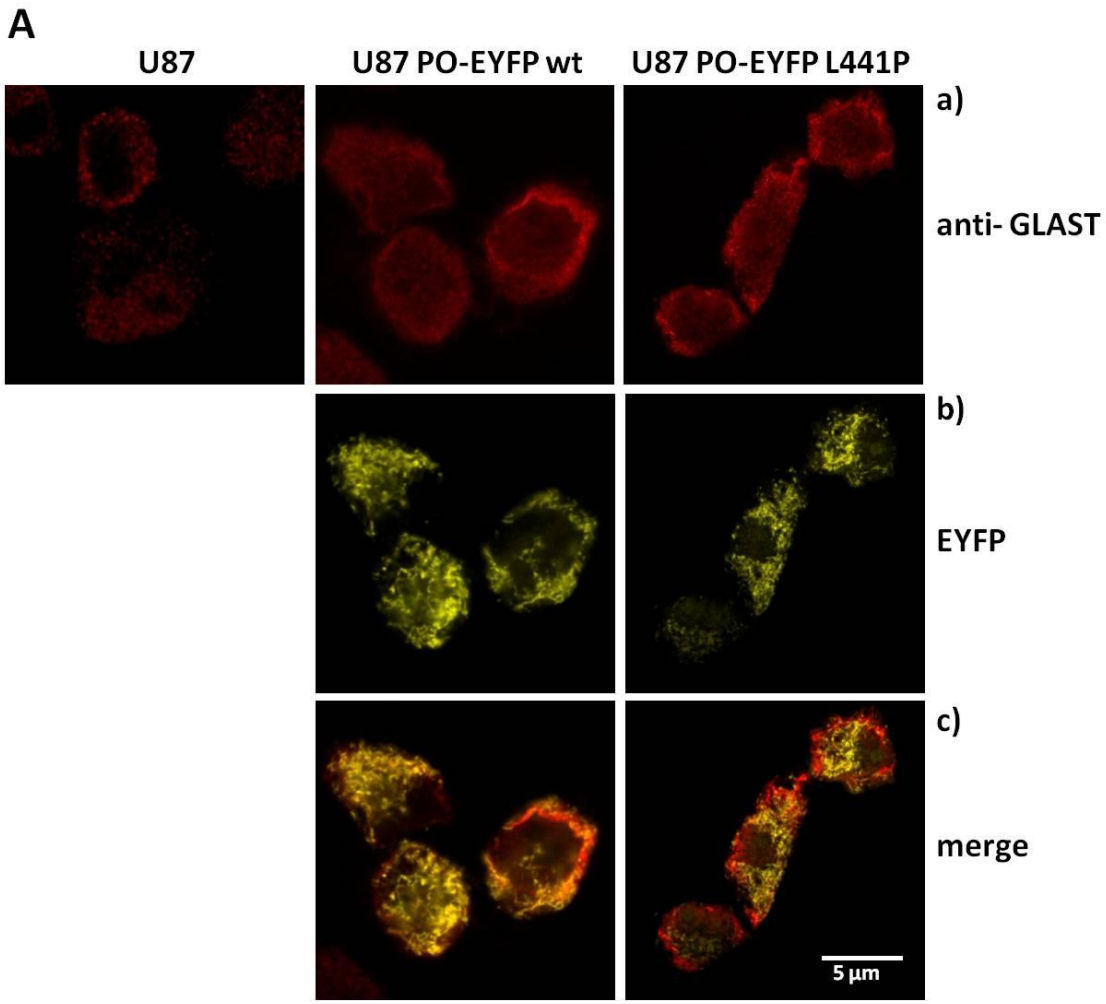
A
U87
U87 PO-EYFP wt
U87 PO-EYFP L441P
a)
anti- GLAST
b)
EYFP
c)
merge
5 µm

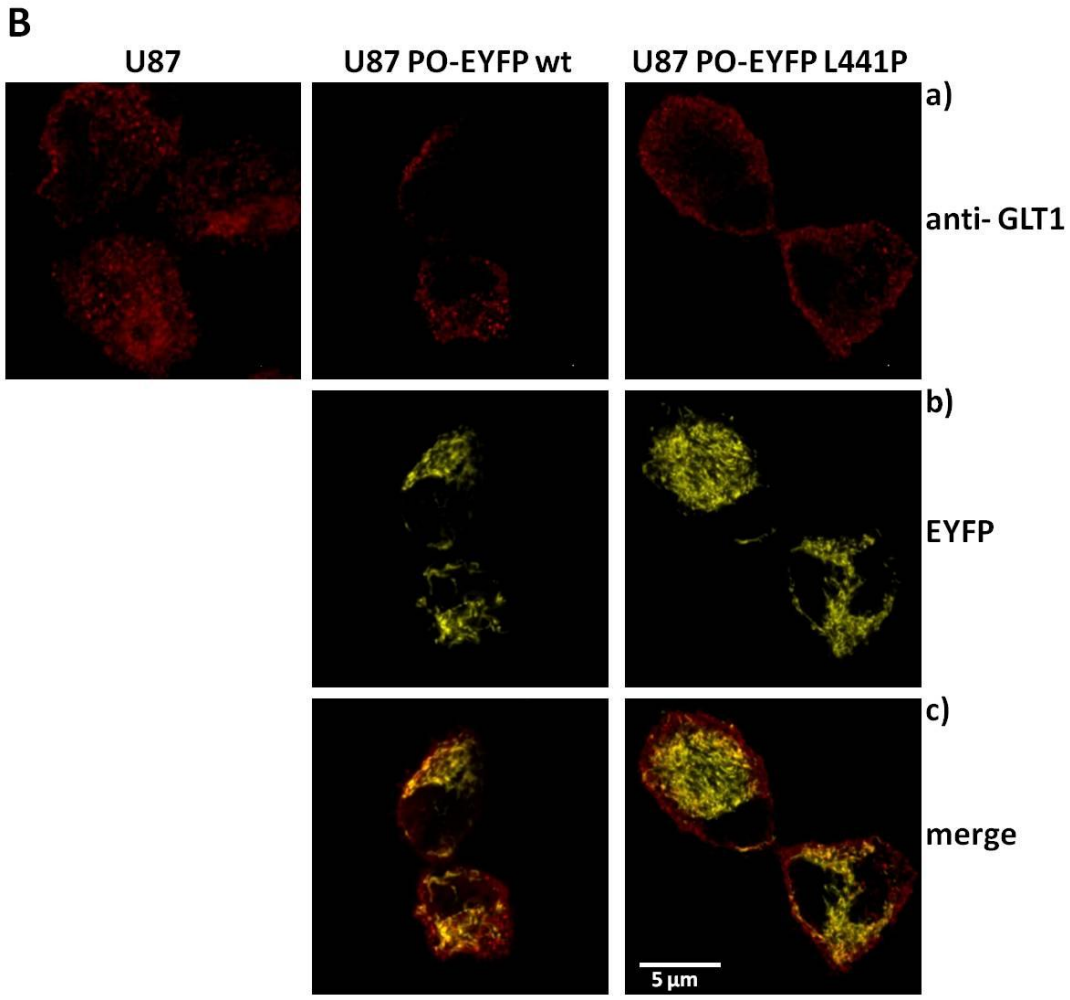
B
U87
U87 PO-EYFP wt
U87 PO-EYFP L441P
a)
anti- GLT1
b)
EYFP
c)
merge
5 µm

4 Discussion

Glutamine and glutamate with proline, histidine, arginine and ornithine, comprise the 25% of the dietary amino acid intake and constitute the “glutamate family” of amino acids, which are disposed to conversion to glutamate [86]. Glutamate is the most abundant free amino acid in the brain and it is the major excitatory neurotransmitters of the vertebrate central nervous system [48]. The reversible cyclization of glutamate produces proline, a key imino acid in bioenergetics, cellular redox control, apoptosis cancer and as recently observed, neurological and cognitive dysfunctions associated to neurodegenerative and psychiatric diseases [9, 33 and references herein]. Accordingly, there is a great interest in understanding the biological roles and biochemical functions of the enzymes that catalyze proline synthesis and degradation.

Since its nitrogen is contained within a pyrrolidine ring, proline is not a substrate for the classical amino acid-metabolizing enzymes (decarboxylases, aminotransferases and racemases): remarkably, a family of proline metabolic enzymes evolved with specific cellular localization and regulation mechanisms [8]. Starting from proline catabolism, all organisms oxidize proline to glutamate in two enzymatic steps coupled by a non equilibrium step: 1) proline is oxidized to Δ^1-pyrroline-5-carboxylic acid (P5C) by the FAD dependent enzyme proline oxidase (PO, EC 1.5.99.8); P5C forms a non enzymatic pH-dependent equilibrium with glutamate semyaldehyde (GSA); 2) P5C dehydrogenase (P5CDH, EC 1.5.1.12) completes the transformation of proline to glutamate by catalyzing the oxidation of GSA, utilizing NAD^+ as the electron acceptor. The biosynthetic pathways for proline has two routes for the formation of GSA from glutamate or ornithine. The glutamate route involves the reaction catalyzed by P5C synthetase (P5CS). The route from ornithine to GSA is catalyzed by the pyrodoxal-5’-phosphate-dependent enzyme ornithine aminotransferase (OAT, EC 2.6.1.13). Finally reduction of P5C to proline is catalyzed by the NADPH-dependent enzyme P5C reductase (P5CR, EC 1.5.1.2) [9; Fig. 1, Fig. 2]. Thus, the aforementioned enzymes constitute a “proline cycle” which represents an important and complex crossroad with other metabolic pathways, through the P5C intermediate which is the connection in this intermediary pathways [8, 24]. Within the cell, the conversion of P5C to proline takes place in the cytosol and participates as a metabolic interlock with the pentose phosphate pathway, while the other metabolic steps of the “proline cycle” take place into mitochondria and link proline and P5C with the TCA cycle and the urea cycle [8]. All these metabolically relevant relationships shall be taken into account in the attempt to define the proline biological functions.

Several inborn errors of proline metabolism caused by impairments in the functionality of the enzymes involved in the "proline cycle" [35], lead to the accumulation of the metabolic intermediates. In the present study, we focused our attention on those related to the mitochondrial inner membrane flavoenzyme PO: PO deficiency has been related to hyperprolinemia type I, a disorder characterized by elevated plasma proline levels caused by deficiency or inactivation of proline oxidase activity. Interestingly, in a significant fraction of hyperprolinemic patients, the disease is frequently associated with mental seizures [38]; moreover, several experimental evidences demonstrated that hyperprolinemia could affect patients with 22q11 deletion syndrome (Di George syndrome, velo-cardio-facial syndrome). Over the past years, it has been shown that the 22q11 deletion predisposes to a range of psychotic conditions prompting the hypothesis that the deleted region represents a predisposition locus for psychotic illness. Notably, there is a large increased risk of schizophrenia and other mental disorders in people with 22q11 deletion syndrome [44] and a recent study on metabolic profile associated with psychotic disorders demonstrated that increased levels of serum proline was specific to schizophrenia [87]. A common feature of 22q11 deletion syndrome is the hemizygous deletion of the *PRODH* gene, encoding for proline oxidase, which is located on chromosome 22q11 [53]. Since the identification of *PRODH,* various mutations (heterozygous and homozygous) have been identified in hyperprolinemic patients with various phenotypes (patients with schizophrenia, 22q11 microdeletion, and/or early neurological impairments). These studies show unambiguously that the severe form of HPI, characterized by neurological manifestation, results from homozygous inactivation/alteration of *PRODH* [35]. In particular, among the reported 16 missense mutation that could affect PO functionality [6], the L441P substitution results in severe reduction of PO activity and, worthy of note, is one of the allele typically found in schizophrenic patients [4]. The *PRODH* gene has been proposed as a candidate risk factor for schizophrenia [55]; the selection of candidate genes usually arise from their known function or their chromosomal localization, and in the last decade it has been established that the most promising susceptibility loci for the onset of schizophrenia were located on chromosome 6q, 13q, 18 and 22q, where also the *PRODH* gene maps [22, 58]. Despite several promising evidences, actually no specific gene variants could be univocally and functionally associated with the disease, so the products of those susceptibility loci need to be biochemically characterized in detail in order to validate at the molecular level the genetic evidences.

Considering the possible intriguing role of proline oxidase in several human pathological conditions, this PhD project focused on the functional characterization of the human PO enzyme

in order to shed light on the complex net of interconnected metabolic pathways that could link intracellular proline levels with glutamate and glutamatergic neurotransmission.

The first part of the project was aimed to the expression of the human recombinant PO in *E. coli*, the most used organism for heterologous protein expression, to subsequently proceed to the biochemical characterization of the flavoprotein. However, the expression of a foreign protein in *E. coli* is often hampered by the presence of peculiar protein features (e.g., post translational modification, the presence of transmembrane domains and/or targeting sequences for specific compartments) and this is exactly the case of proline oxidase: a very low amount of the full length flavoenzyme was produced (< 0.1 mg/L of fermentation broth). Thus were designed deletion variants of human PO lacking the protein regions potentially affecting the expression. We identified the catalytic domain by aligning the sequence of the human enzyme with that of *E. coli* PutA, and we generated a model of its three dimensional structure by using the I-Tasser server. Moreover, *in silico* analysis of the primary sequence of the protein revealed the presence of two regions with high propensity to structural disorder in the N-terminal end of PO that might affect the solubility of the recombinant protein. Based on these analyses, seven deletion variants were designed encompassing a core region corresponding to the entire predicted catalytic site; the variants differ for the presence or the absence of additional upstream or downstream sequences. Among the seven deletion variants designed, only the PO-barrelN-His variant was produced as a soluble active holoenzyme. Despite the produced variant possesses the typical spectral properties and flavin reactivity of flavoprotein oxidases (i.e. a tight interaction with the flavin cofactor and with the inhibitor THFA), PO-barrelN-His specific activity is 3-fold lower than the value previously estimated for the full length PO (0.032 and 0.1 U/mg, respectively) and high K_m values for proline [89]. Different factors, ranging from differences in the sequences of the gene used for the design of the recombinant PO to differences in activity assay and/or protein preparation, might account for the observed discrepancy. Furthermore, we assumed that the fold of PO-barrelN-His variant strictly resembles that of the full length human PO based on the investigated properties, but we cannot rule out that the structural determinants deleted in the PO variants affect in some way the overall conformation, preventing the enzyme from reaching full activity. Nevertheless the purification of a soluble, active human PO variant represents a crucial step in elucidation of the structure-function relationships of this enzyme. Moreover the expressed variant represents the starting point for the generation of active-site variants containing those substitutions that have been shown to be related to human pathologies, and the elucidation of their actual effect on the enzyme functionality.

In the second part of the project we reported the expression of the human recombinant full length PO in U87 glioblastoma cells: we obtained both the wild-type and the L441P inactive variant enzyme as chimeric proteins fused with EYFP at the C-terminus (in order to leave the N-terminal mitochondrial targeting sequences unmasked). By confocal analysis of U87 cells stably expressing PO-EYFP and PO-EYFP L441P we observed that both enzyme variants were properly localized to the mitochondria, this suggesting that neither the EYFP fused protein nor the substitution introduced to inactivate the flavoenzyme (L441P) affected the correct folding of the protein, since the protein variants were correctly targeted and no evidence of protein aggregates was apparent.

By the way, since the fused EYFP tag could in some way affect PO catalytic activity we expressed also both wild-type and L441P PO variant as untagged recombinant proteins. To investigate PO biological function in the U87 cell system, we tried to evaluate the activity of the PO variants in the cell extracts of U87 cells stably expressing PO EYFP, PO EYFP L441P, PO and PO L441P by using the o-AB method [90]. Unfortunately we were unable to obtain consistent activity values. In order to evaluate PO activity in the cell, the variation in the intracellular proline content was assessed by HPLC analyses. U87 cells expressing PO-EYFP and PO-EYFP L441P were used (chosen because we can verify at each step the fraction of cells expressing the chimeric proteins at the fluorescence microscope). In U87 cells stably expressing PO-EYFP a 2.3-fold lower intracellular proline content with respect to U87 control cells was observed, while in U87 cells stably expressing the PO-EYFP L441P inactive variant, a progressive accumulation of proline was evident: a 1.6-fold higher intracellular concentration compared to control cells was detected. These results show that PO-EYFP is active, while PO-EYFP L441P activity is largely affected by the introduced substitution.

Subsequently, we tempted to correlate proline oxidase activity with glutamate cellular concentration in order to expand the overview on the “proline cycle” and the linked, complex metabolic network. PO-EYFP L441P cells show higher intracellular glutamate level compared to U87 PO-EYFP and the control cells. An explanation of this scenario is possible, if we consider glutamate as a precursor of proline, in this perspective it is conceivable that when proline degradation is prevented (by the over-expression of an inactive proline oxidase) “proline cycle” is unbalanced and the shift in the equilibrium results in the intracellular glutamate accumulation. We analyzed also the extracellular glutamate content, detecting significant differences among cultures of cells expressing the different PO variants. In particular, higher glutamate level were observed in the medium of U87 PO EYFP cells then in control ones. Considering that in these cells the rate of proline degradation is boosted by the over-expression of the flavoenzyme, we

supposed that proline itself can unbalance the "proline cycle" (becoming the most abundant metabolic glutamate precursor) and cause the release by the cells of the glutamate produced.
We then investigated the expression of two glial glutamate transporters: GLAST and GLT-1 which (in physiological conditions) are the two major Na^+-dependent glutamate transporters in CNS. Termination of glutamatergic activity occurs through the glial uptake of the neurotransmitters: the maintenance of the extracellular glutamate concentration below neurotoxic level is a critical function of glial glutamate transporters [91]. Interestingly, glioma cells demonstrate impaired glutamate transporter expression [84]: they most likely results mislocalized, drastically reducing the cells capability of glutamate uptake. Moreover these tumor cells display a strong Na^+-independent cystine/glutamate exchange which induces glutamate efflux outside the cells and outweighs the inward glutamate transport leading to the accumulation of glutamate in the extracellular space [91]. Notably, in the U87 model cell system, we observed that the over-expression of the PO-EYFP L441P variant, which increases proline cellular levels, influences the level of expression of the selected glutamate transporter. On the other hand, GLAST levels in U87 cells expressing PO-EYFP and U87 PO-EYFP L441P cells appear very similar, even though the amount of expressed PO between the two cells clones is substantially different. Moreover, confocal analysis showed that even though the transporters are mainly located in the cell membrane, in part they appeared diffused in the cytosol: this result agrees with previously reported observations that in glioma cell the transporters are often mislocalized and their expression and traslocation at the plasma membrane could be reduced [92]. These findings suggest that the U87 glioblastoma cell system is too complex to investigate the effect of the variation of proline cellular concentration on the synthesis and release of glutamate. Further studies in a most physiological cellular system are needed in this regard. However, the produced U87 cells represent a suitable expression system to produce significant levels of human full length PO variant and to assess its role on proline levels.

The expression of the soluble active PO-barrelN-His variant, as obtained in the first part of this PhD project represents a fundamental step in elucidating the structure-function relationships of human proline oxidase: to our knowledge, this is the first biochemical characterization of the human PO. This result paves the way for studying the effect of the reported polymorphisms associated with pathological conditions (HPI and psychiatric diseases) at the molecular level allowing to answer the many question regarding proline/P5C redox cycle and possibly to design new structure-based drugs that will modulate the cellular concentration of proline (and glutamate) by affecting PO activity. The L441P mutation we introduced to inactivate PO

flavoenzyme, is considered one of the most deleterious mutation: Leu 441 is located in the active site of the enzyme, and its substitution by Pro has been shown to inactivate PO by disrupting the correct interaction between the substrate (proline) and the FAD cofactor [6].

Further studies, will allow to design new molecules that by specifically binding to PO active site will modulate its activity and consequently proline cellular concentration, likely inducing a concomitant variation in glutamate levels. In this regard, we demonstrated at the molecular and cellular level that the expression of an active or an inactive form of PO differently affect the intracellular equilibrium of the metabolite pathways linked with the “proline cycle”. Nevertheless, further investigations are required to elucidate the mechanisms by which proline might exert its function as a putative neuromodulator in physiological and pathological conditions. Considering our preliminary results it is tempting to speculate that proline and glutamate are strictly interconnected and that proline is not less important than glutamine as metabolic precursor of glutamate.

Our work is aimed at shed light on the role exerted by proline oxidase in the framework of glutamatergic neurotransmission; this will be useful to elucidate the molecular mechanism responsible of the schizophrenia onset. In this prospective the flavoenzyme would become a new putative therapeutic target.

5 References

[1] J.M. Phang, W. Liu, Proline metabolism and cancer; Frontiers in Bioscience 17: 1835-1845, 2012.

[2] J.M. Phang, G.C. Yeh, C.H. Hagendorm, The intracellular proline cycle; Life Science 28: 53-58, 1981.

[3] C. Servet, T. Ghelis, L. Richard, A. Zilberstein, A. Savoure, Proline dehydrogenase: a key enzyme controlling cellular homeostasis; Frontiers in bioscience 17 (1): 607-620, 2012.

[4] A. Willis, H.U. Bender, G. Steel, D. Valle, Prodh variants and risk for schizophrenia; Amino Acid 35: 673-679, 2008.

[5] J.M. Phang, W. Liu, C. Hancock, K.J. Christian, The proline regulatory axis and cancer; Frontiers in Oncology 2: 1-12, 2012.

[6] H.U. Bender, S. Almashanu, G. Steel, C.A. Hu, W.W. Lin, A. Willis, A. Pulver, D. Valle, Functional consequence of prodh missense mutation; American Journal of Human Genetics 76: 409-420, 2005.

[7] L. Szabados, A. Savourè, Proline: a multifunctional amino acid; Trends in Plants Science 15: 89-97, 2009.

[8] J.M. Phang, C.A. Hu, D. Valle, Disorders of proline and hydroxyproline metabolism. The Metabolic and Molecular Bases of Inherited Disease, 8th ed. Scriver C.R., Beaudet A.R., Sly W., Valle D. (eds), McGraw-Hill, New York, 1821-1838, 2001.

[9] J.J. Tanner, Structural biology of proline catabolism; Amino Acid 35: 719-730, 2008.

[10] R.K. Singh, J.J. Tanner, Unique structural features and sequences motifs of proline utilization A (PutA); Frontiers in Bioscience 17: 556-568, 2012.

[11] S. Vilchez, M. Manzanera, J.L. Ramos, Control of expression of divergent pseudomaonas putida put promoters for proline catabolism; Applied Environment Microbiology 66 (12): 5221-5225, 2000.

[12] M.A. Moxley, J.J. Tanner, D.F. Becker, Steady-state kinetic mechanism of the proline: ubiquinone oxidoreductase activity of proline utilization A (PutA) from *Escherichia coli*; Archives of Biochemistry and Biophysics 516 (2): 113-120, 2011.

[13] M. Luo, B.W. Arentson, D. Srivastava, D.F. Becker, J.J. Tanner, Crystal structure and kinetics of monofunctional proline dehydrogenase provide insight into substrate recognition and conformational changes associated with flavin reduction and product release; Biochemistry 51: 10099-10108, 2012.

[14] T.A. White, N. Krishnan, D.F. Becker, J.J. Tanner, Structure and kinetics of monofunctional proline dehydrogenase from thermus thermophilus; Journal of Biological Chemistry 282 (19): 14316-14327, 2007.

[15] W. Zhang, M. Zhang, W. Zhu, Y. Zhou, S. Wanduragala, D. Rewinkel, J.J. Tanner, D.F. Becker, Redox-induced changes in flavin structure and roles of flavin N(5) and the ribityl 2'-OH group in regulating PutA-membrane binding; Biochemistry 46: 483-491, 2007.

[16] N. Krishnan, D.F. Becker, Oxygen Reactivity of PutA from helicobacter species and proline-linked oxidative stress; Journal of Bacteriology 188 (4): 1227-1235, 2006.

[17] S. Wanduragala, N. Sanyal, X. Liang, D.F. Becker, Purification and characterization of Put1p from *Saccharomices cerevisiae*; Archives of Biochemistry and Biophysics 498: 136-142, 2010.

[18] V. Massey, F. Muller, R. Fedelberg, M. Schuman, P.A. Sullivan, L.G. Howell, S.G. Mayhew, R.G. Matthews, G.P. Foust, The reactivity of flavoproteins with sulfite; The Journal of Biological Chemistry 244 (15): 3999-4006, 1969.

[19] M.P. Vinod, P. Bellur, D.F. Becker, Electrochemical and functionsl characterization of the proline dehydrogenase domain of PutA flavoprotein from *E. coli*; Biochemistry 41: 6525-6532, 2002.

[20] M.A. Moxley, D.F. Becker, Rapid reaction kinetics of proline dehydrogenase in the multifunctional proline utilization a protein; Biochemistry 51: 511-520, 2012.

[21] V. Massey, The chemical and biological versatility of riboflavin; Biochemical Society Translation 28: 283-296, 2000.

[22] H. Liu, G.R. Abecasis, S.C. Health, A. Knowles, S. Demars, Y.J. Chen, J.L. Roos, J.L. Rapoport, J.A. Gogos, M. Karayorgou, Genetic variation in the 22q11 locus and susceptibility to schizophrenia; Proceeding of the National Academy of Science USA 99: 16859-16864, 2002.

[23] S.K. Cooper, J. Pandhare, S.P. Donalds, J.M. Phang, A novel function of hydroxyproline oxidase in apoptosis through generation of reactive oxygen species; Journal of Biological Chemistry 283 (16): 10485-10492, 2008.

[24] J.M. Phang, S.P. Donald, J. Pandhare, Y.Liu, The metabolism of proline, a stress substrate, modulates carcinogenic pathways; Amino Acid 35: 681-690, 2008.

[25] S.A. Maxwell, A. Rivera, Proline oxidase induces apoptosis in tumor cells, and its expression is frequently absent or reduced in renal carcinomas; Journal of Biological Chemistry 278: 9784-9789, 2003.

[26] C.A.A. Hu, J. Yu, W.W. Lin, S.P. Donald, X.Y. Sun, S. Almashanu, G. Steel, J.M. Phang, B. Volgestein, D. Valle, Overexpressionof proline oxidase, a p53 induced genes (PIG6) induces reactive oxygen species generation and apoptosis in cancer cells; Proceedings of the American Association for Cancer Research 42: 225-232, 2001.

[27] Y. Liu, G.L. Borchert, S.P. Donald, B.A. Diwan, M. Anver, J.M. Phang, Proline oxidase functions as a mitochondrial tumor suppressor in human cancers; Cancer Research 69 (16): 6414-6422, 2009.

[28] J. Dobruckia, Z. Darzynkiewicz, Chromatin condensation and sensitivity of DNA in situ to denaturation during cell cycle and apoptosis - a confocal microscopy study; Micron 32: 645-652, 2001.

[29] Y. Liu, G.L. Borchert, A. Surazynski, C.A. Hu, J.M. Phang, Proline oxidase activates both intrinsic and extrinsic pathways for apoptosis: the role of ROS/superoxides, NFAT and MEK/ERK signaling; Oncogene 25: 5640-5647, 2006.

[30] O. Zabirnyk, W. Liu, S. Khalil, A. Sharma, J.M. Phang, Oxidized low-density lipoproteins upregulate proline oxidase to initiate ROS-dependent autophagy; Carcinogenesis 31: 446-454, 2010.

[31] L. Galluzzi, J.M. Vicencio, O. Kepp, E. Tasdemir, M.C. Maiuri, G. Kroemer, To die or not to die: that is the autophagic question; Current Opinion in Molecular Medicine 8: 78-91, 2008.

[32] J.M. Phang, J. Pandhare, Y.Liu, The metabolism of proline as microenvironmental stress substrate; The Journal of Nutrition 138: 2008 -2015, 2008.

[33] A.T.S. Wyse, C.A. Netto, Behavioral and neurochemical effects of proline; Metabolic Brain Disease 26: 159-172, 2011.

[34] J.A. Gogos, D.J. Gerber, Schizoprenia susceptibility genes: emergence of positional candidates and future directions; Trends in Pharmacological Science 27(4): 226-233, 2006.

[35] H. Mitsubuchi, K. Nakamura, S. Matzumoto, F. Endo, Inborn errors of proline metabolism; The Journal of Nutrition 138: 2016-2020, 2008.

[36] M. Van Spronsen, C.C. Hoogenraad, Synapse pathology in psychiatric and neurologic disease; Current Neurology and Neuroscience Reports 10 (3): 207-214, 2010.

[37] P. Roussous, S.G. Giakoumaki, P. Bitsios, A risk PRODH haplotype affects sensorimotor gating, memory, schizotypy, and anxiety in healthy male subjects; Biological Psychiatry 65 (12): 1063-1070, 2009

[38] S.M. Cohen, J.V. Nadler, Proline induced inhibition of glutamate release in hippocampal area CA1; Brain Research 769: 333-339, 1997.

[39] J.V. Nadler, Sodium-dependent proline uptake in the rat hyppocampal formation: association with ipsilateral commissural projection of CA3 pyramidal cells; Journal of Neurochemistry 49: 1155-1160, 1987.

[40] F.T. Crump, R.T. Fremau Jr., A.M. Craig, Localization of the brain-specific high-affinity L-proline transporter in cultured hippocampal neurons: molecular heterogeneity of synaptic terminals; Molecular and Cellular Neuroscience 13: 25-39, 1999.

[41] S.E. Renick, D.T. Kleven, J. Chan, K. Stenius, T.A. Milner, V.M. Pickel, R.T. Fremau Jr., The mammalian brain high-affinity L-proline transporter is enriched preferentially in synaptic vescicles in a subpopulation of excitatory nerve terminals rat forebrain; The Journal of Neuroscience 19 (1): 21-33, 1999.

[42] R.T. Fremau Jr., M.G. Caron, R.D. Blakely, Molecular cloning and expression of high affinity proline transporter expressed in putative glutamatergic pathway of rat brain; Neurons 8: 915-926, 1992.

[43] D.C. Hayward, S.J. Delaney, H.D. Cambell, A. Ghysen, S. Benzer, A.B. Kasprazak, J.N. Cotsell, I.G. Young, G.L. Gabor Miklos, The sluggish-A gene of *Drosophila melanogaster* is expressed in the nervpous system and encodes proline oxidase, a mitochondrial enzyme involved in glutamate biosynthesis; Proceeding of the National Academy of Science 90: 2979-2983, 1993.

[44] M. Paterlini, S.S. Zakharenko, W.S. Lai, J. Qin, H. Zhang, J. Mukai, K. Westphal, B. Olivier, D. Sulzer, P. Pavlidis, S.S. Siegelbaum, M. Karayiorgou, J.A. Gogos, Transcriptional and behavioral interaction between 22q11.2 orthologs modulates schizophrenia–related phenotypes in mice; Nature Neuroscience 11 (8): 1586-1594, 2005.

[45] A. Cherkin, M.J. Eckardt, L.K. Gerbrandt, Memory: proline induces retrograde amnesia in chicks; Science 193: 242-244, 1976.

[46] J.C. Moreira, C.M. Wannmacher, S.M. Costa, M. Wajner, Effect of proline administration on rat behavior in aversive and non aversive tasks; Pharmacology Biochemistry and Behavior 32: 885-890, 1989.

[47] N.J. Maragakis, J.D. Rothstain, Glutamate transporters in neurological disease; Archives of Neurology 58: 365-370, 2001.

[48] N.C. Danbolt, Glutamate uptake; Progress in Neurobiology 65: 1-105, 2001.

[49] V.D.B. Henzi, S.W. Helm, A.B. MacDermott, L-Proline activates glutamate and glicine receptors in cultured rat dorsal horn neurons; Molecular Pharmacology 41: 793-801, 1992.

[50] X.C. Yu, W. Zhang, A. Oldham, E. Buxton, S. Patel, N. Nghi, D. Tran, T.H. Lanthorn, C. Bomont, Z.C. Shi, Q. Liu, Discovery and characterization of potent small molecule inhibitors of the high-affinity proline transporter; Neuroscience Letter 451: 212-216, 2009.

[51] D. Delwing, C.S. Bavaresco, C.M. Wannmacger, M. Wajner, C.S Dutra-Hilgo, A.T. Wyse, Proline induces oxidative stress in cerebral cortex of rat; International Journal of Developmental Neuroscience 21: 105-110, 2003.

[52] Y. Liu, G.L. Borchert, S.P. Donalds, A. Surazynski, C.A. Hu, C.J. Weydert, L.W. Oberley, J.M. Phang, MnSOD inhibits proline oxidase induced apoptosis in colorectal cancer cells; Carcinogenesis 26: 1335-1342, 2005.

[53] C.L. Clelland, L.L. Read, A.N. Baraldi, C.P. Bart, C.A. Pappas, L.J. Panek, R.H. Nadrich, J.D. Clelland, Evidence for association of hyperprolinemia with schizophrenia and a measure of clinical outcome; Schizophrenia Research 131: 139-145, 2011.

[54] H. Jacquet , G. Raux, F.F. Thibaut, B. Hecketsweiler, E. Houy, C. Demilly, S. Haouzir, G. Allio, G. Fouldrin, V. Drouin, J. Bou, M. Petit, D. Campion, T. Frébourg, PRODH mutation and hyperprolinemia in a subset of schizophrenic patients; Human molecular genetics (11) 19: 2243-2249, 2002.

[55] C.M.P. O'Tuathaigh, D. Bobovic, G. O'Meara, J.J. Clifford, D.T. Croke, J.L. Waddington, Susceptibility genes for schizophrenia: characterization of mutant mouse models at the level of phenotypic behavior; Neuroscience and Biobehavioural Reviews 31: 60-78, 2007.

[56] G.K. Thaker, W.T. Carpenter, Advances in schizophrenia; Nature Medicine 7: 667-671, 2001.

[57] R. Freedman, Schizophrenia; New England Journal of Medicine 349: 1738-1749, 2003.

[58] R.Tandon, M.S. Keshavan, H.A. Nasrallah, Schizophrenia, "just the facts" what we know in 2008. 2: epidemiology and etiology; Schizophrenia Research 102: 1-18, 2008

[59] D.C. Javitt, Glutamatergic theories of schizophrenia; Israel Journal of Psychiatry & Related Sciences 47 (1): 4-16, 2010.

[60] D. G. Pearlson, Neurobiology of schizophrenia; Annals of Neurology 48 (4): 556-566, 2000.

[61] U.E. Lang, I. Puls, D.J. Müller, N. Strutz-Seebohm, J. Galliant, Molecular mechanism of schizophrenia; Cellular Physiology Biochemistry 20: 687-702, 2007.

[62] A. Sawa, S.H. Snyder, Schizophrenia: neural mechanism for novel therapies; Molecular Medicine 9(1-2): 3-9, 2003.

[63] J.S. Kim, H.H. Korhuber, W. Schmid-Burgk, B. Holzmuller, Low cerebrospinal fluid glutamate in schizophrenic patients and a new hypothesis on schizophrenia; Neuroscience Letter 20: 379-382, 1980.

[64] M.S. Keshavan, R. Tandon, N.N. Boutros, H.A. Nasrallah, Schizophrenia, "just the facts" what we know in 2008. 3: neurobiology; Schizophrenia Research 106: 89-107, 2008.

[65] C. Konradi, S. Heckers, Molecular aspects of glutamate dysregulation; implications for schizophrenia and its treatment; Pharmacology and Therapeutics 97: 153-179, 2003.

[66] T.L. Schwartz, S. Sachdeva, S.M. Stahl, Glutamate neurocircuitry: theoretical underpinnings in schizophrenia; Frontiers in Pharmacology 3 (195): 1-11, 2012.

[67] J.T. Coyle, G. Tsai, D. Goff, Converging evidences of NMDA receptor hypofunction in the pathophysiology of schizophrenia; Annals of the New York Academy of Science 1003: 318-327, 2003.

[68] K. Prybylowski, R.J. Wenthold, N-methyl-D-aspartate receptors: subunit assembly and trafficking to the synapse; Journal of Biological Chemistry 279: 9673-9676, 2004.

[69] J.A. Kemp, R.M. Mckeran, NMDA receptor pathways as drug targets, Nature Neuroscience 5: 1038-1042, 2002.

[70] A. Inanobe, H. Furukawa, E. Gouaux, Mechanisms of partial agonist action at the NR1 subunit of NMDA receptors, Neuron 47: 71-84, 2005.

[71] R.J. Wenthold, K. Prybylowski, S. Stanley, N. Sans, R.S. Petralia, Trafficking of NMDA receptors; Annual Review of Pharmacology 43: 335-358, 2003.

[72] H.V. Friedman, T. Bresler, C.C. Garner, N.E. Ziv, Assembly of new individual excitatory synapses, time course and temporal order of synaptic molecular recruitment; Neurons 27: 57-69, 2000.

[73] A.F. Schinder, E.C. Olson, N.C. Spintzer, M. Montal, Mitochondrial dysfunction is a primary event in glutamate neurotoxicity; Journal of Neuroscience 16: 6125-6133, 1996.

[74] J.T. Kantrowitz, D.C. Javitt, N-methyl-D-aspartate (NMDA) receptor dysfunction or deregulation: The final common pathway on the road to schizophrenia?; Brain Research Bulletin 83: 108-121, 2010.

[75] M.J. Niciu, B. Kelmendi, G. Sanacora, Overview of glutamatergic neurotransmission in the nervous system; Pharmacology, Biochemistry and Behavior 100: 656-664, 2012.

[76] T. Walsh, J.M. McClellan, S.E. McCarthy, A.M. Addington, S.B. Pierce, G.M. Cooper, A.S. Nord, M. Kusenda, D. Malhotra, A. Bhandari, S.M. Stray, C.F. Rippey, P. Roccanova, V. Makarov, B. Lakshmi, R.L. Findling, L. Sikich, T.Stromberg, B. Merriman, N. Gogtay, P. Butler, K. Eckstrand, L. Noory, P. Gochman, R. Long, Z. Chen, S. Davis, C. Baker, E.E. Eichler, P.S. Meltzer, S.F. Nelson, A.B. Singleton, M.K. Lee, J.L. Rapoport, M.C. King, J. Sebat, Rare structural variants disrupt multiple genes in neurodevelopmental pathways in schizophrenia; Science 320: 539-543, 2008.

[77] R.M. Karlsson, K. Tanaka, L.M. Saksida, T.J. Bussey, M. Heilig, A. Holmes, Assessment of glutamate transporter GLAST (EAAT1)-deficient mice for phenotypes relevant to the negative and executive/cognitive symptoms of schizophrenia; Neuropsychopharmacology 34: 1578-1589, 2009.

[78] F. Papaleo, B.K. Lipska, D.R. Weinberger, Mouse models of genetic effects on cognition: relevance to schizophrenia; Neuropharmacology 62: 1204-1220, 2012.

[79] A. Furuta, J.D. Rothstain, L.J. Martin, Glutamate transporter protein subtype are expressed differentially during rat CNS development; Journal of Neuroscience 17: 8363-8375, 1997b.

[80] N.C. Danbolt, J. Storm-Mathisen, B.I. Kanner, An [Na^+K^+]-coupled L-glutamate transporter purified from rat brain is located in glial cell processes; Neuroscience 51: 295-310, 1992.

[81] W. Chen, C. Aoki, V. Mahadomrongkul, C.E. Gruber, G.J. Wang, R. Blitzlzau, N. Irwin, P.A. Rosenberg, Expression of a variant form of the glutamate transporter GLT1 in neuronal cultures and in neurons and astrocytesin the rat brain; Journal of Neuroscience 22: 2142-2152, 2002.

[82] Y. Kanai, M.A. Hediger, Primary structure and functional characterization of high affinity glutamate transporter; Nature 360: 467-471, 1992.

[83] O. Barpeled, H. Benhur, A. Biegon, Y. Groner, S.Dewhurst, A. Furuta, J.D Rothstein, Distribution of glutamate transporter subtypes during human brain development; Journal of Neurochemistry 69: 2571-2580, 1997.

[84] D.V. Pow, N.L. Barnett, Developmental expression of excitatory amino acid transporters: a photoreceptor and bipolar cell glutamate transporter in rat retina; Neuroscience 280: 21-24, 2000.

[85] N.J. Maragakis, J.D. Rothstein, Glutamate transporters: animal models to neurological disease; Neurobiology of Diseases 15: 461-473, 2004.

[86] H. Tapiero, G. Mathé, P. Couvreur, K.D. Tew, Glutamine and glutamate; Biomedicine and Pharmacotherapy 56: 446-457, 2002.

[87] M. Oresic, J. Tang, T. Seppanen-Laasko, I. Mattila, S.E. Saarni, S.I. Saarni, J. Lonnqvist, M. Sysi-Aho, T. Hyotylainen, J. Perala, J. Suvisaari, Metabolome in schizophrenia and other psychotic disorders: a general population-based study; Genome Medicine 3: 19-33, 2011.

[88] E. Tallarita, L. Pollegioni, S. Servi, G. Molla, Expression in Escherichia coli of the catalytic domain of human proline oxidase; Protein Expression and Purification 82: 345-351, 2012.

[89] N. Krishnan, M.B. Dickman, D.F. Becker, Proline modulates the intracellular redox environment and protects mammalian cells against oxidative stress; Free Radical Biology and Medicine 44: 671- 681, 2008.

[90] J. Pandhare, S.P. Donalds, S.K. Cooper, J.M. Phang, Regulation and function of proline oxidase under nutrient stress; Journal of cellular Biochemistry 107: 759-768, 2009.

[91] E. Lopez-Bayghen, A. Ortega, Glial glutamate transporters: new actors in brain signaling; Life 63 (10): 816-823, 2011.

[92] Z.C. Ye, J.D. Rothstein, H. Sontheimer, Compromised glutamate transport in human glioma cells: reduction-mislocalization of sodium-dependent glutamate transporters and enhanced activity of cystine-glutamate exchange; The Journal of Neuroscience 19 (24): 10767-10777, 1999.

6 Other publication

Comparison of the baculovirus-insect cell and *Pichia pastoris* heterologous systems for the expression of the human tumor suppressor protein RNASET2

Biotechnology and Applied Biochemistry

Paola Campomenosi,[1] Raffaella Cinquetti,[1] Elena Tallarita,[1] Christer Lindqvist,[2] Ivan Raimondi,[1] Paola Grassi,[3] Johnny Näsman,[2] Anne Dell,[3] Stuart M. Haslam,[3] Roberto Taramelli,[1] and Francesco Acquati[1*]*

[1]*Department of Biotechnology and Molecular Sciences, University of Insubria, Varese, Italy*

[2]*Department of Biosciences, Åbo Akademi University, Turku, Finland*

[3]*Division of Molecular Biosciences, Faculty of Natural Sciences, Imperial College London, London, UK*

Abstract.

We report the expression of recombinant RNASET2, the only human member of the Rh/T2/S family of acid ribonucleases, in the yeast *Pichia pastoris* and the baculovirus-insect cell heterologous systems. In both models, the yield of recombinant protein was comparable and ranged between 5 mg/L (for a catalytically impaired mutant version of RNASET2) and 30 mg/L for the wild-type protein. Thus, the produced protein version rather than the expression system used appears to influence protein yield after optimization of culture conditions. The recombinant protein was found to undergo heterogeneous glycosylation in both systems, particularly in *P. pastoris*. Most importantly, the wild-type protein purified from both systems was found to be catalytically competent. The expression of recombinant RNASET2 in both systems will allow the implementation of functional assays *in vivo* and *in vitro* to better define the antioncogenic properties of this member of the Rh/T2/S ribonuclease family.

Volume 58, Number 1, January/February 2011, Pages 39–49 •

E-mail: paola.campomenosi@uninsubria.it; francesco.acquati@uninsubria.it

Keywords: RNASET2, tumor suppressor, ribonuclease, heterologous protein expression, protein glycosylation

1. Introduction

Ribonucleases have been the subject of extensive studies in recent years, due to their involvement in several biological processes besides RNA metabolism. Indeed, RNAses have been involved in a host of cellular processes such as viral infections, cell proliferation, tumor cell growth, and angiogenesis [1],[2]. The transferase-type ribonucleases have long been ranked into three main families (ribonuclease A, Rh/T2/S, and T1) according to their biochemical properties [1]. The main feature of the Rh/T2/S family of ribonucleases is represented by two conserved active-site segment (CAS) motives, in which two histidine residues play an essential role in catalysis [1],[2]. These proteins are acid ribonucleases displaying a pH optimum below 6.0 for catalytic activity and are either secreted extracellularly or targeted to the vacuolar or lysosomal compartments after their transit through the secretory pathway, where they usually undergo *N*-glycosylation and chaperone-assisted folding [2].

RNASET2 is to date the only member of the Rh/T2/S family described in humans [3]. Besides its activity as a ribonuclease [4], we previously demonstrated an oncosuppressive function for this protein [5–7]. Strikingly, this role appeared to be independent of catalytic activity because a mutant RNASET2 protein in which the two key CAS histidine residues were replaced by phenylalanine (H65/118F RNASET2) was found to be still highly effective in suppressing tumorigenesis *in vivo* when compared with the wild-type protein [6],[7]. However, in order to further characterize this protein (both structurally and functionally) and to better define its potential as an antitumorigenic agent, it would be crucial to have recombinant RNASET2 available.

Ribonucleases of the Rh/T2/S family have been purified from different sources, either directly from the host organisms in which they are expressed (such as in fungi or plants) or in different heterologous protein expression systems [1],[2]. As these proteins are usually modified post-translationally by *N*-glycosylation and targeted to the secretory pathway, the expression strategy of choice usually relies on a eukaryotic system, in particular the baculovirus expression vector system (BEVS) or the yeast *Pichia pastoris*.

However, finding the system that grants the best expression levels is mandatory for obtaining sufficient amounts of pure protein for *in vivo* experiments and for conformational and

Abbreviations: CAS, conserved active-site segment; H65/118F, mutant RNASET2 version with histidine at positions 65 and 118 substituted with phenylalanines; BEVS, baculovirus expression vector system; anti-HA, anti-hemagglutinin; Mut$^+$, methanol utilization plus; Mut^S, methanol utilization slow; MOI, multiplicity of infection.

*Address for correspondence: Paola Campomenosi, BSc, PhD, Department of Biotechnology and Molecular Sciences, University of Insubria, Via J.H. Dunant 3, 21100 Varese, Italy. Tel.: +39-0332-421518; Fax: +39-0332-421500; e-mail: paola.campomenosi@uninsubria.it.

*Address for correspondence: Francesco Acquati, BSc, PhD, Department of Biotechnology and Molecular Sciences, University of Insubria, Via J.H. Dunant 3, 21100 Varese, Italy. Tel.: +39-0332-421512; Fax: +39-0332-421500; e-mail: francesco.acquati@uninsubria.it.

Received 30 November 2010; accepted 20 December 2010

DOI: 10.1002/bab.7

Published online 30 March 2011 in Wiley Online Library (wileyonlinelibrary.com)

structural studies. In independent reports, yields of a few milligrams per liter of culture have been reported for members of this family of ribonucleases [1],[2]. However, to our knowledge, no comparisons have ever been made among the expression levels obtained in different systems for a specific ribonuclease of this family.

In this work, we set out to define the best conditions for RNASET2 production in heterologous systems and we report the expression of this protein in both *P. pastoris* and BEVS by showing that both systems produce a catalytically competent RNASET2 with comparable levels of expression and catalytic activity. *P. pastoris* thus represents the expression system of choice for this protein, being more cost-effective compared with the baculovirus system and allowing the secretion of the protein in a relatively protein-free supernatant from which RNASET2 can be easily purified [8–10].

2. Materials and methods

2.1. Reagents and media

All reagents were from Sigma–Aldrich (Milan, Italy), unless otherwise specified. The "easy select" *Pichia* expression kit was purchased from Invitrogen (Milan, Italy). Phusion high-fidelity DNA polymerase, restriction/modification enzymes, and peptide-*N*-glycosydase F were from New England Biolabs (Milan, Italy). Zeocin was purchased from InvivoGen (Milan, Italy), yeast nitrogen base from Difco BD, and Bradford reagent and Polyprep columns from Biorad. Ultrafree centrifugal concentrators (cutoff 5,000 Da) were purchased from Millipore and NiNTA resin from Qiagen (Milan, Italy). BA85 nitrocellulose membrane was from Schleicher & Schuell (Varese, Italy), supersignal *West Dura* extended duration chemiluminescent substrate and horseradish peroxidase-conjugated secondary antibodies were from Thermo Scientific (Milan, Italy).

A rabbit polyclonal antibody raised against a truncated version of human RNASET2 expressed in bacteria (anti-RNASET2) [6] and a rabbit polyclonal antibody against purified full-length human recombinant RNASET2 from the baculovirus-insect cell system (anti-RNASET2-2) were used as primary antibodies and were raised by Dabio (Germany). The mouse monoclonal anti-HA tag (clone 12CA5) was purchased from Roche (Monza, Italy).

The following media for insect cell culture were used: Sf900 II medium supplemented with 2 mM L-glutamine, 10 U/mL penicillin G (sodium salt), 10 μg/mL streptomycin sulfate (GIBCO, Invitrogen), and 0.1% pluronics (Sigma–Aldrich); TMN-FH (Fully Supplemented Grace's Medium) medium, supplemented with 2 mM L-glutamine, 10 U/mL penicillin G (sodium salt), and 10 μg/mL streptomycin sulfate plus 5% Fetal Bovine Serum (FBS) (GIBCO, Invitrogen, Milan, Italy). Media for *P. pastoris* cell growth and screening of the methanol utilization phenotype were prepared as described in the Invitrogen "EasySelect™ *Pichia* Expression kit."

2.1.1. Cloning of the human RNASET2 coding sequence in plasmid vectors

Cloning of RNASET2 coding sequence fused at the 3′ end to sequences coding for both HA (hemagglutinin) and 6× histidine tags into the pFASTBAC1 vector for expression in the BEVS has been described previously [4]. The RNASET2 coding sequence included the human endogenous N-terminal signal peptide. Two versions of RNASET2 were cloned, coding either for the wild-type protein or the catalytically impaired H65/118F mutant.

The same HA and 6× histidine-tagged RNASET2 coding sequence without endogenous signal peptide (aa 25–256) was PCR amplified for cloning in pPICZ A (Invitrogen) in order to express RNASET2 in frame with the vector-encoded *Saccharomyces cerevisiae* factor signal peptide for secretion of the recombinant protein.

Primers for PCR amplification were as follows:

RNASET2 Forward:
5′TGACGAATTCGACAAGCGCCTGCGTGACA3′
RNASET2 Reverse:
5′TGACGAATTCTCAGTGATGATGGTGGTGATGAGCGTAGTCTGGC-ACGTCGTATGGG3′

The PCR products were gel purified, digested with EcoRI, and cloned into pPICZ A before transformation in the JM109 *Escherichia coli* strain. Plasmid DNA was purified from several transformed colonies and, after sequencing (CRIBI, Padova, Italy), the empty vector and the two RNASET2-encoding constructs (pPICZ A-wtRNASE and pPICZ A-mutRNASE) were used to transform several *P. pastoris* strains.

2.1.2. Transformation of P. pastoris and "methanol utilization" phenotype screening

Five micrograms of each RNASET2 construct or empty vector were linearized within the 3′AOX region with PmeI and transformed into *P. pastoris* by the lithium chloride method [11]. Three strains were transformed: GS115 [His4] and X33 [wild type], which are both methanol utilization plus (Mut^+), and KM71H [arg4, AOX1::ARG4], which is methanol utilization slow (Mut^S). Transformants were selected on Yeast, Peptone, Dextrose (YPD) plates (1% yeast extract, 2% bactopeptone, 2% dextrose, 20 g/L bactoagar) containing 100 μg/mL zeocin and confirmed by streaking on the same plates. Zeocin-resistant clones were picked and lysed by boiling at 100°C for 10 Min in 20 mL of bidistilled water. Five microliters of each lysate was used for PCR amplification, using two pairs of primers. The first primer pair (5′AOX and 3′AOX) was designed according to manufacturer's instructions (Invitrogen) to discriminate integration of the empty vector (producing a 590 bp PCR product) from integration of RNASET2-containing constructs (producing a 1,340 bp PCR product). The second primer pair (RNASET2 *forward 2*: 5′ GACAAGCGCCTGCGTGACA 3′ and RNASET2 *reverse 2*: 5′ TGCTTGGTCTTTTTAGGTGG 3′) was RNASET2-specific and was expected to yield a 700 bp band only when RNASET2-containing constructs were integrated.

Mut^+ strain colonies positive for integration were also screened for the methanol utilization phenotype by streaking on MDH and MMH plates (Minimal Dextrose Histidine and Minimal Methanol Histidine: 1.34% yeast nitrogen base, 4×10^{-5}% biotin, 0.004% histidine, 15 g/L bactoagar, and either 2% dextrose for MDH or 0.5% methanol for MMH plates). Clones maintaining the Mut^+ phenotype grew approximately

at the same efficiency on both plates, whereas clones that have turned to Mut^S phenotype grew very slowly on MMH plates.

2.2. Optimization of RNASET2 expression from *P. pastoris*

Buffered minimal glycerol or buffered minimal methanol medium (BMGH/BMMH) (100 mM potassium phosphates pH 6.0, 1.34% yeast nitrogen base, 4×10^{-5}% biotin, 0.004% histidine, and either 1% glycerol or 0.5% methanol) and buffered complex glycerol or buffered complex methanol medium (BMGY/BMMY) (1% yeast extract, 2% bactopeptone, 1.34% yeast nitrogen base, 4×10^{-5}% biotin, and either 1% glycerol or 0.5% methanol) media were used to grow cells and analyze the expression of RNASET2. Selected clones were freshly plated and grown for 2 days at 30°C. One colony was picked and inoculated into 50 mL of BMGH or BMGY medium. Cultures were grown at 30°C with 180 rpm shaking overnight until they reached an Optical Density at 600 nm (OD_{600}) between 2 and 6. They were then centrifuged and the pellet was resuspended in the appropriate methanol-containing medium at a starting OD_{600} of 1 for induction of protein expression. Fresh methanol (0.5% final concentration) was added to the culture each day to replace for evaporation. From time 0 to 240 H, 300-mL aliquots were taken from the culture every 24 H. Cells at each time point were centrifuged at 2,000*g* and both pellets and supernatants were stored at −80°C for subsequent immunoblot analysis. To select the best RNASET2-expressing clones, eight clones transformed with either wild type or H65/118F mutant RNASET2 construct and two control clones transformed with empty vector were grown in 50 mL conical tubes in 5 mL of BMGY. When cultures reached an OD_{600} of 3, the cells were transferred in BMMY medium at a density of 1 OD_{600}. Induction was performed for 168 H (optimal time as determined during the time course assay), then cultures were centrifuged and supernatants stored at −80°C for subsequent analysis.

2.2.1. Expression and purification of wild-type RNASET2 using the BEVS

The Sf9 insect cell line [12] from the pupal ovarian tissue of the fall army worm *Spodoptera frugiperda* was cultured at 27°C as suspension and/or monolayer cultures and infected with the recombinant baculovirus batches FastBac1-wtRNASE (wild-type RNASET2) or FastBac1-MutRNASE (H65/118F mutant) at a multiplicity of infection (MOI) of 5–10 plaque-forming units per cell. Supernatants were collected 96–144 H after infection. Protein purification was performed as previously described [4].

2.2.2. Expression and purification of wild-type RNASET2 from P. pastoris strain X33

One recombinant clone from the X33 strain was selected to express the protein for subsequent purification. The BMGY/BMMY medium was used for generating biomass and inducing expression and cultures were processed after 7 days from induction. After pelleting the cells at 2,500*g* in a swinging rotor, the supernatant was filtered with a 0.45 μm pore size filter unit and processed as described in ref. [4] for RNASET2 expressed in the baculovirus system. Briefly, supernatants were concentrated 10-fold on Ultrafree centrifugal concentrators and extensively dialyzed against 50 mM Tris–HCl, 100 mM KCl, and 5 mM 2-mercaptoethanol (base solution) at pH 8.0, to improve subsequent binding to the Ni-NTA resin (Qiagen). After addition of 10 mM imidazole, binding to the resin was allowed to proceed for 2 H at 4°C, before applying the solution onto an empty column. After washing with 10-column volumes of wash solution (base solution plus 20 mM imidazole), elution was performed with four column volumes (one volume at a time) of base solution plus 250 mM imidazole. The amount of protein in the eluted fractions was checked both spectrophotometrically and by Sodium Dodecyl Sulphate-Polyacrylamide Gel Electrophoresis (SDS-PAGE) followed by Coomassie R250 staining. Protein-containing fractions were pooled and dialyzed against 10 mM potassium phosphate, 0.2 mM 2-mercaptoethanol (pH 6.6), and stored at −20°C in small aliquots.

2.2.3. Analysis of RNASET2 expression by immunoblotting

Ten/fifteen microliters of supernatant from RNASET2-expressing *Pichia* or baculovirus system cultures or 10–50 ng of purified recombinant proteins were prepared in LaemmLi sample buffer, denatured at 95°C for 5 Min, resolved on 13% SDS-PAGE and transferred to BA85 nitrocellulose membrane. Membranes were blocked with 4% nonfat dry milk in 0.1% Tween-20 in phosphate-buffered saline (PBST) overnight at 4°C, then incubated 1 H at room temperature with the appropriate primary antibody at the following dilution in 2% nonfat milk in PBST: rabbit polyclonal anti-RNASET2: 1:600; rabbit polyclonal anti-RNASET2-2: 1:1,000; mouse monoclonal anti-HA tag: 1:4,000. Subsequently, membranes were incubated with horseradish peroxidase-conjugated anti-mouse or anti-rabbit secondary antibodies at a 1:900 dilution in 2% nonfat milk in PBST. Detection was carried out with chemiluminescent substrate.

2.2.4. RNASET2 deglycosylation

Five hundred nanograms of purified recombinant RNASET2 obtained from the baculovirus-insect cell system or supernatants from RNASET2-expressing *P. pastoris* clones were denatured and either treated with peptide-*N*-glycosydase F to remove all *N*-linked glycosylation or mock treated. After treatment, samples were processed for immunoblotting as described above.

2.3. Analysis of the glycosylation pattern of recombinant RNASET2 purified from the two expression systems

Approximately 10 μg of RNASET2 obtained from either baculovirus or *P. Pastoris* was subjected to reduction, carboxymethylation, and tryptic digestion; the samples were reduced at 37°C in water bath for 1 H in 1 mL of 50 mM Tris–HCl buffer (pH 8.5) containing 10 mg/mL dithiothreitol.

Carboxymethylation was carried out by the addition of iodoacetic acid (fivefold molar excess over dithiothreitol), and the reaction was allowed to proceed at room temperature in the dark for 1 and 5 H. After carboxymethylation, samples were dialyzed against 4×4.5 L of 50 mM ammonium bicarbonate (pH 8.5) at 4°C for 48 H, and subsequently lyophilized.

The reduced carboxymethylated proteins were then digested with *N-p*-tosyl-l-phenylalanine chloromethyl

ketone-pretreated bovine pancreas trypsin (EC 3.4.21.4; Sigma) for 16 H at 37°C in 50 mM ammonium bicarbonate buffer (pH 8.4). After trypsin digestion, samples were purified by C18 Sep-Pak® (Waters Corp., Milford, MA, USA) as described previously [13].

Releasing of *N*-glycans from tryptic glycopeptides was obtained by addition of *N*-glycosidase F in 50 mM ammonium bicarbonate (pH 8.5). The digestion was carried on for 20 H at 37°C with 5 units of enzyme (Roche Applied Science, UK). The released *N*-glycans were purified from O-glycopeptides and peptides by chromatography on a Sep-Pak C18 cartridge (Waters) and subsequently methylated using the sodium hydroxide permethylation procedure as described previously [14].

Briefly, five to seven NaOH pellets were ground to fine powder and mixed with 2–3 mL anhydrous dimethylsulfoxide (Romil, UK) before adding to each dried sample. This is followed by the addition of 0.6 mL of methyl iodide and vigorous shaking at room temperature for 15 Min. Permethylated glycans were extracted with chloroform and then purified by using Sep-Pak C18 cartridges.

The cartridges were successively conditioned with methanol (5 mL), water (5 mL), acetonitrile (5 mL), and water (15 mL). Each sample was dissolved in 200 μL of methanol/water (1:1) solution before loading onto the cartridges. The cartridges were washed with 5 mL of water and then eluted sequentially with 3 mL of each 15%, 35%, 50%, and 75% acetonitrile solution in water.

Acetonitrile/water fractions (35%, 50%, and 75%) were collected and then concentrated with a Savant SpeedVac (ThermoFisher Scientific, Horsham, West Sussex, UK) and subsequently lyophilized.

The permethylated glycans were subsequently analyzed by mass spectrometry (MS). Briefly, Matrix Assisted Laser Desorption/Ionization-Time of Flight (MALDI-TOF) data were acquired on a Voyager-DE STR mass spectrometer (Applied Biosystems, Foster City, CA, USA) in the reflectron mode with delayed extraction. Permethylated samples were dissolved in 10 μL of methanol, and 1 μL of dissolved sample was premixed with 1 μL of matrix [20 mg/mL 2,5-dihydroxybenzoic acid in 70% (v/v) aqueous methanol], spotted onto a target plate and dried under vacuum.

The MS data were processed using Data Explorer 4.9 software (Applied Biosystems, UK). The mass spectra were baseline corrected (default settings) and noise filtered (with correction factor of 0.7), and then converted to ASCII format. The processed spectra were then subjected to manual assignment and annotation with the aid of a glycobioinformatics tool known as GlycoWorkBench [15].

Peak picking was done manually and proposed assignments for the selected peaks were based on molecular mass composition of the ^{12}C isotope together with knowledge of the biosynthetic pathways.

2.4. Analysis of the catalytic activity of recombinant RNASET2

To assess the catalytic activity of RNASET2 purified from the baculovirus-insect cell system or *P. pastoris*, zymogram gel electrophoresis was performed as described [16],[17]. Briefly, SDS polyacrylamide gels were prepared according to standard procedures, except total RNA from torula yeast was added in resolving (2 mg/mL final concentration) and stacking (0.3 mg/mL final concentration) gel solutions. Proteins were prepared in nonreducing sample buffer (125 mM Tris–HCl pH 6.8, 2% SDS, 10% glycerol, 0.02% blue bromophenol) and directly loaded into gels without boiling. After electrophoresis, proteins were allowed to renature by removing SDS with 25% isopropanol prepared in 10 mM Tris–HCl (pH 7.4) and the gel was washed extensively with 10 mM Tris–HCl (pH 7.4) and incubated at 51°C in freshly prepared KCl 100 mM, Na acetate 100 mM at pH 5,0. After washing with 10 mM Tris–HCl (pH 7.4), enzymatic activity was detected by toluidine blue staining followed by destaining in 10 mM Tris–HCl (pH 7.4), leaving a negative image where RNase activity was present. After image acquisition with a Biorad GS800 densitometer, gels were destained as much as possible from toluidine blue with 10 mM Tris–HCl (pH 7.4), soaked for 30 Min in transfer buffer and processed for immunoblotting as described above. In this case, detection was performed with the sensitive anti-RNASET2-2 antibody.

2.4.1. Spectrophotometric discontinuous method for catalytic activity measurement

To better quantify the enzymatic activity of the two recombinant proteins, a spectrophotometric discontinuous method was also used. The protein concentration was estimated assuming an extinction coefficient at 280 nm of 61,920 M^{-1} cm^{-1} for the denatured amino acid sequence without the signal peptide (aa 25–256), calculated with the ProtParam bioinformatics tool at Expasy (www.expasy.ch) and measuring the absorbance of the protein solution in 8 M urea, sodium phosphate buffer (pH 6.5). Enzymatic activity toward torula yeast total RNA was measured by following the increase in absorbance at 260 nm due to acid soluble nucleotides release at pH 5.0 and 37°C. Briefly, 3 μg/mL of RNASET2 was added to a reaction mix, pre-equilibrated at 37°C, containing total RNA at a final concentration of 0.4 mg/mL in 0.1 M sodium acetate, 0.1 M KCl (pH 5.0). This concentration has been previously shown to ensure that we worked in excess of substrate. At each time point, a 300 μL aliquot of the reaction was taken and transferred to a tube containing 100 μL of 25% perchloric acid with 0.75% uranyl acetate. After centrifugation, supernatants, containing the free nucleotides, were diluted 1:5 and absorbance at 260 nm was measured. At least two measures were performed for each protein preparation and two independent protein preparations were analyzed for each type of recombinant RNASET2. The software Kaleidagraph was used to build and analyze kinetics.

3. Results

To express recombinant RNASET2 in *P. pastoris*, the coding sequences of both wild-type and H65/118F mutant RNASET2 were cloned into the pPICZ A vector. Both recombinant constructs and empty vector were transformed into three *Pichia* strains (GS115, KM71H, and X33) and several clones were checked by PCR for integration of the construct in the host genome. As expected, integrant clones containing the RNASET2-coding

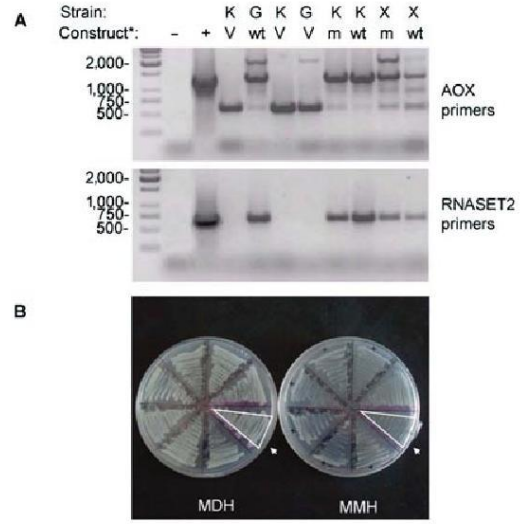

Fig. 1. Screening of *Pichia pastoris* zeocin-resistant clones for RNASET2–pPICZaA or pPICZaA vector integration and for methanol utilization phenotype. (A) AOX1-specific primers (upper panel) or RNASET2-specific primers (lower panel) were used for colony PCR to check for integration of the constructs into the AOX1 locus. Clone strains are indicated as X, K, and G for X33, KM71H, and GS115, respectively. The type of construct used for transformation (*) is also indicated as "V" (vector only), "wt" (wild-type RNASET2 construct), or "m" (H65/118F mutant RNASET2 construct). (B) MDH or MMH plates were used to screen for the methanol utilization phenotype. Arrows indicate a Mut^S control that was streaked on both plates and shows a slower growth on MMH plates compared with MDH plates.

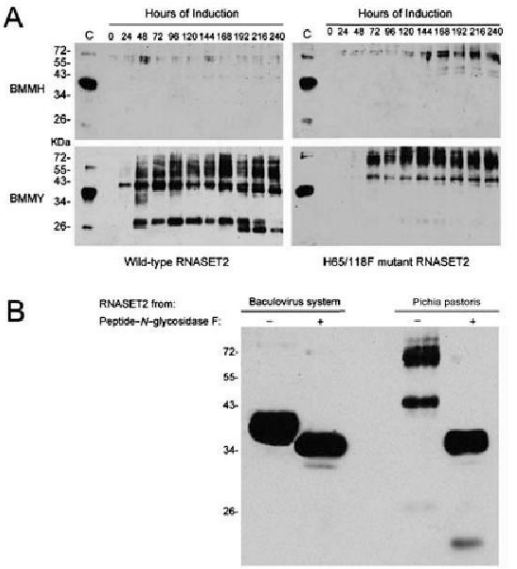

Fig. 2. Analysis of time-dependent RNASET2 expression in different media formulations. (A) Wild-type and H65/118F mutant RNASET2-expressing clones from the GS115 strain were induced up to 240 H in BMMH or BMMY media. Supernatants were immunoblotted and detected with anti-RNASET2-specific antibody. Lane C shows recombinant RNASET2 purified from the baculovirus-insect cell system. (B) Analysis of recombinant RNASET2 after peptide-*N*-glycosidase F treatment. Supernatants from RNASET2-expressing, baculovirus-infected cells or from a single *Pichia pastoris* clone were either treated with peptide-*N*-glycosidase F (+) or mock treated (–). Reactions were immunoblotted and detected with anti-HA specific antibody.

sequence showed a 700 and a 1,400 bp amplification product when RNASET2-specific primers or 5′ and 3′ AOX primer pairs were used, respectively (Fig. 1A). By contrast, integrants for the empty vector did not amplify with the RNASET2 primer pair and gave rise to a 600 bp band with the AOX primers (Fig. 1A). The orientation of the insert was also checked by PCR using a forward or a reverse RNASET2-specific primer together with the 3′ AOX primer (data not shown). Clones from Mut^+ strains were checked for maintenance of the methanol utilization phenotype. All clones in KM71H and X33 strains showed comparable growth rates on methanol or glycerol containing plates, indicating that they had maintained the Mut^+ phenotype (Fig. 1B).

One wild-type and one H65/118F mutant clone from the GS115 (Mut^S) strain were selected for pilot expression experiments aimed at defining the best conditions for RNASET2 expression. We chose this strain because it has already been used for expression of ribonucleases from the T2 family [18]. Cell pellets and supernatants were collected every 24 H for 10 days and stored until the end of the experiment. As shown in Fig. 2A, samples grown in BMMY medium showed a strong positivity to the anti-RNASET2-specific antibody in immunoblotting. These anti- RNASET2 positive bands showed a wide range of molecular masses, suggesting that following expression in *P. pastoris* RNASET2 undergoes a complex posttranslational modification. Indeed, besides proteins in the 38–45 kDa range, which is similar to that observed following expression of RNASET2 in the BEVS system, several bands in the 50–80 kDa range were also observed. Occasionally, a few bands were also observed at about 26 kDa in the wild-type RNASET2-expressing clone. This band(s) was recognized by two different anti-RNASET2 polyclonal antibodies and by the anti-HA antibody, confirming its identity as RNASET2 (Fig. 2, panel B and data not shown). A band of the same approximate molecular weight has been sometimes observed also in the baculovirus system and is likely to

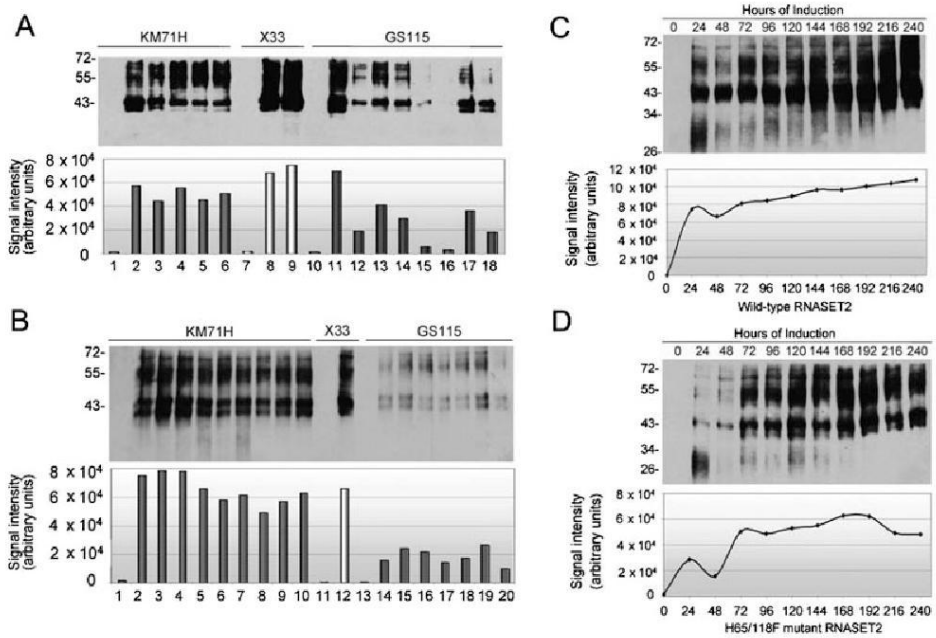

Fig. 3. Comparison of RNASET2 expression levels among different *Pichia pastoris* strains. Clones with integrated wild-type (A) or H65/118F mutant (B) RNASET2 constructs from strains GS115, X33, and KM71H were induced with methanol. Supernatants were collected after 168 H, immunoblotted and detected with anti-RNASET2-specific antibody. As a control, clones obtained by integration of empty pPICZaA vector were used (lanes and columns 1, 7, and 10 for wild- type and 1, 11, and 13 for mutant clones). (C, D) RNASET2 expression levels as a function of time in wild-type and mutant RNASET2-expressing clones from strain X33. The graphs below each immunoblot detected with anti-RNASET2 antibody show wild-type (C) or H65/118F mutant (D) expression levels as a function of induction time, and are reported as "signal intensity" arbitrary units which were calculated by band scanning and quantification with ImageJ software. The reported data represent the result of two independent experiments.

represent a degradative product. To investigate the nature of the different RNASET2 positive bands, supernatants from both RNASET2-expressing baculovirus-infected insect cells and a *Pichia* recombinant clone were treated with peptide-*N*-glycosidase F prior to Western blot analysis. A main band of 33 kDa was detected with an anti-HA antibody either in the sample from the baculovirus system or in that from *Pichia* after deglycosylation (Fig. 2B), suggesting that all anti-RNASET2 reactive forms shown in Fig. 2A represent mildly glycosylated or hyperglycosylated forms of RNASET2. The 26 kDa band, upon deglycosylation with PNGase F, shifted to a 19 kDa band and this confirmed that also this band was indeed glycosylated (Fig. 2B).

The time-course experiment in GS115 also allowed us to estimate the best time for optimal expression in this strain. At each time point, cell supernatants were immunoblotted and detected with anti-RNASET2-specific antibody. The expression levels were found to increase rapidly, reaching maximum levels between 144 and 168 H after induction (data not shown). We also tried to define the best RNASET2-expressing strain by the analysis of several clones from the three strains. Although we found evidence for intraclone variability in the expression levels, a trend was observed (for wild-type RNASET2-expressing clones), whereby the X33 strain was in general a better expressor when compared with both KM71H and GS115 strains (Fig. 3A), whereas for the H65/118F mutant RNASET2-expressing clones, the expression levels were quite similar in both X33 and KM71H strains and much higher when compared with strain GS115 (Fig. 3B). Being the best expressor strain for both RNASET2 forms, we thus chose the X33 strain for further expression experiments, and a new time course was performed on two selected wild-type and mutant clones, in order to define the best time for optimal expression in this strain. For both proteins, all clones showed a rapid increase in RNASET2 protein levels within 24 H from induction (Figs. 3C and 3D), followed by a flex between 24 and 72 H and a further wave of slow increased expression. As for clones in the GS115 strain, 168 H (7 days) was chosen as the best time for subsequent induction.

Table 1
RNASET2 expression levels in the two heterologous expression systems

	Pichia pastoris	BEVS
Wild-type RNASET2	36 ± 4.26	33 ± 3.35
H65/118F mutant RNASET2	6.9 ± 1.09	5.6 ± 1.39

Values are expressed in mg/L of cell culture supernatants and represent the mean of four independent experiments ± standard error.

Preliminary attempts to express recombinant RNASET2 in the baculovirus-insect cell system have been previously carried out in our laboratory [4], with estimated yields in the range of 1–2 mg/L of cell culture supernatant. We thus tried to optimize RNASET2 expression levels also in this heterologous system by using different media formulations and collecting supernatants at different times after infection (ranging from 96 to 144 H). Comparison among different media allowed us to conclude that maximum RNASET2 expression levels were obtained in TNM-FH medium supplemented with 5% FBS. In this medium, the wild-type protein was expressed at about 30 mg/L (Table 1), which represents a 15-fold improvement in expression levels compared with cultures in the previously used serum-free medium. The expression levels of the H65/118F mutant, however, did not improve as much as the wild type in the same conditions.

Next, we compared the expression levels of wild type and mutant RNASET2 in *P. pastoris* with those in the BEVS. To this aim, identical volumes of unprocessed supernatant samples were immunoblotted and detection was performed with anti-RNASET2 and anti-HA antibodies. A calibration curve was constructed on each immunoblot by loading increasing known amounts of pure recombinant RNASET2 previously purified from the BEVS. This allowed us to determine the concentration of RNASET2 in the supernatants, which was estimated to range between 30 and 40 mg/L for the wild-type form in both expression systems, whereas the H65/118F mutant was expressed at about 7 mg/L in *P. pastoris* and at about 5 and 6 mg/L in the BEVS (Table 1).

Purification of recombinant RNASET2 was performed from supernatants after 168 H (7 days) of induction in *P. pastoris* and from supernatants of recombinant baculovirus-infected insect cells 144 H (6 days) after infection. The same protocol previously described for purification of RNASET2 from the baculovirus-insect cell system [4] was applied to both types of supernatant. By SDS-PAGE analysis of the purified proteins, RNASET2 from the baculovirus system showed two main bands of 37 and 39 kDa (Fig. 4A, lanes 1–3), whereas RNASET2 purified from *P. pastoris* showed two bands of 41 and 43 kDa (Fig. 4A, lanes 4–6). The hyperglycosylated forms with a molecular weight above 55 kDa were barely visible only when high amounts (0, 5 μg) of

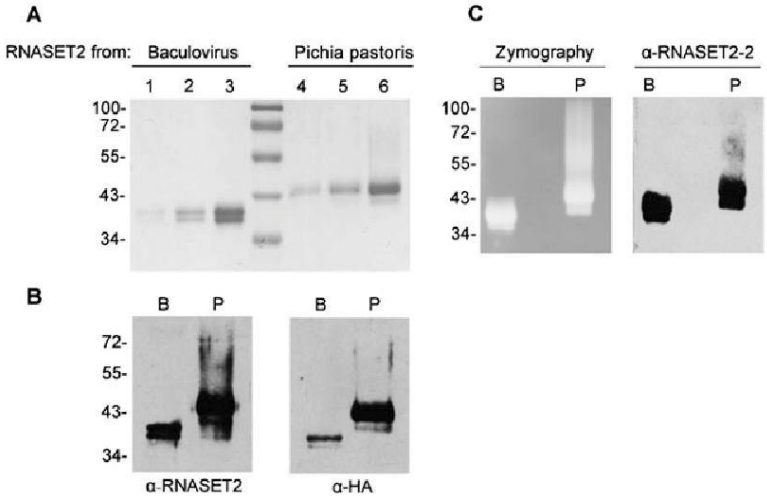

Fig. 4. Analysis of wild-type RNASET2 purified from baculovirus-infected insect cells or from a *Pichia pastoris* strain X33 clone. (A) Coomassie staining of an SDS-PAGE gel loaded with three different volumes of RNASET2 from either baculovirus-infected insect cells (lanes 1–3) or *P. pastoris* (lanes 4–6). A prestained protein marker was loaded in the middle lane. (B) Immunoblots were detected with anti-RNASET2 antibody (left) or anti-HA antibody (right) to confirm the identity of the purified proteins. (C) Zymography was performed using total RNA from torula yeast as substrate to analyze RNASET2 purified from the two heterologous systems. The identity of the bands showing ribonucleolytic activity was confirmed by immunodetection with anti- RNASET2-2 antibody. In all panels, P and B indicate supernatants from *P. pastoris* or the BEVS, respectively.

RNASET2 from *P. pastoris* were loaded (data not shown). Western blot analysis with anti-RNASET2 or anti-HA monoclonal antibodies confirmed the identity of the purified proteins (Fig. 4B). Both purified preparations were judged to be >95% pure by Coomassie staining of SDS-acrylamide gels.

Finally, as we previously showed that human RNASET2 is a functional ribonuclease [4], the purified proteins were checked for proper folding and functionality by zymographic analysis. Equal amounts of each purified protein, as determined both spectrophotometrically and by Coomassie blue staining, were loaded on a zymographic gel containing torula yeast's total RNA as a substrate. RNASET2 purified from both *P. pastoris* and baculovirus systems showed a strong signal after toluidine blue staining, indicative of ribonucleolytic activity (Fig. 4C, left panel). Molecular weights corresponding to RNA hydrolyzation activity were compatible with those observed from the forms obtained after purification. Moreover, the same forms showing ribonucleolytic activity were detected by the anti-RNASET2-2-specific antibody (Fig. 4C, right panel).

To evaluate whether the wild-type proteins from the two expression systems showed comparable levels of catalytic activity, a spectrophotometric method to measure the ribonucleolytic activity in solution was applied. At least two measures were performed for each protein preparation and two independent protein preparations were tested for each type of RNASET2. The two preparations of each recombinant protein gave very similar results, showing that the recombinant protein produced in the BEVS has an activity, expressed as Abs260/Min, of 0.67 $\pm$ 0.009 against an activity of 1.02 $\pm$ 0.013 Abs260/Min for the recombinant protein expressed in *P. pastoris*. Therefore, RNASET2 purified from *P. pastoris* shows a 30% higher activity than the protein purified from the baculovirus system in the conditions tested.

Defining one unit as the amount of enzyme which produces a change of 1 OD_{260} absorbance in 15 Min at 37°C, wild-type human RNASET2 purified from baculovirus appeared to contain 3,390 units/mg of protein, whereas the protein purified from *P. pastoris* contained 5,100 units/mg of protein in the preparations and the conditions tested.

Taken together, these data show that recombinant RNASET2 expressed in both *P. pastoris* and BEVS expression systems have catalytic activity.

Finally, we investigated the nature of the carbohydrate modifications on the proteins purified from the two heterologous expression systems. Analysis of MALDI spectra of *N*-glycans released by PNGaseF digestion of the tryptic peptides and subsequently permethylated (spectra A and B in Fig. 5) showed a wide variation in molecular weight of the glycans attributable to the products from baculovirus and *P. Pastoris* systems. Thus, the protein purified from the baculovirus system is characterized by a major hexasaccharide whose composition is consistent with a core fucosylated trimannosyl *N*-glycan (*m/z* 1,345; see Fig. 5 A). Less abundant components are high mannose structures of composition Man5GlcNac2 (*m/z* 1,580), Man6GlcNac2 (*m/z* 1,784), and Man7GlcNac2 (*m/z* 1,988) (see Fig. 5 A). In contrast, the sample purified from *Pichia* is dominated by polymannose glycans of composition Man5GlcNac2 (*m/z* 1,580), Man6GlcNac2 (*m/z* 1,784), Man7GlcNac2 (*m/z* 1,988), Man9GlcNac2 (*m/z* 2,396), Man10GlcNac2 (*m/z* 2,600), Man11GlcNac2 (*m/z* 2,804), Man12GlcNac2 (*m/z* 3,008), Man13GlcNac2 (*m/z* 3,212), Man14GlcNac2 (*m/z* 3,416), and Man15GlcNac2 (*m/z* 3,623) (see Fig. 5 B), and has none of the hexasaccharide at *m/z* 1,345 detected in the protein from the baculovirus system.

4. Discussion

In this paper, we describe the expression of RNASET2, the only human member of the Rh/T2/S family of ribonucleases, in both *P. pastoris* and baculovirus-insect cell-based expression systems. The two systems were compared in terms of expression levels and functionality of the produced protein. To our knowledge, this is the first report comparing two different heterologous expression systems for expression of a ribonuclease of the Rh/T2/S family.

Pichia pastoris and baculovirus-insect cell systems were chosen because RNASET2 is a secreted protein which undergoes a series of posttranslational modifications in the endoplasmic reticulum and Golgi apparatus. Indeed, RNASET2 expression has been previously attempted in *E. coli* by our group, but the expression levels were quite low, likely due to either toxicity to the host cells or lack of stability in *E. coli*.

By contrast, in this work, RNASET2 was successfully expressed in both eukaryotic heterologous expression systems following optimization of culture conditions. The expression levels in these heterologous expression systems were comparable and ranged between 5 and 30 mg/L, depending on the protein version expressed (mutant or wild-type RNASET2), whereas the expression system did not appear to significantly influence the amount of protein produced. These expression levels represent the result of an accurate optimization strategy, as we previously described a yield of just 1–2 mg of protein/L of baculovirus-infected insect cell supernatants [4]. As long as expression in *P. pastoris* is concerned, three different strains were used as host cells and the X33 strain turned out to be a better expressor with respect to the GS115 and KM71H (Mut^S) strains. When compared with other proteins, the expression levels obtained for RNASET2 are rather low [8]; nevertheless, they rank in the high range of expression levels when published data reporting heterologous expression of members of the Rh/T2/S family of ribonucleases are taken into account [1],[2]. In one report, heterologous expression of RNase Rh from *Rhizopus niveus* in *S. cerevisiae* gave high expression levels, ranging from 40 to 70 mg/L, depending on the signal peptide used [19]. In another paper, two S-ribonucleases of *Petunia inflata* were expressed in the baculovirus expression system with yields of 1 mg of protein/L of cell supernatant [20]. Later, Huang et al. described expression of E^{rns}, a ribonuclease from classical swine fever virus, in *P. pastoris* at 27 mg/L [21]. The same protein had been previously produced in insect cells but expression levels were not reported [22]. Wild type and mutant versions of ribonuclease MC from *Momordica charantia* (bitter gourd) were expressed both in *E. coli* and *P. pastoris*. Although expression levels in bacteria were in the order of 0, 5 mg/L, the same protein was expressed

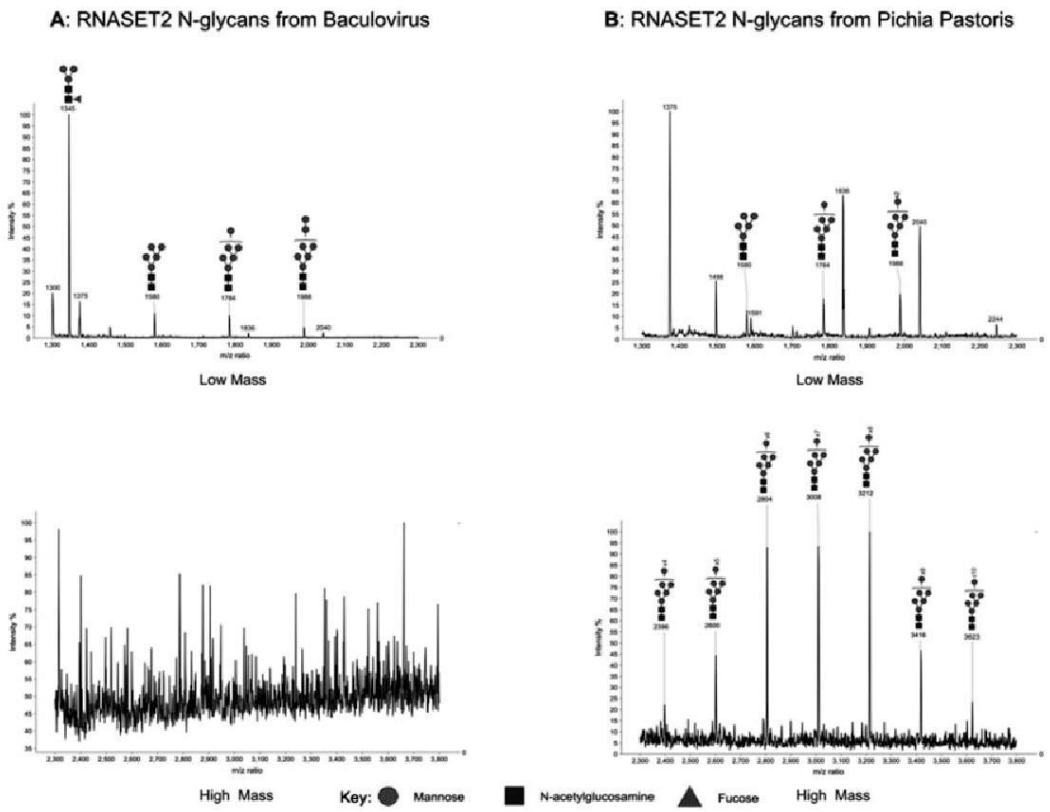

Fig. 5. *N*-glycan structures released from RNASET2 by PNGase F digestion and analyzed by MALDI-TOF MS. (A) Profile of total permethylated *N*-glycans in RNASET2 isolated from the baculovirus-insect cell heterologous systems. Upper panel: Low Masses (*m*/*z* interval: 1,300–2,300), fraction eluted in 50% acetonitrile/water during Sep-Pak purification. Annotated structures correspond to a core fucosylated glycan and high mannose glycans (Man2–Man4). Nonannotated peaks correspond to impurities and glycans originated from animal proteins included in the media used for baculovirus growth. Lower panel: High Masses (*m*/*z* interval: 2,300–3,800), fraction eluted in 75% acetonitrile/water during Sep-Pak purification. The signals spikes observed correspond to electrical and chemical noise. (B) Profile of total permethylated *N*-glycans in RNASET2 isolated from *Pichia pastoris*. Upper Panel: Low Masses (*m*/*z* interval: 1,300–2,300), fraction eluted in 50% acetonitrile/water during Sep-Pak purification. Annotated structures correspond to high mannose glycans (Man2–Man4). Nonannotated peaks correspond to impurities and glycans originated from animal proteins included in the media used for *P. Pastoris* growth. Lower panel: High Masses (*m*/*z* interval: 2,300–3,800), fraction eluted in 75% acetonitrile/water during Sep-Pak purification. Annotated *m*/*z* values correspond to high mannose glycans (Man6–Man12) detected in *P. Pastoris* sample.

with a yield of 7–20 mg/L in *P. pastoris* [23],[24]. Strikingly, in keeping with our data, a significant variation in expression levels between different protein versions was observed in the latter study, suggesting that intrinsic protein properties can influence expression levels.

RNASET2 is an *N*-glycosylated protein and three asparagines residues have been predicted *in silico* and experimentally validated as glycosylation sites *in vitro* [4]. Indeed, treatment of human cell extracts with peptide-*N*-glycosydase F confirmed that at least 7 kDa of the total apparent mass of RNASET2 in SDS-PAGE are contributed by carbohydrates [4]. In our hands, human recombinant RNASET2 expressed in the BEVS displayed a limited glycosylation heterogeneity, as demonstrated by the occurrence of bands ranging from 36 to 40 kDa detected with

an anti-RNASET2-specific antibody. By contrast, the same protein expressed in *P. pastoris* showed greater heterogeneity, as both mildly glycosylated (ranging from 38 to 45 kDa) and highly glycosylated forms (ranging from 50 to 80 kDa) of RNASET2 were detected in immunoblotting. As expected, all these forms turned into a single band of about 31 kDa in both *P. pastoris* and in the BEVS following enzymatic deglycosylation.

Preliminary data regarding the purification of RNASET2 from *P. pastoris* showed that the 39–45 kDa glycosylated forms were purified more efficiently than the hyperglycosylated forms. This could be explained by sterical hindrance of the abundant carbohydrates that could render the 6× histidine tag less accessible for binding to the resin. Therefore, although produced, these hyperglycosylated forms of RNASET2 (that do not usually occur in human cell extracts) represent a negligible fraction of the purified protein. In both heterologous expression systems used in this study, an anti-RNASET2 reactive form of 26 kDa was also occasionally observed, which probably represents a proteolytic degradation product, as deglycosylation treatment produced a further shift of MW down to 19 kDa. The 26-kDa form we observed is recognized by two different polyclonal antibodies against RNASET2 and also by an antibody against the C-terminal HA tag, suggesting that spontaneous proteolysis occurs at the N-terminus. Indeed, ribonucleases from the Rh/T2/S family have been described to possess protease-sensitive regions [25] and we previously showed that RNASET2 undergoes physiological proteolysis in mammalian cells, resulting in 31 and 27 kDa isoforms, which are targeted to the lysosome [4]. However, further analysis of the human forms showed that they were both generated by a cleavage event occurring in the C-terminal moiety of the RNASET2 protein. By contrast, the 26-kDa band occasionally observed in *Pichia* clones likely originated from a cleavage event at the N-terminus, as the C-terminal tag is still present. Taken together, these data suggest that the latter likely represents the result of a host-specific cleavage event of little physiological relevance.

Human RNASET2 was recently expressed in *P. pastoris* by another group [20], who described a single 27 kDa form whose expression levels were not reported. Although this molecular weight could be ascribed to the RNASET2 protein without signal peptide, it is not compatible with the glycosylation pattern that was described *in vivo* for RNASET2.

To better define the structural and functional features of recombinant RNASET2, we have also characterized the glycosylation pattern and the catalytic activity of the proteins purified from the two heterologous protein expression systems. Very distinct patterns of glycosylation were observed with the baculovirus system producing a largely glycosylated protein with a core fucosylated paucimannose glycan, whereas *P. Pastoris* expressed RNASET2 protein with polymannose structures, as expected for this expression system [8],[9].

Finally, recombinant wild-type RNASET2 purified from both systems was found to be catalytically competent. In the conditions tested, RNASET2 purified from *P. pastoris* showed a 30% higher activity than the protein purified from the baculovirus system, the activity of the first being 1.02 (0.013 Abs260/Min) against 0.67 (0.009 Abs260/Min) for the recombinant protein expressed in *P. pastoris*.

This result is of great practical relevance for future molecular and functional assays, whose goal is to achieve a detailed functional characterization of this protein. In recent years, RNASET2 has been shown by our group to behave as a potent oncosuppressor *in vivo* [5–7],[18]. This finding, coupled to the fact that RNASET2 is a secreted extracellular protein whose antiproliferative role was recently found to be carried out in a non-cell autonomous manner [26], makes the use of catalytically competent recombinant RNASET2 in both *in vitro* and *in vivo* cancer models a powerful tool to shed light on the functional roles of this unusual class of ribonucleolytic enzymes.

Acknowledgements

We thank Luciano Piubelli for his help in evaluation of enzyme activity and Mauro Fasano and Tiziana Alberio for helpful discussion. Francesco Acquati was supported by a grant from the Fondazione Comunitaria del Varesotto ONLUS. Christer Lindqvist was supported by grants from The Academy of Finland and The Albin Johansson Foundation. The mass spectrometry work was supported by the Biotechnology and Biological Sciences Research Council (BBF0083091) and Marie Curie Initial Training Network, EuroglycoArrays Project, part of the FP7 People Programme.

References

[1] Luhtala, N. and Parker, R. (2010) *Trends Biochem Sci.* **35**, 253–259.
[2] Deshpande, R. A. and Shankar, V. (2002) *Crit. Rev. Microbiol.* **28**, 79–122.
[3] Trubia, M., Sessa L., and Taramelli, R. (1997) *Genomics* **42**, 342–344.
[4] Campomenosi, P., Salis, S., Lindqvist, C., Mariani, D., Nordstrom T., Acquati F., and Taramelli, R. (2006) *Arch. Biochem. Biophys.* **449**, 17–26.
[5] Acquati, F., Morelli, C., Cinquetti R., Bianchi, M. G., Porrini, D., Varesco, L., Gismondi, V., Rocchetti, R., Talevi, S., Possati, L., Magnanini, C., Tibiletti, M. G., Bernasconi, B., Daidone, M. G., Shridhar, V., Smith, D. I., Negrini, M., Barbanti-Brodano, G., and Taramelli, R. (2001) *Oncogene* **22**, 980–988.
[6] Acquati, F., Possati, L., Ferrante, L., Campomenosi, P., Talevi, S., Bardelli, S., Margiotta, C., Russo, A., Bortolotto, E., Rocchetti, R., Calza, R., Cinquetti, R., Monti, L., Salis, S., Barbanti-Brodano, G., and Taramelli, R. (2005) *Int. J. Oncol.* **26**, 1159–1168.
[7] Monti, L., Rodolfo, M., Lo Russo, G., Noonan, D., Acquati, F., and Taramelli, R. (2008) *Oncol. Res.* **17**, 69–74.
[8] Cereghino, J. L. and Cregg, J. M. (2000) *FEMS Microbiol. Rev.* **24**, 45–66.
[9] Cregg, J. M., Cereghino, J. L., Shi, J., and Higgins, D. R. (2000) *Mol. Biotechnol.* **16**, 23–52.
[10] Daly, R. and Hearn, M. T. J. (2005) *Mol. Recognit.* **18**, 119–138.
[11] Gietz, R. D., Schiestl, R. H., Willems, A. R., and Woods, R. A. (1995) *Yeast* **11**, 355–360.
[12] Vaughn, J. L., Goodwin, R. H., Tompkins, G. J., and McCawley, P. (1977) *In Vitro* **13**, 213–217.
[13] Dell, A., Reason, A. J., Khoo, K. H., Panico, M., McDowell, R. A., and Morris H. R. (1994) *Methods Enzymol.* **230**, 108–132.
[14] Jang-Lee, J., North, S. J., Sutton-Smith, M., Goldberg, D., Panico, M., Morris, H., Haslam, S., and Dell, A. (2006) *Methods Enzymol.* **415**, 59–86.
[15] Ceroni, A., Maass, K., Geyer, H., Geyer, R., Dell, A., and Haslam, S. M. (2008) *J. Proteome Res.* **7**, 1650–1659.
[16] Blank, A. and Dekker, C. A. (1981) *Biochemistry* **20**, 2261–2267.
[17] Brown, P. H. and Ho, T. H. (1986) *Plant Physiol.* **82**, 801–806.
[18] Smirnoff, P., Roiz, L., Angelkovitch, B., Schwartz, B., and Shoseyov, O. (2006) *Cancer* **107**, 2760–2769.
[19] Ohgi, K., Horiuchi, H., Watanabe, H., Takagi, M., Yano, K., and Irie, M. (1991) *J. Biochem.* **109**, 776–785.
[20] Mu J. and Kao, T. H. (1992) *Biophys. Res. Commun.* **187**, 299–304.

[21] Huang, C., Chien, M. S., Hu, C. M., Chen, C. W., and Hsieh, P. C. J. (2006) *Virol. Meth.* **132**, 40–47.
[22] Hulst, M. M., Panoto, F. E., Hoekman, A., van Gennip, H. G., and Moormann, R. J. (2000) *J Virol.* **74**, 9553–9561.
[23] Numata, T., Suzuki, A., Kakuta, Y., Kimura, K., Yao, M., Tanaka, I., Yoshida, Y., Ueda, T., and Kimura, M. (2003) *Biochemistry* **42**, 5270–5278.
[24] Kimura, K., Numata, T., Kakuta, Y., and Kimura, M. (2004) *Biosci. Biotechnol. Biochem.* **68**, 1748–1757.
[25] Iwama, M., Kusano, A., Ogawa, Y., Ohgi, K., and Irie, M. (1998) *Biol. Pharm. Bull.* **21**, 634–637.
[26] Acquati, F., Bertilaccio, S., Grimaldi, A., Monti, L., Cinquetti, R., Bonetti, P., Lualdi, M., Vidalino, L., Fabbri, M., Sacco, M.G., van Rooijen, N., Campomenosi, P., Vigetti, D., Passi, A., Riva, C., Capella, C., Sanvito, F., Doglioni, C., Gribaldo, L., Macchi, P., Sica, A., Noonan, D.M., Ghia, P., and Taramelli, R. (2011) *Proc. Natl. Acad. Sci. USA.* **108**, 1104–1109.